A study of nuclear matter with a parity doublet model (パリティ２重項模型を用いた核物質の研究)

Yuichi Motohiro

Contents

Chapter 1

Introduction

Nuclear matter is one of the most important subjects to be studied in nuclear physics. A long-standing issue in nuclear physics is the lack of deep understanding and knowledge of the nucleus structure and nuclear matter has contributed to it.

In general, a nucleus is a many-body system of nucleons bounded by "strong", short-range nuclear forces. In addition, surface tension and the Coulomb force exist between protons and these complicate the theoretical analysis of the nuclear structure. The study of nuclear matter is an ideal method to approach such a complicated subject. The study of nuclear matter makes the following assumptions:

- the number of nucleons, A, is sufficiently "large".
- Coulomb force between the protons and the surface tension are ignored.

The second assumption implies that the nuclear matter is an infinite system. These assumptions simplify the theoretical analysis of nuclear matter. Based on these assumptions, the structure of the nuclear matter and nucleus have been investigated in nuclear physics [1].

Observation and verification are important to understand physics. Several experiments performed in the field of nuclear physics have revealed the properties [1] of various nuclei. The results of such experiments have enhanced our understanding and knowledge of nuclear matter. For example, the binding energy of nuclear matter is 16 MeV[2] when their densities equal 0.16 fm^{-3}. This density is called the saturation density of normal nuclear matter, which is referred to as ρ_0 in this thesis. The incompressibility and symmetry energy of nuclear matter have also been actively investigated.

Several experiments have been performed to study the above and the normal properties of nuclear matter have been revealed. However, accessing a high-density and/or asymmetric environment is a difficult issue because of the difficulties in creating such an environment. In spite of this fact, some experiments have been performed under such extreme environments ([2]). With the advent of next-generation radioactive beam facilities[3], isospin-asymmetric nuclear matter has claimed much attention in contemporary nuclear physics. These facilities allow us to create a terrestrial environment to study dense matter containing a large neutron or proton excess created by nuclear reactions with radioactive nuclei.

One environment that has asymmetric and dense nuclear matter is a neutron star. Therefore, the study of dense, asymmetric nuclear matter will give us a better understanding of neutron

[1] Mass, composition of the nucleus, energy per nucleon, size, magnetic and electric moments, spin, and parity are examples of such properties.

[2] The binding energy of nucleus is $\approx$ 8 MeV. It is the effect of surface tension and Coulomb force of the nucleus.

[3] RIBF at RIKEN, RAON at RISP

stars. Neutron star was predicted in early 1930 and it was observed as a pulsar later. A neutron stars is the remnant of a supernova explosion of a heavy star with mass of ~ 20 solar masses. As the name indicates, neutrons are the main components of this star and the gravitational force on the star balances the pressure of the degenerate neutron gas. A large number of neutrons are created by inverse beta decay[4] during the collapse of the heavy star. Because the radius is of the order of 10 km, we can ignore the surface tension in the neutron star. In addition, the number of protons and electrons is sufficiently small to ignore the electromagnetic force. Because of these condition, the maximum mass of neutron stars have been estimated using nuclear matter model and considered to be approximately 1.5 solar masses.

In 2010 and 2013, "heavy" neutron stars having twice the solar mass were observed [3, 4]. Because very heavy neutron stars have been detected precisely, several nuclear matter models that do not reproduce their mass and radius were excluded from acceptable models. Each model has its own equation of state (EoS) and we can test it by observation of the neutron star. Neutron stars are very cold, asymmetric, and the densest nuclear matter in the world. It may also be noted that neutron stars may include hyperons in their cores. If there are hyperonic degrees of freedom, it is expected that the EoS will become "softer" and the neutron star will become lighter because hyperons restrict the fermi-momenta of other constituents, mainly protons and neutrons. Another important astrophysical entity for nuclear matter is a hybrid star whose center is a quark matter ([5]).

The EoS for (asymmetric) nuclear matter has been investigated using various approaches [6, 7, 8, 9, 10, 11, 12, 13, 14, 15]. There are two main streams in nuclear-matter study: (a) we determine the potential between nucleons by two- and/or three-body interactions and include many-body effect into particle mass and energy; (b) we determine the Lagrangian of model and obtain the nuclear-matter potential. This is called relativistic mean field (RMF) approach.

The above was the overview of nuclear matter, which is the subject of our study. Next, we introduce the "parity doublet model" and explain the background behind its construction.

In this thesis, we use RMF approach and construct an "effective model " that contains the "parity doublet " structure [16, 17]. This "parity doublet" concept states that positive- and negative-parity baryons have a degenerate mass when the chiral symmetry is restored. We will briefly state the concept of effective hadron model and the concept of parity doublet model below.

Hadrons are composite particles of quarks, which are descrived in quantum chromodynamics (QCD). QCD is an SU(3) gauge theory, which describes the interactions between quarks and gluons. It is very difficult to investigate hadron phenomena directly using QCD due to the strong coupling between quarks and gluons[5]. One approach to study hadron physics is to use effective models of the hadron[6]. Effective hadron-models are constructed based on the chiral symmetry of QCD. We know that the chiral symmetry of QCD is broken spontaneously at "low energy" and its order parameter is the "chiral condensate"[7]. There are some relatinos that must be satisfied from low-energy behaviors of hadrons and we discuss some relevant aspects of the QCD in the appendix A.

Spontaneous chiral symmetry breaking is used to explain the mass of hadrons. For example, a nucleon is composed of three quarks and the mass is ~ 1000 MeV, although the total mass of its components is ~ 10 MeV. A portion of the hadron mass is come from the spontaneous

[4]Also called electron capture; $\mathrm{p} + \mathrm{e}^- \to \mathrm{n} + \nu_\mathrm{e}$. Charge neutrality, chemical equilibrium, and baryon-number conservation constrain the inverse process.

[5]Therefore, we could not use the perturbative approach.

[6]The lattice QCD is an established approach for studying QCD A.

[7]Pion is the lightest observed meson and it is considered as a Nambu-Goldstone boson with spontaneous chiral symmetry breaking.

chiral symmetry breaking. According to QCD, a vacuum is filled with chiral condensate and this gives mass to the quark. This is one of the explanations for the origin of hadron masses.

Parity doublet model is an effective model for hadrons.The basic concept of parity doublet model was written in [16] in a purely theoretical form. However, a realistic model was established in [17, 18]. The motivations to study the parity doublet model are not only theoretical interest but also the indications of the existence of a doublet structure as suggested from previous lattice QCD simulations [19]. The important finding in [19] is that there are two kinds of degenerate baryons, which have a finite mass called "chiral invariant mass", m_0, after chiral restoration. A recent lattice study [20] also supports the existence of m_0 and claims that the chiral partner of nucleon is N(1535). These lattice results prefer high chiral invariant mass although lattice QCD has some uncertainty related to interpolation.

There are the other points of view that support the interest in parity doublet structure. Many experiments have revealed that there are baryons that have the same quantum numbers as the nucleon but have different masses. We assume that the nucleon is composed of three quarks. Although the mass of the nucleon N(939) can be explained by spontaneous chiral symmetry breaking, it is difficult to explain the masses of other heavy baryons using the same theory. The parity doublet structure offers an explanation for the mass spectrum of hadrons.

Some studies using parity doublet models [24, 25, 26, 27, 28, 29, 30, 31] indicate that m_0 should not be small. These results are consistent with [19, 20]. On the other hand, in [18], the authors determined m_0 from the decay width of $N(1535) \to N\pi$ to be approximately one-third of m_N. Similarly, [27] used the decay modes of $N^* \to N\pi$ and $a_1 \to \pi\gamma$ to obtain m_0 as approximately half of m_N. These studies suggest that a light m_0 is preferred from vacuum properties such as the decay modes. Although m_0 may change in dense matter, it is hard to understand why the value of m_0 shows such variation. This fact also motivates us to seek ways to reproduce the normal properties of nuclear matter with a medium chiral invariant mass.

We invoke some studies on asymmetric matter using various approaches [6, 7, 8, 9, 10, 11, 12, 13, 14, 15, 32]. These results predicted that some properties of symmetric nuclear matter such as the order and temperature of phase transition are changed in asymmetric matter.

The original parity doublet model [17] does not include vector mesons. However, the nuclear force is generated from the attractive scalar forces and repulsive vector forces. Therefore, to study the nuclear matter, we added vector mesons in this model and used hidden local symmetry (HLS) [21, 22, 23] in this study (appendix G).

We used the finite-temperature field theory and introduced temperature and density into this model in order to investigate the EoS and phase structure. Then, we compared the behavior of the EoS with those of other studies and demonstrated the phase structure of this model. We would like to clarify that our analysis was based on the effective model. Therefore, our model does not explicitly include quarks. As a result, the quarks in our model were confined in hadrons even after the chiral symmetry was restored. Therefore, our phase diagram does not have quark-gluon plasma and color superconductivity phase (we will explain them in more detail in the appendix A).

At the end of this thesis, we will analyze finite-size nuclear matter[8]. This was because we were interested in investigating whether our model could reproduce finite matter or not. We analyzed the finite-size nuclear matter based on our model and compared the strength of the spin-orbit potential that is affected strongly from behavior of the vicinity of surface [33]. We used relativistic Thomas-Fermi approximation to verify our model and derived the strength of single-particle spin-orbit potential based on [34]. It may be noted that the spin-orbit interaction has been studied for a long time in nuclear physics and they are closely related with the well-

[8]The electromagnetic interaction in the nucleus was ignored in this study.

established shell structure of the nucleus.

This thesis is organized as follows: In chapter 2, we introduce the parity doublet structure and briefly review the construction of the model. In addition, the extension of the parity doublet model with HLS is explained. In chapter 3, we present the analysis of the nuclear matter using our model. We calculated the thermodynamic potential (pressure) of this model and derived the gap equations. Then, we explained the method to determine the parameters. We used saturation density, binding energy, incompressibility, and symmetry energy as inputs and calculated the parameter values. Several figures for the pressure, binding energy, σ_0, ρ_B, and effective masses are shown. Next, we plotted phase diagrams of this model. In chapter 4, we analyzed the finite-size nuclear matter using Thomas-Fermi approximation. Following a brief introduction, we verified the density distribution and radius and determined the strength of the spin-orbit potential. In chapter 5, we have summarized this study and given suggestions for future studies in this field based on our model.

This thesis is mainly based on our previous paper [35]. The review parts are included in the appendix. The appendix also discusses important facts that are not directly related to our main article.

The conventions followed in this article are given below: We used natural units in the entire study. Therefore the speed of light, Dirac constant, and Boltzmann constant are unity[9].

$$\hbar = 1,\ \ c = 1,\ \ k_{\rm B} = 1$$

The Minkowski metric is $g_{\mu\nu} = \mathrm{diag}(+1, -1, -1, -1)$.

We expressed the chiral representation for Dirac matrices as

$$\gamma^0 = \begin{pmatrix} 0 & 1 \\ 1 & 0 \end{pmatrix},\ \ \gamma^i = \begin{pmatrix} 0 & -\tau^i \\ \tau^i & 0 \end{pmatrix},\ \ \gamma_5 \equiv i\gamma^0\gamma^1\gamma^2\gamma^3 = \begin{pmatrix} 1 & 0 \\ 0 & -1 \end{pmatrix}.$$

Here, τ^i $(i = 1, 2, 3)$ are 2×2 Pauli matrices.

[9] $\hbar c = 197.3269788(12)$ MeV·fm is quoted from Particle Data Group (PDG 2016 Review [60].

Chapter 2

Parity doublet model

In this chapter, we will construct an effective model based on the parity doublet structure [17, 18]. In section 2.1, we will briefly review the parity doublet model. In section 2.2, we will explain our model based on the parity doublet structure.

2.1 Parity doublet structure

We will explain the parity doublet structure based on the chiral symmetry of quark. We note that the chiral symmetry is explicitly broken if quarks have the mass, and we negrect the mass of quarks here.

We have assumed the chiral symmetry to be $\mathrm{SU}(2)_{\mathrm{L}}\times\mathrm{SU}(2)_{\mathrm{R}}$. A quark belongs to the fundamental representation:

$$q :: \left(\frac{1}{2}, 0\right) \oplus \left(0, \frac{1}{2}\right). \tag{2.1}$$

Here the left and right components in round brackets correspond to the representation of $\mathrm{SU}(2)_{\mathrm{L}}$ and $\mathrm{SU}(2)_{\mathrm{R}}$:

$$(\mathrm{Rep.}(\mathrm{SU}(2)_{\mathrm{L}}), \mathrm{Rep.}(\mathrm{SU}(2)_{\mathrm{R}}).) \tag{2.2}$$

An ordinal baryon is composed of three quarks and we can assume the representation of baryon as a direct product of three quarks. By means of further calculation, we can reduce them into an irreducible representation given by

$$q\otimes q\otimes q :: 5\left(\left(\frac{1}{2}, 0\right) \oplus \left(0, \frac{1}{2}\right)\right) \oplus 3\left(\left(\frac{1}{2}, 1\right) \oplus \left(1, \frac{1}{2}\right)\right) \oplus \left(\left(\frac{3}{2}, 0\right) \oplus \left(0, \frac{3}{2}\right).\right) \tag{2.3}$$

$\left(\frac{1}{2}, 0\right) \oplus \left(0, \frac{1}{2}\right)$ represents protons and neutrons and we used this representation for baryons in this model. The central expression, $\left(\frac{1}{2}, 1\right) \oplus \left(1, \frac{1}{2}\right)$, also includes the representation of nucleons. However, we have to include spin-one particle Δ in the model simultaneously.

Based on this construction of the baryon ψ, we have two choices for assignment of transformation properties under the chiral transformation, which are given by

$$\psi :: \left(\frac{1}{2}, 0\right) \oplus \left(0, \frac{1}{2}\right) \text{ or } \left(0, \frac{1}{2}\right) \oplus \left(\frac{1}{2}, 0\right). \tag{2.4}$$

This degree of freedom of choice comes from the quark model and it allows us to consider the chiral invariant mass.

Next, we consider positive and negative parity nucleons: ψ_1 has positive parity and ψ_2 has negative parity. As we saw earlier, we have two options for assignment of the chiral transformation properties of baryon. Therefore, we can assign the transformation properties of ψ_1 and ψ_2 as

$$\psi_1 :: \left(\frac{1}{2},0\right) \oplus \left(0,\frac{1}{2}\right), \ \psi_2 :: \left(0,\frac{1}{2}\right) \oplus \left(\frac{1}{2},0\right). \tag{2.5}$$

With regard to the Dirac field components, the transformation properties of left- and right-handed components of baryons are

$$\psi_1 = \begin{pmatrix}\psi_{1r}\\ \psi_{1l}\end{pmatrix}, \ \psi_2 = \begin{pmatrix}\psi_{2r}\\ \psi_{2l}\end{pmatrix} \tag{2.6}$$

$$\psi_{1r} \to g_{\rm R}\psi_{1r}, \quad \psi_{1l} \to g_{\rm L}\psi_{1l} \tag{2.7}$$

$$\psi_{2r} \to g_{\rm L}\psi_{2r}, \quad \psi_{2l} \to g_{\rm R}\psi_{2l}. \tag{2.8}$$

Here $g_{\rm R}$ ($g_{\rm L}$) is an element of $\mathrm{SU(2)_R}$ ($\mathrm{SU(2)_L}$) chiral group, and ψ_{1r} and ψ_{2r} (ψ_{1l} and ψ_{2l}) are the right- (left-) handed fields. This choice of chiral transformation properties is called as "mirror assignment"[1].

The mirror assignment allows us to make a chiral-invariant Dirac mass term and this is one of the most important characteristics of the parity doublet structure. This statement implies that the mass origin of nucleon is not only due to chiral symmetry breaking but also due to the chiral invariant mass. The next section describes the mass functions of nucleons.

In order to include the breakdown of the chiral symmetry in our model, we chose the linear sigma potential and the scalar fields were introduced as

$$M = \sigma + i\pi^a\tau^a \ , \tag{2.11}$$

where σ denotes an isosinglet scalar field and π^a denotes the isotriplet pion fields. The chiral transformation property of M under $\mathrm{SU(2)}_L\times\mathrm{SU(2)}_R$ is given by

$$M \to g_{\rm L} M g_{\rm R}^\dagger \ . \tag{2.12}$$

By using these fields, we can construct the model Lagranian for nucleons as [2]

$$\begin{aligned}\mathcal{L}_{\rm N} =& \bar\psi_{1r} i\gamma^\mu D_\mu^{\mathcal{R}} \psi_{1r} + \bar\psi_{1l} i\gamma^\mu D_\mu^{\mathcal{L}} \psi_{1l} \\ &+ \bar\psi_{2r} i\gamma^\mu D_\mu^{\mathcal{L}} \psi_{2r} + \bar\psi_{2l} i\gamma^\mu D_\mu^{\mathcal{R}} \psi_{2l} \\ &- m_0 \left[\bar\psi_{1l}\psi_{2r} - \bar\psi_{1r}\psi_{2l} - \bar\psi_{2l}\psi_{1r} + \bar\psi_{2r}\psi_{1l}\right] \\ &- g_1 \left[\bar\psi_{1r} M^\dagger \psi_{1l} + \bar\psi_{1l} M \psi_{1r}\right] \\ &- g_2 \left[\bar\psi_{2r} M \psi_{2l} + \bar\psi_{2l} M^\dagger \psi_{2r}\right] \ .\end{aligned} \tag{2.13}$$

[1] Chiral transformation properties can also be expressed as

$$\psi_{1r} \to g_{\rm R}\psi_{1r}, \quad \psi_{1l} \to g_{\rm L}\psi_{1l} \tag{2.9}$$

$$\psi_{2r} \to g_{\rm L}\psi_{2r}, \quad \psi_{2l} \to g_{\rm R}\psi_{2l} \ , \tag{2.10}$$

naively. This assignment is called as "naive assignment". We can easily check that the naive assignment does not have $N^* \to N\pi$ decay mode after diagonalization for mass, in which case we do not consider it.

[2] Familiar form of this Lagrangian is

$$\begin{aligned}\mathcal{L}_{\rm N} =& \psi_1 i\gamma^\mu\partial_\mu\psi_1 + \bar\psi_2 i\gamma^\mu\partial_\mu\psi_2 - m_0\left(\bar\psi_1\gamma_5\psi_2 - \bar\psi_2\gamma_5\psi_1\right) \\ &- g_1\bar\psi_1\left(\sigma + i\gamma_5\vec\pi\cdot\vec\tau\right)\psi_1 - g_2\bar\psi_2\left(\sigma - i\gamma_5\vec\pi\cdot\vec\tau\right)\psi_2 \ .\end{aligned}$$

Here m_0 is the chiral invariant mass, which mixes two nucleon fields, and g_1 and g_2 are the coupling constants with scalar mesons. The covariant derivatives include the external gauge fields $\mathcal{R}_\mu$ and $\mathcal{L}_\mu$ as[3].

$$D_\mu^{\mathcal{R}}\psi_{1r,2l} = (\partial_\mu - i\mathcal{R}_\mu)\,\psi_{1r,2l}\ , \tag{2.15}$$

$$D_\mu^{\mathcal{L}}\psi_{1l,2r} = (\partial_\mu - i\mathcal{L}_\mu)\,\psi_{1l,2r}\ . \tag{2.16}$$

The external fields, $\mathcal{R}_\mu$ and $\mathcal{L}_\mu$, included in the analysis are considered as gauge fields of the chiral symmetry. The chiral symmetry $\mathrm{SU(2)_L}\times\ \mathrm{SU(2)_R}$ is broken into vector $\mathrm{SU(2)_V}$ spontaneously. We can arrange these external fields as

$$\mathcal{V}_\mu = \mathcal{L}_\mu + \mathcal{R}_\mu \tag{2.17}$$

$$\mathcal{A}_\mu = \mathcal{L}_\mu - \mathcal{R}_\mu, \tag{2.18}$$

for ease of analysis. Using the above form, we can easily visualize the broken and unbroken symmetries. With regard to thermodynamics of our model, these external fields are manipulated to introduce the baryon and isospin chemical potential into our model[4];

$$\mathcal{V}_\mu = \left(\mu_B + \mu_I\frac{\tau^3}{2}\right)\delta_{0\mu} \tag{2.20}$$

$$\mathcal{A}_\mu = 0. \tag{2.21}$$

Next, we analyzed the scalar meson field in our model. The Lagrangian of the scalar field is given as

$$\mathcal{L}_\mathrm{M} = \frac{1}{4}\mathrm{tr}\left[\partial_\mu M\partial^\mu M^\dagger\right] - V_\mathrm{M} - V_\mathrm{SB}\ , \tag{2.22}$$

where V_M and V_SB are the potentials of the meson field and explicit chiral symmetry breaking respectively.

$$\begin{aligned} V_\mathrm{M} = &-\frac{1}{4}\bar{\mu}^2\mathrm{tr}\left[MM^\dagger\right] + \frac{1}{16}\lambda\left\{\mathrm{tr}\left[MM^\dagger\right]\right\}^2 \\ &-\frac{1}{48}\lambda_6\left\{\mathrm{tr}\left[MM^\dagger\right]\right\}^3\ , \end{aligned} \tag{2.23}$$

$$V_\mathrm{SB} = -\frac{1}{4}\varepsilon\left(\mathrm{tr}\left[\mathcal{M}^\dagger M\right] + \mathrm{tr}\left[\mathcal{M}M^\dagger\right]\right)\ . \tag{2.24}$$

We chose the linear sigma type potential as a scalar potential, and we added the six-point interaction. We note that the six-point interaction term plays an important role in reproducing the normal nuclear matter properties explained in a later section. Explicit symmetry breaking

[3]Transformation properties of external fields are shown below ($\mathcal{L}$ also has the same properties).

$$\mathcal{R}_\mu \to g_R\mathcal{R}_\mu g_R^{-1} - i(\partial_\mu g_R)g_R^{-1} \tag{2.14}$$

[4]It may be noted that nucleon fields $\psi_{1,2}$ are the doublets of protons and neutrons. Considering a finite μ_I system, we can express these fields as

$$\psi_{1,2} = \begin{pmatrix}\psi_{1,2}^\mathrm{p}\\ \psi_{1,2}^\mathrm{n}\end{pmatrix} \tag{2.19}$$

term (2.24) contains a mass-matrix of quark, $\mathcal{M}$, which has up and down quark masses (m_u and m_d). The mass matrix can be expressed as

$$\mathcal{M} = \begin{pmatrix} m_u & 0 \\ 0 & m_d \end{pmatrix}. \tag{2.25}$$

This mass matrix gives us the quark-level isospin breaking and ε is a constant with mass dimension two. Entire this analysis, we neglected the electromagnetic interaction and the mass difference between proton and neutron. Consequently, the quark mass matrix becomes $m_u = m_d \equiv \bar{m}$. This implies that the isospin asymmetry at quark level was ignored. Therefore, the mass difference between proton and neutron was derived from the isospin chemical potential alone in this model.

2.2 An effective model based on the parity doublet structure

In the previous section, we chose the linear sigma potential for scalar mesons. However, our model does not have vector mesons, which generate repulsive forces in the nuclear matter. Now, we consider the introduction of vector mesons into our model based on the HLS theory [21, 22, 23].

HLS is a useful method that denotes the low energy behavior of NG bosons and vector particles simultaneously. In the case of chiral symmetry, π represented the NG boson and vector mesons were introduced as gauge bosons of hidden symmetry. We assumed that ω_μ and ρ_μ alone are applicable to our model, as is customary. ω meson is the lightest isosinglet vector meson and ρ is the lightest isotriplet vector meson. The group of HLS is $\mathrm{U(1)_{HLS}}$ and $\mathrm{SU(2)_{HLS}}$. We use the facts relating to HLS in this section and a detailed discussion of HLS is included in the appendix G.

In order to introduce vector mesons based on the HLS, we performed the polar decomposition of the field M as

$$M = \xi_L^\dagger \sigma \xi_R = \sigma \xi_L^\dagger \xi_R = \sigma U, \tag{2.26}$$

where σ is a scalar meson field and ξ_L and ξ_R transforms as

$$\xi_{L,R} \to h_\omega h_\rho \xi_{L,R} g_{L,R}^\dagger \tag{2.27}$$

with $h_\omega \in \mathrm{U(1)_{HLS}}$ and $h_\rho \in \mathrm{SU(2)_{HLS}}$. In the unitary gauge, ξ_R and ξ_L are parameterized as

$$\xi_R = \xi_L^\dagger = \exp(i\pi^a T^a / f_\pi) \ , \tag{2.28}$$

where $T^a = \tau_a/2$ $(a = 1, 2, 3)$ with τ_a being the Pauli matrix. In the HLS, the vector mesons are introduced as gauge bosons of the HLS, which transform as

$$\omega_\mu \to h_\omega \cdot \omega_\mu \cdot h_\omega^\dagger + \frac{i}{g_\omega} \partial_\mu h_\omega \cdot h_\omega^\dagger \tag{2.29}$$

$$\rho_\mu \to h_\rho \cdot \rho_\mu \cdot h_\rho^\dagger + \frac{i}{g_\rho} \partial_\mu h_\rho \cdot h_\rho^\dagger \ , \tag{2.30}$$

where g_ω and g_ρ are the corresponding gauge coupling constants.

To construct a model Lagrangian with the HLS, it is convenient to introduce the following Maurer-Cartan 1-forms:

$$\hat{\alpha}_{\perp}^{\mu} \equiv \frac{1}{2i}\left[D^{\mu}\xi_R \cdot \xi_R^{\dagger} - D^{\mu}\xi_L \cdot \xi_L^{\dagger}\right] \ , \tag{2.31}$$

$$\hat{\alpha}_{\parallel}^{\mu} \equiv \frac{1}{2i}\left[D^{\mu}\xi_R \cdot \xi_R^{\dagger} + D^{\mu}\xi_L \cdot \xi_L^{\dagger}\right] \ , \tag{2.32}$$

where the covariant derivatives are given as

$$D_{\mu}\xi_L = \partial_{\mu}\xi_L - ig_{\rho}\rho\xi_L - \frac{i}{2}g_{\omega}\omega_{\mu}\xi_L + i\xi_L\mathcal{L}_{\mu}^{I} \ , \tag{2.33}$$

$$D_{\mu}\xi_R = \partial_{\mu}\xi_R - ig_{\rho}\rho_{\mu}\xi_R - \frac{i}{2}g_{\omega}\omega_{\mu}\xi_R + i\xi_R\mathcal{R}_{\mu}^{I} \ . \tag{2.34}$$

It should be noted that ρ_{μ} represents isotriplet vector meson contracted with T^a,

$$\rho_{\mu} = \rho_{\mu}^{a}T^{a}, \tag{2.35}$$

and we added the factor $1/2$ to ω in the equations (2.33) and (2.34), which are used for easy analysis later in the thesis. There are no meson fields that carry the baryon charge. The external fields include the isospin chemical potential alone and in order to avoid confusion, we attached the suffix I to the external gauge fields. The one-forms transform as

$$\hat{\alpha}_{\perp,\parallel}^{\mu} \to h_{\omega}h_{\rho}\hat{\alpha}_{\perp,\parallel}^{\mu}h_{\rho}^{\dagger}(x)h_{\omega}^{\dagger}. \tag{2.36}$$

With respect to (2.36) and using 1-forms (**??**,**??**), we can write the meson Lagrangian as:

$$\begin{aligned}\mathcal{L}_{\mathrm{M}} =& \frac{1}{2}\partial_{\mu}\sigma\partial^{\mu}\sigma + \sigma^2\mathrm{tr}\left[\hat{\alpha}_{\perp\mu}\hat{\alpha}_{\perp}^{\mu}\right] - V_{\sigma} - V_{\mathrm{SB}} \\ &+ \frac{m_{\rho}^2}{g_{\rho}^2}\mathrm{tr}\left[\hat{\alpha}_{\parallel\mu}\hat{\alpha}_{\parallel}^{\mu}\right] + \left(\frac{m_{\omega}^2}{2g_{\omega}^2} - \frac{m_{\rho}^2}{2g_{\rho}^2}\right)\mathrm{tr}\left[\hat{\alpha}_{\parallel\mu}\right]\mathrm{tr}\left[\hat{\alpha}_{\parallel}^{\mu}\right] \\ &- \frac{1}{2}\mathrm{tr}\left[\rho_{\mu\nu}\rho^{\mu\nu}\right] - \frac{1}{4}\omega_{\mu\nu}\omega^{\mu\nu}.\end{aligned} \tag{2.37}$$

Kinetic terms and interaction terms of scalars are given in the first line of the expression. The second line expresses the mass terms of vector mesons and the third line expresses the kinetic terms of the vector mesons. The vector meson terms of $\hat{\alpha}_{\parallel}^{\mu}$ when $\xi_{L,R} = 1$[5] can be written as:

$$\hat{\alpha}_{\parallel}^{\mu} = -g_{\rho}\rho^{\mu} - \frac{g_{\omega}}{2}\omega^{\mu} + \mathcal{V}_{I}^{\mu}. \tag{2.38}$$

It may be noted that the mass of a vector meson is related to its gauge coupling, which is a feature of HLS (G) and $\mathcal{V}_{I}^{\mu}$ has been defined in equation (2.43).

In the above Lagrangian, we introduced field strength tensors of the vector fields:

$$\omega_{\mu\nu} = \partial_{\mu}\omega_{\nu} - \partial_{\nu}\omega_{\mu} \tag{2.39}$$

$$\rho_{\mu\nu} = \partial_{\mu}\rho_{\nu} - \partial_{\nu}\rho_{\mu} - ig_{\rho}\left[\rho_{\mu}, \rho_{\nu}\right] \tag{2.40}$$

and the following forms of potentials:

$$V_{\sigma} = -\frac{1}{2}\bar{\mu}^2\sigma^2 + \frac{1}{4}\lambda\sigma^4 - \frac{1}{6}\lambda_6\sigma^6 \tag{2.41}$$

$$V_{\mathrm{SB}} = -\frac{1}{4}\bar{m}\epsilon\sigma\,\mathrm{tr}\left[U + U^{\dagger}\right] \ . \tag{2.42}$$

[5]This condition corresponds to vacuum where the chiral symmetry is already broken.

These potentials are easily derived from equations (2.23) and (2.24).

We introduced the chemical potential of nuclear matter into our model using external fields. Because we have only meson fields, we have considered isospin chemical potential in the model.

$$\mathcal{V}^I_\mu = \mathcal{L}^I_\mu + \mathcal{R}^I_\mu \equiv \mu_I T^3, \tag{2.43}$$
$$\mathcal{A}^I_\mu = \mathcal{L}^I_\mu + \mathcal{R}^I_\mu \equiv 0. \tag{2.44}$$

Next, we introduce the interactions among mesons and baryons using Maurer-Cartan 1-forms based on the chiral transformation. We can rewrite the nucleon Lagrangian with $\hat{\alpha}^\mu_\parallel$ as

$$\begin{aligned}
\mathcal{L}_{\rm N} =& \bar{\psi}_{1r} i\gamma^\mu D_\mu \psi_{1r} + \bar{\psi}_{1l} i\gamma^\mu D_\mu \psi_{1l} + \bar{\psi}_{2r} i\gamma^\mu D_\mu \psi_{2r} + \bar{\psi}_{2l} i\gamma^\mu D_\mu \psi_{2l} \\
& - m_0 \left[\bar{\psi}_{1l}\psi_{2r} - \bar{\psi}_{1r}\psi_{2l} - \bar{\psi}_{2l}\psi_{1r} + \bar{\psi}_{2r}\psi_{1l}\right] \\
& - g_1\sigma \left[\bar{\psi}_{1r} U^\dagger \psi_{1l} + \bar{\psi}_{1l} U \psi_{1r}\right] - g_2\sigma \left[\bar{\psi}_{2r} U \psi_{2l} + \bar{\psi}_{2l} U^\dagger \psi_{2r}\right] \\
& + a_\rho \left[\bar{\psi}_{1l}\gamma^\mu (\xi^\dagger_L \hat{\alpha}_{\parallel\mu} \xi_L)\psi_{1l} + \bar{\psi}_{1r}\gamma^\mu (\xi^\dagger_R \hat{\alpha}_{\parallel\mu} \xi_R)\psi_{1r}\right] \\
& + a_\rho \left[\bar{\psi}_{2l}\gamma^\mu (\xi^\dagger_R \hat{\alpha}_{\parallel\mu} \xi_R)\psi_{2l} + \bar{\psi}_{2r}\gamma^\mu (\xi^\dagger_L \hat{\alpha}_{\parallel\mu} \xi_L)\psi_{2r}\right] \\
& + a_0 \,\mathrm{tr}\left[\hat{\alpha}_{\parallel\mu}\right] \left(\bar{\psi}_{1l}\gamma^\mu\psi_{1l} + \bar{\psi}_{1r}\gamma^\mu\psi_{1r} + \bar{\psi}_{2l}\gamma^\mu\psi_{2l} + \bar{\psi}_{2r}\gamma^\mu\psi_{2r}\right).
\end{aligned} \tag{2.45}$$

Interaction terms with scalar mesons are given on the third line and those for vector mesons are given from the fourth to the sixth line. We used a new coefficient a_0, which was defined as

$$a_0 \equiv \frac{1}{2}\left(a_\omega - a_\rho\right). \tag{2.46}$$

The coupling constants between the vector mesons and nucleons are defined as

$$g_{\omega NN} \equiv a_\omega g_\omega, \;\; g_{\rho NN} \equiv a_\rho g_\rho. \tag{2.47}$$

Here, we have assumed that coupling constants of vector mesons are equivalent to two nucleon (ψ_1 and ψ_2).

Therefore the model Lagrangian $\mathcal{L}$ is given as below based on equations (2.37) and (2.45):

$$\mathcal{L} = \mathcal{L}_{\rm N} + \mathcal{L}_{\rm M}. \tag{2.48}$$

We have assumed that the linear sigma potential can be used to determine the vacuum dynamically. In other words, the vacuum expectation value (VEV) of σ, denoted as σ_0, is obtained from the stationary condition of the scalar potential. In addition, σ_0 coincides with the pion decay constant f_π of the vacuum[6].

The non-zero σ_0 generates masses of nucleons and the chiral invariant mass mixes the two nucleons.

$$\mathcal{L}_{\rm mass} = -\begin{pmatrix}\bar{\psi}_1 & \bar{\psi}_2\end{pmatrix}\begin{pmatrix} g_1\sigma_0 & m_0\gamma_5 \\ -m_0\gamma_5 & g_2\sigma_0\end{pmatrix}\begin{pmatrix}\psi_1 \\ \psi_2\end{pmatrix}. \tag{2.49}$$

We obtain the masses of positive-parity and negative-parity nucleons by diagonalization of the mass matrix. The diagonalization yields the mass eigenvalues, which are written as

$$m_\pm = \frac{1}{2}\left(\sqrt{(g_1+g_2)^2\sigma_0^2 + 4m_0^2} \pm (g_1 - g_2)\sigma_0\right), \tag{2.50}$$

[6]The value of σ_0 will change when we consider a finite density system.

where m_+ and m_- are the masses of positive and negative parity baryons, respectively. These equations show that the vacuum expectation value σ_0 generates mass differences between parity partners. Here, the mass eigenstates are defined as N_+ and N_-, and they are related with ψ_1 and ψ_2 as

$$\begin{pmatrix} N_+ \\ N_- \end{pmatrix} = \begin{pmatrix} \cos\theta & \gamma_5 \sin\theta \\ -\gamma_5 \sin\theta & \cos\theta \end{pmatrix} \begin{pmatrix} \psi_1 \\ \psi_2 \end{pmatrix} \ . \tag{2.51}$$

Here, θ is the mixing angle given by

$$\tan 2\theta = \frac{2m_0}{(g_1 + g_2)\sigma_0} \ .. \tag{2.52}$$

γ_5 is used in the rotation matrix to account for the parity difference. Equation (2.52) indicates that the mixing angle depends on the scalar VEV and the restoration of symmetry implies that ψ_1 and ψ_2 are present in the same proportion.

At the end of this section, we would like to mention an important fact regarding the chiral effective model. Let us consider the interaction term of π meson and the nucleons. By expanding U, the interactions between pi and the nucleons are obtained as

$$\begin{aligned} \mathcal{L}_{\pi NN} = &- g_{\pi N_+ N_+} \bar{N}_+ (i\gamma_5 \pi^a \tau^a) N_+ - g_{\pi N_- N_-} \bar{N}_- (i\gamma_5 \pi^a \tau^a) N_- \\ &- g_{\pi N_+ N_-} [(\bar{N}_+ (i\pi^a \tau^a) N_- - \bar{N}_- (i\pi^a \tau^a) N_+]. \end{aligned} \tag{2.53}$$

Here, the Yukawa couplings of π and nucleons are expressed as

$$g_{\pi N_+ N_+} = g_1 \cos^2\theta + g_2 \sin^2\theta \tag{2.54}$$

$$g_{\pi N_- N_-} = -(g_1 \sin^2\theta + g_2 \cos^2\theta) \tag{2.55}$$

$$g_{\pi N_+ N_-} = \frac{g_2 - g_1}{2} \sin 2\theta. \tag{2.56}$$

Now, commutation relations for N_+ and N_- are established as below to consider the axial charge of the nucleons:

$$[Q_A^a, N_+] = \frac{\tau^a}{2} (\cos 2\theta \gamma_5 N_+ - \sin 2\theta N_-) \tag{2.57}$$

$$[Q_A^a, N_-] = \frac{\tau^a}{2} (-\sin 2\theta N_+ - \cos 2\theta \gamma_5 N_-). \tag{2.58}$$

The above gives us the axial charges in a matrix form defined by

$$\begin{aligned} g_A &\equiv \begin{pmatrix} g_{A++} & -g_{A+-}\gamma_5 \\ -g_{A+-}\gamma_5 & g_{A--} \end{pmatrix} \\ &= \begin{pmatrix} \cos 2\theta & -\sin 2\theta \gamma_5 \\ -\sin 2\theta \gamma_5 & -\cos 2\theta \end{pmatrix}. \end{aligned} \tag{2.59}$$

It may be noted that the axial charges of positive and negative nucleon have the same magnitude and opposite signs.

Equations (2.54-2.56) can be rewritten using g_A as

$$g_{\pi N_+ N_+} = \frac{m_+}{\sigma_0} g_{A++} \tag{2.60}$$

$$g_{\pi N_- N_-} = \frac{m_-}{\sigma_0} g_{A--} \tag{2.61}$$

$$g_{\pi N_+ N_-} = \frac{m_- - m_+}{2\sigma_0} g_{A+-}. \tag{2.62}$$

These equations are considered as generalized versions of Goldberger-Treiman (GT) relations and the ordinal GT relation corresponds to the equation (2.60). Especially, equation (2.62) is a characteristic of the parity doublet model. The GT relation is one of the consequences of low-energy theorem for NG bosons [7]. The parity doublet model satisfies the theorem, which is as expected.

[7]The low energy theorem states the general relations for scattering amplitude of NG bosons. It is determined from the symmetric structure alone. Examples of the low-energy theorem are discussed in [36] (p. 20).

Chapter 3

Nuclear matter

In this chapter, we construct an EoS of the nuclear matter. In section 3.1, we will calculate the thermodynamic potential using our model. Next, we will explain the saturation density, binding energy, incompressibility, and symmetry energy of the nuclear matter that are used as inputs of our model in section 3.2. In last two sections, we will discuss the results of our model.

3.1 Thermodynamic potential

In this section, we will focus on calculating the thermodynamic potential of the nuclear matter. In order to take into account the density, we used baryon and isospin chemical potentials in equations (2.20), (2.21), (2.43), and (2.44). Next, we used Matsubara's imaginary time formalism to consider the finite temperature system [1].

We calculated the thermodynamic potential based on the mean-field approximation for scalar and vector meson fields. Here, we have assumed that the meson fields have no position dependence. The thermodynamic potential is expressed as a function of the four meson fields in our model, σ, π, ω, and ρ. However, we have also assumed that there are no neutral and charged pion condensations because they are too complicated to investigate in this study [2]. The assumption that meson condensations are homogeneous in the space allows us to ignore the space components of the vector mean fields. In addition, the time components of $\rho^{1,2}$ must be zero when the vacuum is isosymmetric. We have summarized these assumptions for the mean fields below.

$$\pi^{1,2,3} = 0, \quad \rho_i^{1,2,3} = 0, \quad \omega_i = 0, \quad \rho_0^{1,2} = 0. \tag{3.1}$$

It may be noted that time components of vector mesons ω_0 and ρ_0^3 can have finite VEV.

Based on the above assumptions, the thermodynamic potential at temperature T is given as

$$\begin{aligned}\frac{\Omega}{V} = &-2T \sum_{\substack{\alpha=+,-\\ i=p,n}} \int \frac{d^3p}{(2\pi)^3} \left\{\ln\left(1 - n_{\alpha i}\right) + \ln\left(1 - \bar{n}_{\alpha i}\right)\right\} \\ &- \frac{1}{2} m_\omega^2 \omega_0^2 - \frac{1}{2} m_\rho^2 \tilde{\rho}_0^2 - \frac{1}{2} \bar{\mu}^2 \sigma_0^2 + \frac{1}{4} \lambda \sigma_0^4 - \bar{m} \epsilon \sigma_0 - \frac{1}{6} \lambda_6 \sigma_0^6. \end{aligned} \tag{3.2}$$

[1] This method is explained in appendix H.

[2] A meson condensation changes the vacuum structure. Although this is an interesting subject, we have not considered it in this thesis.

Here, we have defined $\tilde{\rho}_0$ as given below. The value is used later in the study:

$$\tilde{\rho}_0 \equiv \rho_0^3 - \frac{\mu_I}{g_\rho}. \tag{3.3}$$

This redefinition corresponds to the translation of the saturation point and it does not affect the following discussion.

The Matsubara formalism introduces the Fermi-Dirac distribution function naturally as:

$$\begin{aligned} n_{\pm p} &= \frac{1}{1+e^{(E_\pm - \bar{\mu}_B - \frac{\bar{\mu}_I}{2})/T}}, \quad n_{\pm n} = \frac{1}{1+e^{(E_\pm - \bar{\mu}_B + \frac{\bar{\mu}_I}{2})/T}} \\ \bar{n}_{\pm p} &= \frac{1}{1+e^{(E_\pm + \bar{\mu}_B + \frac{\bar{\mu}_I}{2})/T}}, \quad \bar{n}_{\pm n} = \frac{1}{1+e^{(E_\pm + \bar{\mu}_B - \frac{\bar{\mu}_I}{2})/T}}. \end{aligned} \tag{3.4}$$

$n_{\pm p,(n)}$ corresponds to the proton (neutron) distribution functions of the positive or negative parity nucleons and $\bar{n}_{\pm p,(n)}$ are for anti-particles. We note that the mass difference of protons and neutrons depends only on the effective isospin chemical potential defined below in our model. Other variables used in this thesis are defined as

$$E_\pm = \sqrt{p^2 + m_\pm^2} \tag{3.5}$$

$$\bar{\mu}_B = \mu_B - g_{\omega NN}\omega_0, \tag{3.6}$$

$$\bar{\mu}_I = \mu_I - g_{\rho NN}\tilde{\rho}_0. \tag{3.7}$$

Equations (3.6) and (3.7) correspond to the effective chemical potentials in the nuclear matter.

The physical state is determined by the stationary point of the thermodynamic potential, which corresponds to the principle of least action. Therefore, we obtain the following three-gap equations from the thermodynamic potential.

$$\begin{aligned} \frac{\partial\Omega}{\partial\sigma_0} = 2\sum_{i=\pm}\int \frac{d^3p}{(2\pi)^3}\frac{m_i}{\omega_i}\frac{\partial m_i}{\partial\sigma_0}(n_{ip} + \bar{n}_{ip} + n_{in} + \bar{n}_{in}) \\ - \bar{\mu}^2\sigma_0 + \lambda\sigma_0^3 - \lambda_6\sigma_0^5 - \bar{m}\epsilon \end{aligned} \tag{3.8}$$

$$\frac{\partial\Omega}{\partial\omega_0} = 2g_{\omega NN}\sum_{i=\pm}\int \frac{d^3p}{(2\pi)^3}(n_{ip} - \bar{n}_{ip} + n_{in} - \bar{n}_{in}) - m_\omega^2\omega_0 \tag{3.9}$$

$$\frac{\partial\Omega}{\partial\tilde{\rho}_0} = g_{\rho NN}\sum_{i=\pm}\int \frac{d^3p}{(2\pi)^3}(n_{ip} - \bar{n}_{ip} - n_{in} + \bar{n}_{in}) - m_\rho^2\tilde{\rho}_0. \tag{3.10}$$

Baryon number density ρ_B and isospin density ρ_I are defined as

$$\frac{\partial\Omega}{\partial\mu_B} \equiv \rho_B = 2\sum_{i=\pm}\int \frac{d^3p}{(2\pi)^3}(n_{ip} - \bar{n}_{ip} + n_{in} - \bar{n}_{in}) \tag{3.11}$$

$$\frac{\partial\Omega}{\partial\mu_I} \equiv \rho_I = \sum_{i=\pm}\int \frac{d^3p}{(2\pi)^3}(n_{ip} - \bar{n}_{ip} - n_{in} + \bar{n}_{in}). \tag{3.12}$$

Based on principles of thermodynamics, the relations between the thermodynamic potential and other quantities are

$$p = -\frac{\Omega}{V}, \tag{3.13}$$

$$\varepsilon = -p + Ts + \mu_B\rho_B + \mu_I\rho_I, \tag{3.14}$$

where p, ε, and s correspond to the pressure, energy density, and entropy density respectively.

When $T = 0$, we can perform integrals on thermodynamic potential, gap equations, and densities easily because the distribution functions can be transformed into step functions.

3.2 Parameter determination

In this section, we will discuss the determination of the parameters used in our model.

Our model has 14 parameters[3]. We would like to specify that the value of gauge couplings g_ω and g_ρ is not covered within the current analysis and we have omitted the determination of their values. In addition, we will mainly investigate the m_0 dependence of liquid-gas, chiral phase transition, slope parameter, and spin-orbit force discussed in later sections. The remaining eleven parameters are determined using data pertaining to vacuum and cold nuclear matter at saturation density.

The vacuum data includes particle masses and pion decay constant. When we choose a nucleon as a parity plus particle, we are allowed to choose a negative parity partner. In this analysis, we will use N(1535) as the parity partner of nucleon. Our inputs at vacuum are summarized in table 3.1.

The four values: saturation density, binding energy, incompressibility, and symmetry energy, are used as inputs in our model and these are used to determine the previously mentioned parameters. By definition, the nuclear matter is infinite and composed of nucleons bound by nuclear force. There are no electromagnetic forces and surface tension on the nucleus. However, properties of nuclear matter are estimated from experimental data.

The binding energy of nuclear matter is obtained by adding (or subtracting) energy of one nucleon to (from) the nuclear matter. Here, we have used $E_{\rm bind} = -16$ MeV[4]. Strictly speaking, the thermodynamic potential depends on (T, V, μ_B, μ_I) and we need to consider the chemical potentials as inputs. Therefore, we have set $\mu_B = 923$ MeV and $\mu_I = 0$ MeV as external conditions of the system.

The density of the nucleus has been determined and it was found to be nearly same for various nuclei. This characteristic is called the saturation of nuclei density. We use $\rho_0 = 0.16$ fm^{-3} as the saturation density in our model.

We have summarized these conditions in equation (3.15) and (3.16).

$$E_{bind} \equiv \frac{E}{A} - m_N = \left.\frac{\varepsilon}{\rho}\right|_{\mu_B=923[\mathrm{MeV}]} = -16 \text{ MeV} \tag{3.15}$$

$$\rho_0 \equiv \rho_B|_{\mu_B=923[\mathrm{MeV}]} = 0.16 \text{ fm}^{-3}. \tag{3.16}$$

The nuclear incompressibility, which is given by the curvature of binding energy at saturation density, corresponds to the "hardness" of the matter. We observed the nuclear matter through a giant-monopole resonance (GMR) experiment to detect its incompressibility. In the GMR experiment, we applied an oscillating magnetic field to the nuclei and observed its modification. This experiment detects the incompressibility of the nuclear matter and distinguishes it from "pseudo" infinite matter [5] and surface tension. With respect to nuclear matter, we consider the infinite matter as an input of incompressibility. The definition of incompressibility is shown below.

$$K = 9\rho_0^2 \left.\frac{d^2(E/A)}{d\rho^2}\right|_{\rho_0} = 9\rho_0^2 \left.\frac{d^2(\varepsilon/\rho)}{d\rho^2}\right|_{\rho_0} = 9\rho_0 \left.\frac{d\mu_B}{d\rho}\right|_{\rho_0} = 240 \text{ MeV}. \tag{3.17}$$

The value of incompressibility has experimental uncertainties. However, we will use $K = 240$ MeV as input in this analysis [37, 38]. In a subsequent section, we will change incompressibility

[3] $g_1, g_2, m_0, g_{\omega NN}, g_{\rho NN}, \bar{\mu}^2, \lambda, \lambda_6, f_\pi, \bar{m}\epsilon, m_\omega, m_\rho, g_\omega, g_\rho$

[4] This value corresponds to the volume term of the semi-empirical mass formula (Bethe-Weizäcker mass formula).

[5] Some articles mention it as K_∞..

within the error to investigate the extent to which it affects the slope parameter and spin-orbit interaction.

Light stable-nuclei tend to have the same number of protons and neutrons and the difference in their numbers generates energy, causing the nuclei to become unstable. The symmetry energy gives the energy difference between symmetric nuclear matter[6] and pure neutron matter. The definition of symmetry energy is shown below and we used 31 MeV as the symmetry energy [39].

$$E_{sym}(\rho_0) = \frac{1}{2!}\frac{\partial^2(E/A)}{\partial\delta^2}\bigg|_{\delta=0} = \frac{1}{2!}\frac{\partial^2(\epsilon/\rho)}{\partial\delta^2}\bigg|_{\delta=0} = 31 \text{ MeV}. \tag{3.18}$$

Here, we have defined the asymmetry parameter δ as

$$\delta \equiv \frac{\rho_p - \rho_n}{\rho_B} = \frac{2\rho_I}{\rho_B}. \tag{3.19}$$

It may be noted that the incompressibility and symmetry energy are expansion coefficients of E/A with respect to baryon density ρ_B and asymmetric parameter δ. These values are important to predict the E/A information at high density and/or asymmetricity in the vicinity of saturation density. Although there are many uncertainties, the higher order coefficients are also considered in some articles and studies (e.g. [40]).

There are other properties of nuclear matter as well that are considered such as first-, second- or more derivatives of symmetry energy with respect to baryon density at saturation density. The first derivative of symmetry energy is a "slope parameter" and it is introduced in the next section. The analyses of these coefficients are important to understand the high-density and/or highly asymmetric environment using data pertaining to normal nuclear matter.

The model parameters for a given m_0 and fixed parameters are listed in table 3.1. Table 3.1 also contains the parameters determined from $m_0 = 500$ MeV to $m_0 = 900$ MeV with 100 MeV interval.

Table 3.1: Model parameters for each m_0 are shown below. In order to determine them, we used cold nuclear matter properties (binding energy, saturation density, incompressibility, and symmetry energy) along with these values used as inputs at vacuum: $f_\pi = 92.3$ MeV, $m_\omega = 140$ MeV, $m_\omega = 783$ MeV, $m_\rho = 775$ MeV, $m_N = 939$ MeV and $m_{N^*} = 1535$ MeV. The chiral invariant mass m_0 is given by hand with 100 MeV intervall.

m_0 [MeV]	500	600	700	800	900
g_1	9.03	8.49	7.82	7.00	5.97
g_2	15.5	15.0	14.3	13.5	12.4
$g_{\omega NN}$	6.75	6.60	6.22	5.34	3.49
$g_{\rho NN}$	8.19	8.20	8.24	8.32	8.43
$\bar{\mu}^2/f_\pi^2$	73.5	50.7	30.8	14.9	1.74
λ	1.39×10^2	95.9	58.8	29.4	5.00
$\lambda_6 \cdot f_\pi^2$	62.9	42.9	25.7	12.2	0.952
m_σ [MeV]	489.4	437.3	381.0	322.3	268.8

[6]The number of protons and neutrons are the same.

We have also listed the mass of scalar fluctuation m_σ in this table for reference. In order to determine this, we divided σ into a vacuum part and a part affected by fluctuation $\tilde{\sigma}$ as

$$\sigma = f_\pi + \tilde{\sigma} \tag{3.20}$$

and the mass m_σ is given by

$$m_\sigma = \sqrt{-\bar{\mu}^2 + 3\lambda f_\pi^2 - 5\lambda_6 f_\pi^4}. \tag{3.21}$$

m_σ corresponds to the mass of scalar fluctuation and we can identify it as a scalar mode.

3.3 EoS and order parameter

We will demonstrate the EoS and other quantities of our model constructed in the previous sections. We have used chiral invariant masses of 900 MeV and 500 MeV as typical examples from the various choices for chiral invariant mass available to us.

Figure 3.1 shows the binding energies of symmetric nuclear matter and pure neutron matter. The red line corresponds to symmetric nuclear matter and the black line to pure neutron matter.

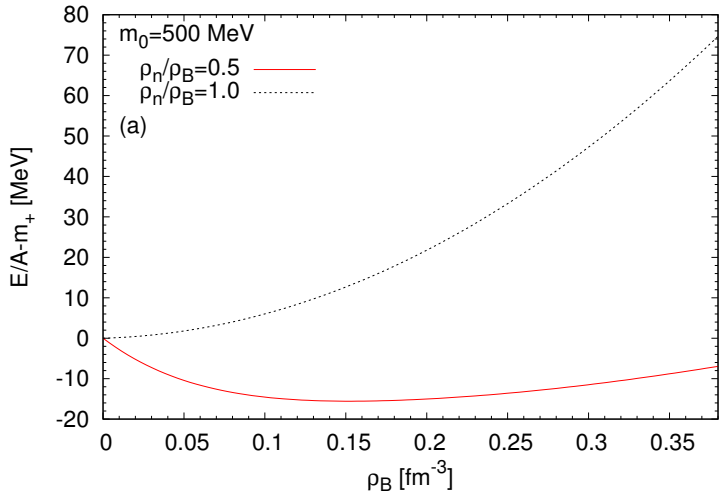

Figure 3.1: Binding energy of symmetric nuclear matter and pure neutron matter

In this figure, we used a ratio of neutron to total baryon, ρ_n/ρ_B, equal to 0.5 for nuclear matter and 1.0 for neutron matter. In order to avoid pion condensation, we restricted the isospin chemical potential within $|\mu_I| < m_\pi$. The red line has a minimum value of -16 MeV at $\rho_B = 0.16$ fm^{-3}. This shows that the binding energy at saturation density has been correctly reproduced in this analysis. In addition, the incompressibility is given by the curvature of the red line as it approaches saturation density and the symmetry energy by the energy difference between the red line and black line at saturation density.

We have also plotted the variation in pressure in the nuclear matter with $\rho_n/\rho_B = 0.5$ and 1.0 in the figure 3.2. This figure shows that we get a negative value of pressure at a certain ρ_n/ρ_B. We note that this negative pressure region is an unstable state where nuclear "gas" and "liquid" states coexist. The important fact here is that this negative pressure region is generated from the coexistence of gaseous and liquid phases. We will analyze this phase of coexistence and the phase transition using the order parameter. Figure 3.2 also shows that

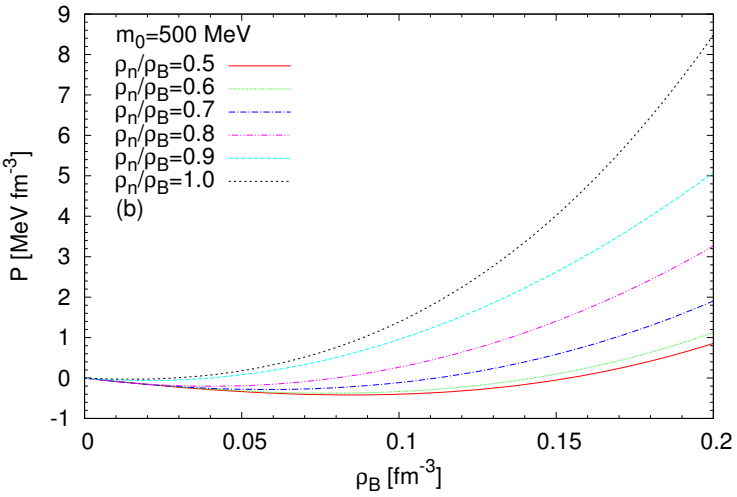

Figure 3.2: Pressure and density relation of nuclear matter and pure neutron matter

the pressure of the system increase monotonically when the asymmetry becomes large. This implies that the coexistence phase tends to disappear with increasing asymmetry. The EoS of asymmetric matter is discussed in molecular dynamics [41] and many-body perturbation [42]. The pressure observed in our model (figure 3.2) shows similar behavior with [41, 42]. For example, there are negative pressure regions below saturation density in the symmetric nuclear matter and pressure is always a positive and monotonically increasing function in the pure neutron matter.

Before we discuss order parameters, we will briefly cover the other characteristics of nuclear matter. As we mentioned in the previous section, there are few expansion coefficients of 1-particle energy and symmetry energy [40] and they were observed experimentally. We have analyzed one of the most important parameters called the slope parameter as an output of this model. It was studied by experiment and the allowed region was shown in[43].

The slope parameter, L, is defined as a gradient of symmetry energy with respect to baryon density at saturation density as,

$$L = 3\rho_0 \left. \frac{dE_{sym}(\rho_B)}{d\rho_B} \right|_{\rho_B=\rho_0} . \tag{3.22}$$

Figure 3.3 shows the predicted values of the slope parameter. The center values of the figure 3.3 correspond to $K = 240$ MeV.

In order to investigate the K dependence of the slope parameter, we varied the incompressibility from $K = 220$ MeV to $K = 260$ MeV. We observed that the upper values are obtained from $K = 260$ MeV and lower values are obtained from $K = 220$ MeV.

We found that a heavier m_0 corresponds to a relatively smaller L in the figure 3.3, which indicates that the slope parameter depends marginally on the chiral invariant mass and incompressibility. The constraint for the value of L is obtained from experiments such as the heavy ion collision experiment, neutron skin thickness of Sn isotopes, and giant monopole resonance [39, 43]. Our value of the slope parameter is partly consistent with the above experiments because the experimental value of the slope parameter has uncertainty depending on the method of the experiment.

There are two order parameters in our model, which are vacuum expectation value of scalar σ_0 and baryon number density ρ_B. Figure 3.4 shows the dependence of σ_0 on the baryon

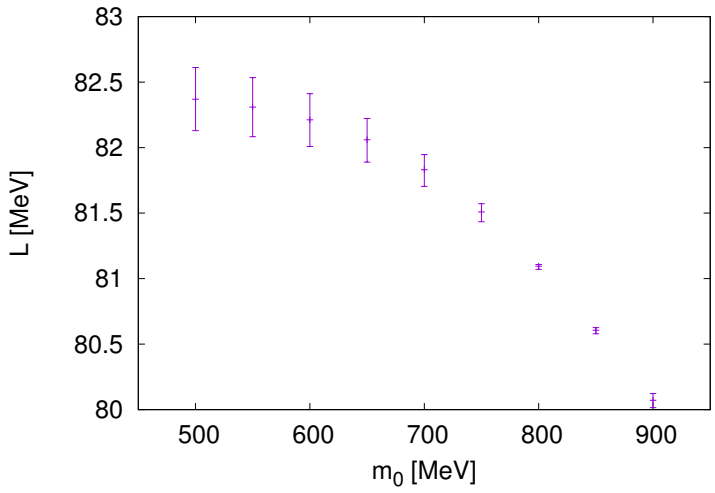

Figure 3.3: Slope parameter L as function of m_0: a heavier m_0 corresponds to a smaller L.

chemical potential μ_B for $m_0 = 500$ MeV. The symmetric nuclear matter is represented by

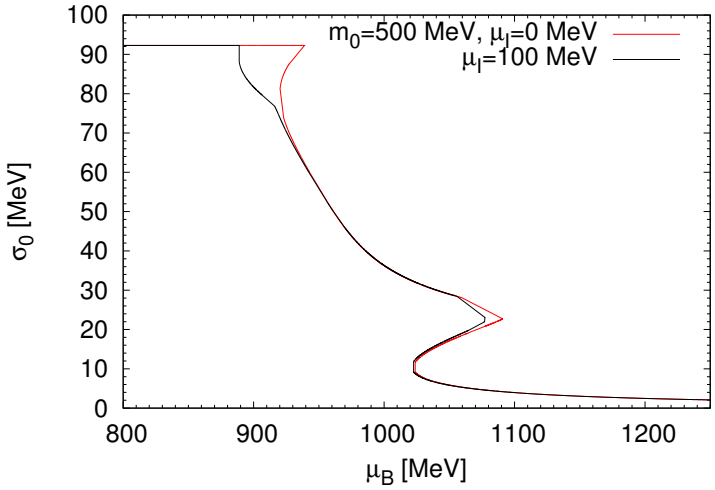

Figure 3.4: Sigma distribution: $m_0 = 500$ MeV case

the red line and the pure neutron matter by the black line. σ_0 decreases rapidly as the graph approaches $\mu_B = 920$ MeV and $\mu_B = 1050$ MeV in the figure 3.4. We conclude that the second drop corresponds to the chiral phase transition. This is because σ_0 is an order parameter of the chiral phase transition and it approaches zero. However, in this analysis, the current quark mass breaks the chiral symmetry and it prevent σ_0 from going to zero.

In order to investigate the first drop, we plot the dependence of the baryon number density of this system on μ_B in the figure 3.5. The red line corresponds to the symmetric nuclear matter and the black line corresponds to the asymmetric matter ($\mu_I = 100$ MeV). These lines show that the baryon density appears abruptly near $\mu_B = 900$ MeV, which is an evidence of liquid-gas phase transition. We determined the order of the transition from the dependence of the density on μ_B. We concluded that the liquid-gas phase transition in symmetric nuclear matter is of first-order and there is a coexisting phase of liquid and gas. The coexisting phase

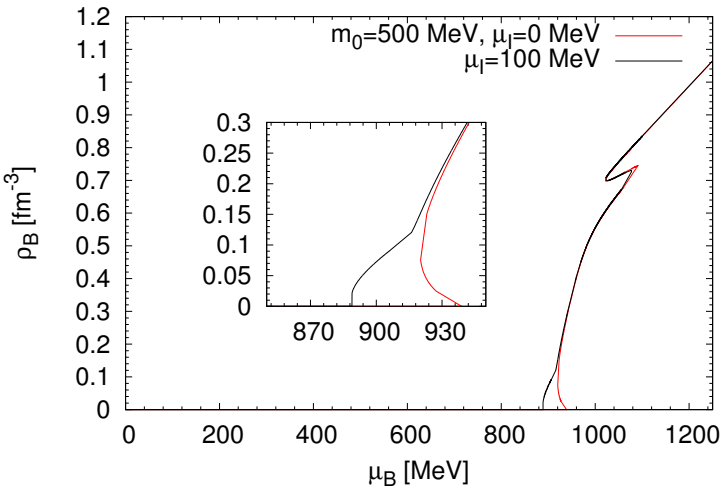

Figure 3.5: Density distribution at $m_0 = 500$ MeV: We can see the density behavior near the liquid-gas and chiral phase transition

was investigated experimentally and its existence was proved in [44]. Our result is consistent with this study. This coexistence phase disappears when μ_I is increased, and the liquid-gas phase transition becomes second order as suggested in [7]. Our result supports this result and prediction.

The density dependence of nucleon masses is plotted in figure 3.6. The red and black curves

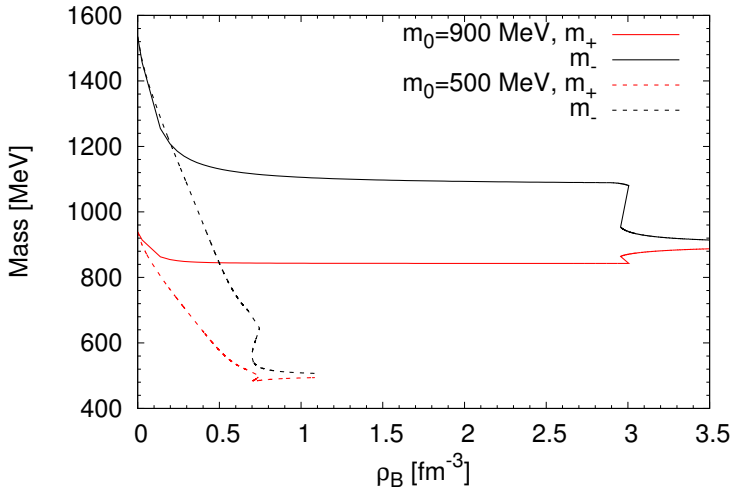

Figure 3.6: Behavior of effective masses at $m_0 = 500$ and 900 MeV:

show the effective masses of nucleons with positive and negative parity, respectively. The solid lines correspond to $m_0 = 900$ MeV and the dotted lines correspond to $m_0 = 500$ MeV. We note that σ_0 becomes zero faster at $m_0 = 500$ MeV than at $m_0 = 900$ MeV. The plot for $m_0 = 500$ MeV ends at $\rho_B \sim 1$ fm^{-3}.

As ρ_B increases, these masses approach zero and finally degenerate to m_0. This is a feature of the parity doublet structure. The critical density of chiral phase transition depends on the

value of the chiral invariant mass m_0[7]. A larger value of m_0 tends to require higher density for the chiral transition. For example, in the case of $m_0 = 500$ MeV, the transition occurs around $\rho_B = 0.7$ fm^{-3}. On the other hand, in the case of $m_0 = 900$ MeV, it occurs around $\rho_B = 2.5$ fm^{-3}.

Our model is an effective model and does not include a detailed discussion of the chiral phase transition. However, it may be noted that the effective masses above the saturation density depend on m_0. This suggests that we may obtain the value of m_0 from observation of the effective masses of nucleon.

Before moving to the next section, we consider the pion decay constant, f_π, in the medium. In this analysis, σ_0 corresponds to the f_π of the medium and figure 3.7 shows the density dependence of σ_0 in the vicinity of the saturation density. The black line corresponds to

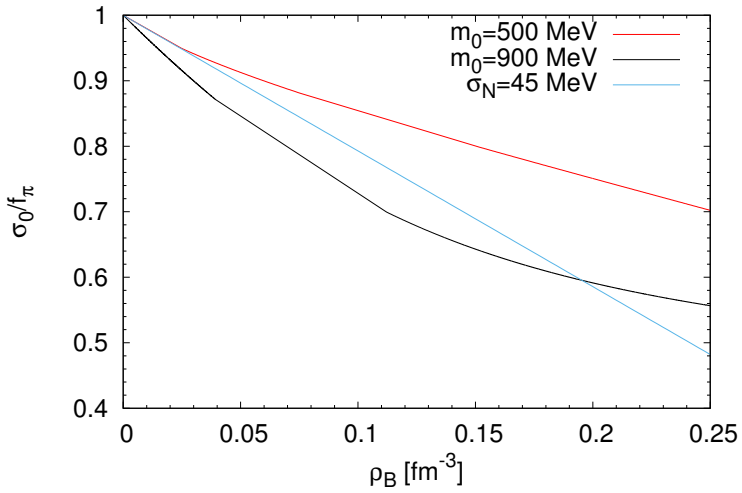

Figure 3.7: Density dependence of σ_0 and theoretical calculation using parameter $\sigma_N = 45$ MeV

$m_0 = 500$ MeV and the red line corresponds to $m_0 = 900$ MeV. When we choose a lighter m_0, the pion decay-constant in the medium, $f_\pi^*(= \sigma_0(\rho_B))$, becomes larger. f_π^* in the vicinity of ρ_0 is estimated from experiments and the observed value is $(f_\pi^*(\rho_0)/f_\pi) \sim 0.8$ [45]. Therefore, we conclude that at $m_0 = 500$ MeV is preferred experimentally [45].

We also determined the density dependence of the chiral condensate, $\frac{\langle\bar{q}q\rangle(\rho_B)}{\langle\bar{q}q\rangle_{\text{vac.}}}$, on low-density expansion. In this model, the density dependence is written as

$$\frac{\langle\bar{q}q\rangle(\rho_B)}{\langle\bar{q}q\rangle_{\text{vac.}}} = \frac{\sigma_0(\rho_B)}{f_\pi} = 1 - \frac{\sigma_N}{m_\pi^2 f_\pi^2}\rho_B. \tag{3.23}$$

This formula is model independent [46]. The parameter σ_N is called "sigma term" and its accepted value is $\sigma_N = 45$ MeV. Because the equation (3.23) is valid near the low-density region, the slope near $\mu_B \sim 0$ is important. From this point of view, the result for $m_0 = 500$ MeV will reproduce the theoretical slope near $\rho_B \sim 0$ fm^{-3}. Our results indicate that $m_0 = 500$ MeV reproduces experimental data [45] and coincides with the theoretical prediction [46].

[7]The liquid-gas phase transition does not depend on m_0.

3.4 Phase diagram

In this section, we will explore the phase structure of our model in finite temperature and density with isospin asymmetry. We investigated not only the asymmetry (μ_I) but also temperature dependence of the liquid-gas and chiral phase transition structures in our study. These phase structures were investigated using $m_0 = 500$ MeV and $m_0 = 900$ MeV. We would like to discuss the characteristics of the phase structure for each m_0.

The value of μ_I affects the particles that have isospin charge. When μ_I exceeds the mass of isospin-charged particles, these particles are usually condensed. Therefore, charged pion, which is the lightest particle having isospin charge, is the first to condense in the vacuum [47, 48] when we take μ_I into account. The pion condensation is an interesting phenomenon. However, we do not consider it in this study and so we restrict our investigation to $|\mu_I| < m_\pi$. It may be noted that this is a same situation with a lattice simulation[20], which suggests the existence of a chiral invariant mass.

Figure 3.8 shows the phase diagram at $m_0 = 900$ MeV and $\mu_I = 0$ MeV case. Each line

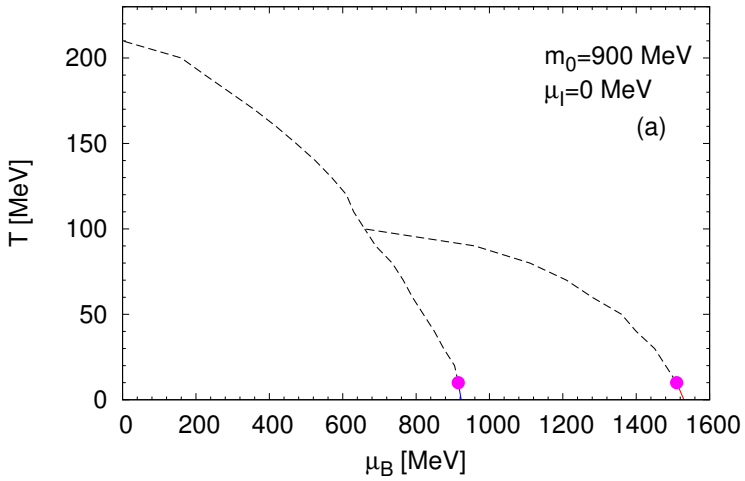

Figure 3.8: Phase diagram at $m_0 = 900$ MeV and $\mu_I = 0$ MeV: refer text for detailed explanation.

represents the phase transition and the order of transition is determined from the behavior of the order parameters. The dashed line corresponds to the crossover phase transition and the solid line corresponds to the first-order phase transition. The blue one represent the liquid-gas phase transition and the red one the chiral phase transition. The magenta dots represent the second order critical point. This diagram is drawn from the behavior of the order parameters[8], σ_0 and ρ_B. We note that the crossover phase transition is defined by a local maximum of susceptibility derived from the order parameters.

The vertical line from $\mu_B = 923$ MeV represents the liquid-gas phase transition. At zero temperature, it is a first-order phase transition and corresponds to $\rho_B = 0.16$ fm^{-3}. As the temperature rises, this phase transition occurs "earlier" in terms of μ_B[9] and the order changes to second and crossover occurs gradually. The critical point where the first-order transition changes to the second-order is $(\mu_B, T) =$(MeV, MeV).

[8]Figure 3.4 and 3.5 show the behavior of the order parameters at zero temperature.

[9]The words earlier and later are often used to explain the phase transition

A line from $\mu_B \sim 1500$ corresponds to the chiral phase transition. This transition is also a first-order transition, which changes to the second order and undergoes crossover. In addition, the first-order transition continues at a higher temperature than the liquid-gas phase transition. The corresponding density of chiral phase transition at $T = 0$ MeV is $\sim 18\rho_0$, which is a very high density[10].

These two phase transitions seem to meet near $(\mu_B, T) = (700 \text{ MeV}, 100 \text{ MeV})$ because we could not distinguish the two local maximums of susceptibility. This is a feature of parity doublet model and similar phase diagrams are drawn in [28].

Isospin asymmetry hardly changes the chiral phase transition temperature and density (μ_B). However, μ_I mainly affects the liquid-gas phase transition, which changes to second-order as shown in the figure 3.9. The black line shows the combined phase transition of first order.

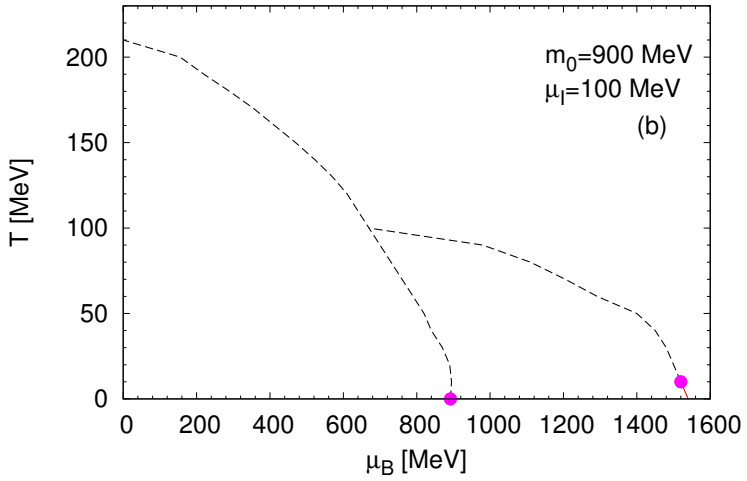

Figure 3.9: Phase diagram at $m_0 = 900$ MeV and $\mu_I = 100$ MeV

Our analysis is based on an effective model because of which we could not discuss the chiral phase transition precisely. The critical point of the liquid-gas phase transition can be observed at (μ_B, T) =(892 MeV, 0 MeV). Our result that asymmetry affects the chiral phase transition marginally is opposed to the lattice QCD result [49] in which it is suggested that the transition temperature is changed by μ_I. However, calculating the finite density region using lattice QCD is difficult[11] and we could not compare our result with [49].

Next, we will discuss the characteristics for $m_0 = 500$ MeV and $\mu_I = 0$ MeV given in the figure 3.10. The situation is different from the case of $m_0 = 900$ MeV except for the order of the liquid-gas phase transition. The chiral phase transition occurs at $\mu_B \sim 1050$ MeV and it corresponds to $4\rho_0$. Therefore, the chiral phase transition occurs "earlier" when m_0 becomes lighter. The value, $4\rho_0$, may exist in a neutron star. We also realize that the order of transition is different from that for $m_0 = 900$ MeV. σ_0 still drops suddenly when T is increased. At this point, the crossover transition of liquid-gas is absorbed into the first-order transition.

Finally, we discuss the characteristics for $m_0 = 500$ MeV and $\mu_I = 100$ MeV shown in figure 3.11. Asymmetric tendency is not different from the case of $m_0 = 900$ MeV: μ_I changes the order of the liquid-gas phase transition from second to first. However, the chiral phase transition is affected only marginally.

[10]The central density of the neutron star is estimated to be approximately $10\rho_0$.

[11]This is the "sign problem" of lattice QCD.

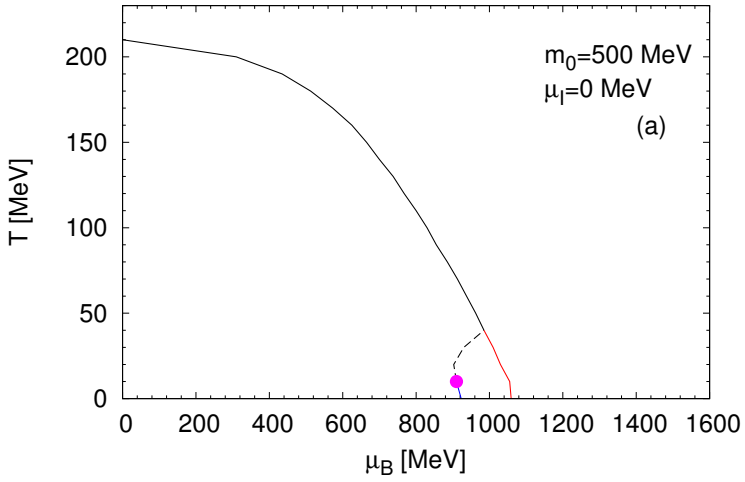

Figure 3.10: Hadron kun $m_0 = 500$ MeV and $\mu_I = 0$ MeV

Therefore, we can conclude that the main differences between $m_0 = 500$ MeV and $m_0 = 900$ MeV is the critical density of chiral symmetry. In addition, μ_I mainly affects the liquid-gas phase transition and the transition-order is second at $\mu_I = 100$ MeV for both m_0. The order of the chiral phase transition is changed and the transition-order after coalescence is different. However, this study is based on the effective model of hadron and the existence of hadron as a particle after chiral restoration is discussed.

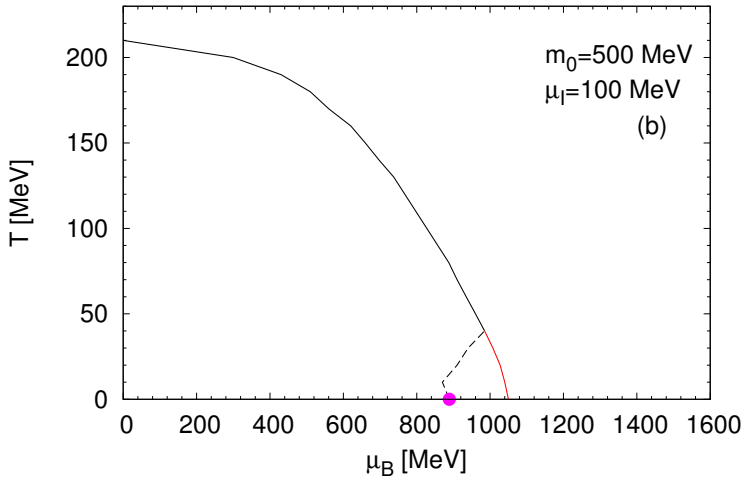

Figure 3.11: Hadron kun $m_0 = 500$ MeV and $\mu_I = 100$ MeV

Chapter 4

Finite-size nuclear matter

In chapter 2, we constructed a model describing the nuclear matter based on the parity doublet structure and showed that the binding energy, saturation density, incompressibility, and symmetry energy of nuclear matter and the predicted slope parameter are reproduced using the chiral invariant mass m_0 in the range from 500 to 900 MeV.

A question that arises is "Can our model make a finite-size nuclear matter?" In order to answer this question, we investigated the spin-orbit potential in our model. We followed the analysis described in [34], where a spin-orbit force of the Walecka model is investigated.

In section 4.1, we explain our analysis of finite-size nuclear matter. In section 4.2, we demonstrate the results for the spin-orbit potential of our model.

4.1 Finite-size model

Unlike the nuclear matter, the finite matter has position dependence. We analyzed our model using mean-field approximation with position dependence. We also applied the Thomas-Fermi approximation to our model.

In this situation, our effective Lagrangian is written as[1]

$$\begin{aligned}\mathcal{L} =&\bar{N}_+(i\partial\!\!\!/ - m_+(r))N_+ + \bar{N}_-(i\partial\!\!\!/ - m_-(r))N_- \\ &- g_{\omega NN}\left(\bar{N}_+\gamma^0\omega_0(r)N_+ + \bar{N}_-\gamma^0\omega_0(r)N_-\right) \\ &- g_{\rho NN}\left(\bar{N}_+\gamma^0\tilde{\rho}_0(r)T^3N_+ + \bar{N}_-\gamma^0\tilde{\rho}_0(r)T^3N_-\right) \\ &- \frac{1}{2}(\nabla\sigma_0(r))^2 + \frac{1}{2}\bar{\mu}^2\sigma_0(r)^2 - \frac{1}{4}\lambda\sigma_0(r)^4 + \frac{1}{6}\lambda_6\sigma_0(r)^6 + \bar{m}\epsilon\sigma_0(r) \\ &+ \frac{1}{2}(\nabla\omega_0(r))^2 + \frac{1}{2}m_\omega^2\omega_0(r)^2 + \frac{1}{2}(\nabla\tilde{\rho}_0(r))^2 + \frac{1}{2}m_\rho^2\tilde{\rho}_0(r)^2. \end{aligned} \tag{4.1}$$

The gradient of the meson fields are added to the Lagrangian of nuclear matter and the meson fields have radius dependence with the argument r. We have used the same parameters as those listed in table 3.1. It may be noted that the masses of nucleons depend on the radius via $\sigma_0(r)$.

$$m_\pm[\sigma_0(r)] = \frac{1}{2}\left[\sqrt{(g_1+g_2)^2\sigma_0(r)^2 + 4m_0^2} \pm (g_1-g_2)\sigma_0(r)\right]. \tag{4.2}$$

Here, we omitted r from $\sigma_0(r)$, $\omega_0(r)$, and $\tilde{\rho}_0(r)$. The equations of motion for σ_0, ω_0, and

[1] We have omitted the time component from the vector fields, $\omega_{00} \to \omega_0$ and $\rho^3_{00} \to \rho^3_0$.

$\tilde{\rho}_0$ in the Thomas-Fermi approximation are derived using the above Lagrangian as

$$\left(\nabla^2 + \bar{\mu}^2\right)\sigma_0 = \lambda\sigma^3 - \lambda_6\sigma_0^5 - \bar{m}\epsilon + \frac{\partial m_+}{\partial\sigma_0}\rho_{\mathrm{S}+}(r) + \frac{\partial m_-}{\partial\sigma_0}\rho_{\mathrm{S}-}(r), \tag{4.3}$$

$$\left(\nabla^2 - m_\omega^2\right)\omega_0 = -\,g_\omega\left[\rho_{\mathrm{B}+}(r) + \rho_{\mathrm{B}-}(r)\right], \tag{4.4}$$

$$\left(\nabla^2 - m_\rho^2\right)\tilde{\rho}_0 = -\,g_\rho\left[\rho_{\mathrm{I}+}(r) + \rho_{\mathrm{I}-}(r)\right], \tag{4.5}$$

where the scalar densities $\rho_{\mathrm{S}\pm}(r)$, baryon densities $\rho_{\mathrm{B}\pm}(r)$, and isospin densities $\rho_{\mathrm{I}\pm}(r)$ are defined as

$$\begin{aligned}\rho_{\mathrm{S}\pm} =& \langle\bar{N}_\pm N_\pm\rangle = \frac{2}{(2\pi)^3}\left(\int_0^{p_{f\pm}^{\mathrm{p}}} d^3p\frac{m_\pm}{\sqrt{p^2+m_\pm^2}} + \int_0^{p_{f\pm}^{\mathrm{n}}} d^3p\frac{m_\pm}{\sqrt{p^2+m_\pm^2}}\right)\\ =&\frac{1}{2\pi^2}m_+\left[p_{f\pm}^{\mathrm{p}}\sqrt{{p_{f\pm}^{\mathrm{p}}}^2+m_\pm^2} - m_\pm^2\ln\left(\frac{p_{f\pm}^{\mathrm{p}}+\sqrt{{p_{f\pm}^{\mathrm{p}}}^2+m_\pm^2}}{m_\pm}\right)\right] + [\mathrm{p}\to\mathrm{n}],\end{aligned} \tag{4.6}$$

$$\begin{aligned}\rho_{\mathrm{B}\pm} =& \langle N_\pm^\dagger N_\pm\rangle = \frac{2}{(2\pi)^3}\left(\int_0^{p_{f\pm}^{\mathrm{p}}} d^3p + \int_0^{p_{f\pm}^{\mathrm{n}}} d^3p\right)\\ =&\frac{1}{3\pi^2}{p_{f\pm}^{\mathrm{p}}}^3 + \frac{1}{3\pi^2}{p_{f\pm}^{\mathrm{n}}}^3,\end{aligned} \tag{4.7}$$

$$\begin{aligned}\rho_{\mathrm{I}\pm} =& \langle N_\pm^\dagger T^3 N_\pm\rangle = \frac{1}{(2\pi)^3}\left(\int_0^{p_{f\pm}^{\mathrm{p}}} d^3p - \int_0^{p_{f\pm}^{\mathrm{n}}} d^3p\right)\\ =&\frac{1}{6\pi^2}{p_{f\pm}^{\mathrm{p}}}^3 - \frac{1}{6\pi^2}{p_{f\pm}^{\mathrm{n}}}^3.\end{aligned} \tag{4.8}$$

These densities depend on r through the Fermi momenta $p_{f\pm}^{\mathrm{p,n}}$, which are defined as

$$p_{f\pm}^{\mathrm{p}} = \sqrt{\left[\bar{\mu}_{\mathrm{B}} + \frac{\bar{\mu}_{\mathrm{I}}}{2}\right]^2 - m_+^2}, \tag{4.9}$$

$$p_{f\pm}^{\mathrm{n}} = \sqrt{\left[\bar{\mu}_{\mathrm{B}} - \frac{\bar{\mu}_{\mathrm{I}}}{2}\right]^2 - m_+^2}. \tag{4.10}$$

Now $\bar{\mu}_{\mathrm{B}}$ and $\bar{\mu}_{\mathrm{I}}$ defined in equation (3.6) and (3.7) depend on r through $\omega_0(r)$ and $\tilde{\rho}_0(0)$.

In principle, we can obtain mesons and density distributions by solving (4.6-4.8) under plausible conditions. First, we assigned $r_0 = 6$ fm as the size of nuclear matter. This implies that we have taken the densities into consideration at $r \le r_0$ and we have omitted densities from the equation at $r > r_0$;

$$\rho_{\mathrm{B}\pm} = \rho_{\mathrm{I}\pm} = \rho_{\mathrm{S}\pm} = 0,\ (r > r_0). \tag{4.11}$$

Next, we defined the total number of protons N_{p} and neutrons N_{n}. These give the constraints for the density distribution such as

$$N_{\mathrm{p,n}} = \int_V\int_0^{p_{f+}^{\mathrm{p,n}}} d^3p d^3x. \tag{4.12}$$

In this analysis, we solved these equations by using Green's function method. Then, we assumed the Woods-Saxon density distribution as an initial estimate and we solved these equations

iteratively. Boundary conditions of these equations were chosen as

$$\left.\frac{d\sigma_0}{dr}\right|_{r=0} = 0, \quad \left.\frac{d\omega_0}{dr}\right|_{r=0} = 0, \quad \left.\frac{d\tilde{\rho}_0}{dr}\right|_{r=0} = 0, \tag{4.13}$$

$$\sigma_0|_{r\to\infty} = f_\pi, \quad \omega_0|_{r\to\infty} = 0, \quad \tilde{\rho}_0|_{r\to\infty} = 0. \tag{4.14}$$

We note that σ_0 must coincide with f_π at vacuum in our model.

The total energy of the finite-size nuclear matter E is given as

$$\begin{aligned} E = \int d^3x \Bigg\{ & -\frac{1}{2}\left[(\nabla\omega_0)^2 + m_\omega^2\omega_0^2\right] - \frac{1}{2}\left[(\nabla\tilde{\rho}_0)^2 + m_\rho^2\tilde{\rho}_0^2\right] \\ & + \frac{1}{2}(\nabla\sigma_0)^2 - \frac{1}{2}\bar{\mu}^2\sigma_0^2 + \frac{1}{4}\lambda\sigma_0^4 - \frac{1}{6}\lambda_6\sigma_0^6 - \bar{m}\epsilon\sigma_0 \\ & + g_\omega\omega_0\rho_B + g_\rho\tilde{\rho}_0\rho_I \\ & + \frac{2}{(2\pi)^3}\left[\int_0^{p_{f+}^{\mathrm{p}}} d^3p\sqrt{\boldsymbol{p}^2 + m_+^2} + \int_0^{p_{f+}^{\mathrm{n}}} d^3p\sqrt{\boldsymbol{p}^2 + m_+^2}\right] + [\text{Negative Parity}]\Bigg\}. \end{aligned} \tag{4.15}$$

We can verify equations (4.9) and (4.10) by using Lagrange multipliers. The variation of energy E must be zero in a stable matter. In addition, the total baryon number B and isospin I must be conserved. Therefore, the following equation must be satisfied

$$\delta E - \mu_{\mathrm{B}}\delta B - \mu_{\mathrm{I}}\delta I = 0 \tag{4.16}$$

where μ_{B} and μ_{I} are Lagrange multipliers. From equation (4.16), we obtained these two equations that are same as (4.9) and (4.10):

$$g_\omega\omega_0 + \frac{1}{2}g_\rho\tilde{\rho}_0 + \sqrt{{p_{f+}^p}^2 + m_+^2} = \mu_B + \frac{\mu_I}{2}, \tag{4.17}$$

$$g_\omega\omega_0 - \frac{1}{2}g_\rho\tilde{\rho}_0 + \sqrt{{p_{f+}^n}^2 + m_+^2} = \mu_B - \frac{\mu_I}{2}. \tag{4.18}$$

We omitted the negative parity nucleons from the equations (4.17,4.18) because N^* does not exist in the normal nuclear matter. Actually, figure 3.6 also indicates that N^* does not exist near the saturation density.

4.2 Distributions and spin-orbit interaction

In this section, we discuss the results of finite-size nuclear matter. We chose ^{40}Ca ($N_{\mathrm{p}} = 20$ and $N_{\mathrm{n}} = 20$) for input in this analysis. Because ^{40}Ca is a symmetric nucleus, the ρ meson field does not appear. We also assumed the radius of finite-size nuclear matter as $r_0 = 6$ fm[2] in this analysis. We solved these equations iteratively and the initial estimate of this analysis is the famous Woods-Saxon distribution ([50, 51]). Solving the equation (4.3-4.5) yields the mean fields, densities, and effective mass distributions of the finite matter. It may be noted that we did not consider results that corresponded to the excited state[3]. As a result, we only used results of $m_0 = 700, 800$, and 900 MeV cases.

[2]The radius R of an A (mass number) nucleus is written as

$$R = \bar{r}_0 A^{\frac{1}{3}}, \quad r_0 = 1.1 \sim 1.3\mathrm{fm} \tag{4.19}$$

. This is a popular relation for nucleus radius. This relation is usually given in textbooks such as [**?**].

[3]Smaller m_0 tends to result in an excited state that has one or more intersections with the x-axis.

Our purpose is to obtain the strength of the spin-orbit potential. However, we verified some distributions using radius before investigating the spin-orbit. Mean field distributions are drawn in figure 4.1. We can see that the analysis satisfies the boundary conditions (equation

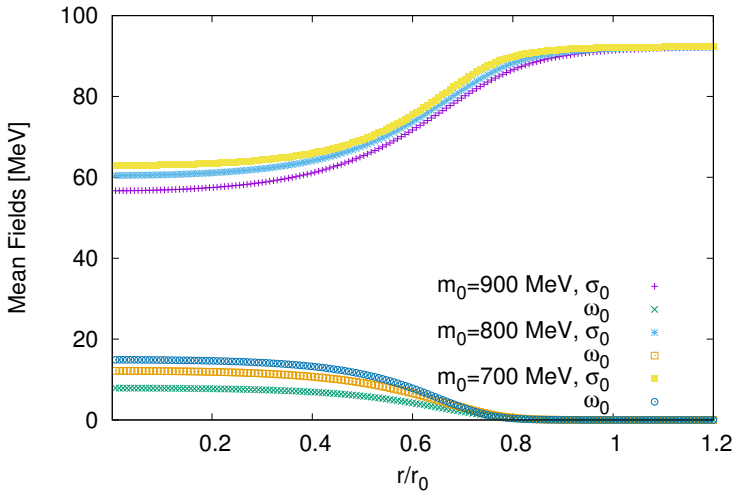

Figure 4.1: Mean fields distributions for each m_0

(4.13) and (4.14)).

Figure 4.2 shows the mass distributions for each m_0. Because the ω field does not affect the

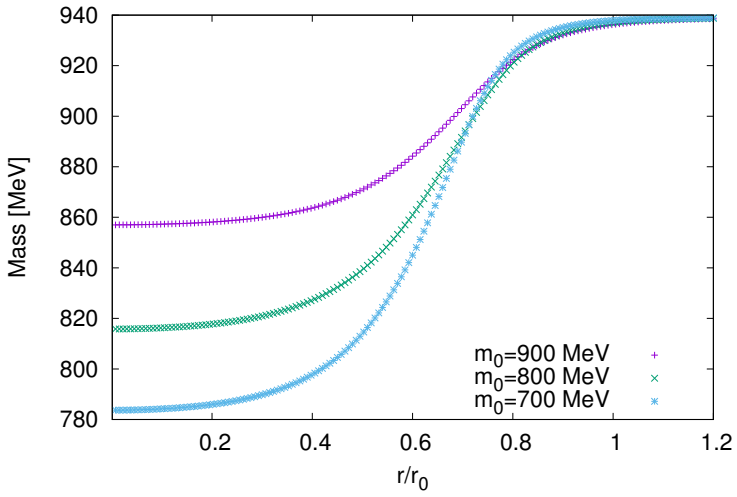

Figure 4.2: Mass distributions

mass distribution (4.2), it is directly affected by σ_0 behavior.

Figure 4.3 shows the density distributions of finite-size nuclear matter. The central density seems to be higher than ρ_0. However, we restricted the nuclear matter within a finite size and used naive approximation (Thomas-Fermi approximation). As a result, it is possible that the central density was changed from ρ_0.

Finally, we will discuss the spin-orbit interaction. The strength of the spin-orbit potential

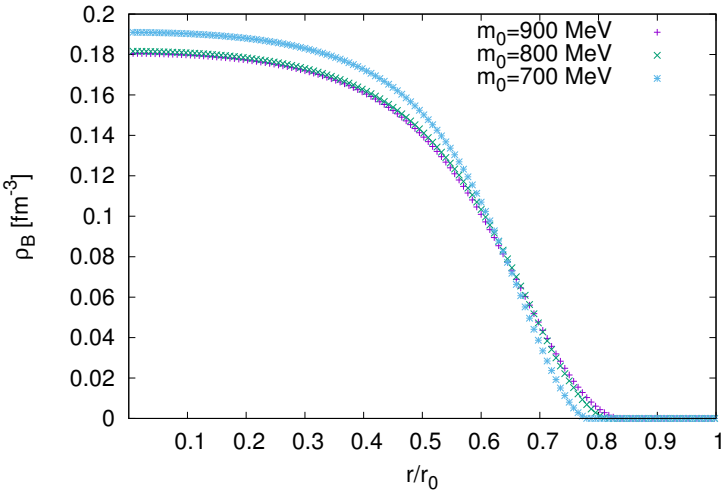

Figure 4.3: Density distributions

in the Thomas-Fermi approximation [34] is given as

$$V_{\rm so}(r) = \frac{1}{2m_+^2 r}\left(g_\omega \frac{d\omega_0}{dr} - \frac{dm_+}{dr}\right)\boldsymbol{s}\cdot\boldsymbol{L} \equiv -\alpha(r)\boldsymbol{s}\cdot\boldsymbol{L} \tag{4.20}$$

in our model[4]. In general, the density distribution of the nuclei approaches zero rapidly in the vicinity of the boundary. Consequently, the gradient of the meson becomes large and the spin-orbit interaction $\alpha_{\rm so}(r)$ gains the largest value here. In order to obtain the equation for this, we used Foldy-Wouthuysen transformation of the Dirac equation. The derivation of $\alpha_{\rm so}(r)$ is summarized in appendix I in detail.

Now, we will discuss the distributions of the strength of spin-orbit potential, $\alpha_{\rm so}(r)$. They are shown in the figure 4.4. This figure shows that $\alpha_{\rm so}^{max}$ is smaller than the experimental value in table 4.1. .

Table 4.1: The strength of the spin-orbit potential: α_{so}^{max}.

m_0 MeV	α_{so}^{max} MeV	α_{so}^{max} MeV
900	0.29	1.80 [34]
800	0.56	
700	0.87	

The values in figure 4.4 are small. However, we have space to change an input, which is incompressibility or K. The observation of incompressibility is difficult because the experimental error is large [37, 38]. Then, we investigated the behavior of $\alpha_{\rm so}^{max}$ with respect to $K = 200--300$ MeV[5]. In order to compare the strength of spin-orbit interactions, we used the maximum value of $\alpha_{\rm so}$ based on [34]. The experimental value of $\alpha_{\rm so}^{max}$ in Ca^{40} is approximately 1.8 MeV [34]. The maximum values of $\alpha_{\rm so}^{max}$ in various situations are summarized in figure 4.5. This figure 4.5 suggests that $\alpha_{\rm so}^{max}$ is sensitive to incompressibility and chiral invariant mass.

[4]The sign of $d\omega/dr$ is negative and dm/dr is positive. Therefore, the spin-orbit force is still an "adding" interaction.

[5]Model parameters are determined in the finite-size nuclear matter.

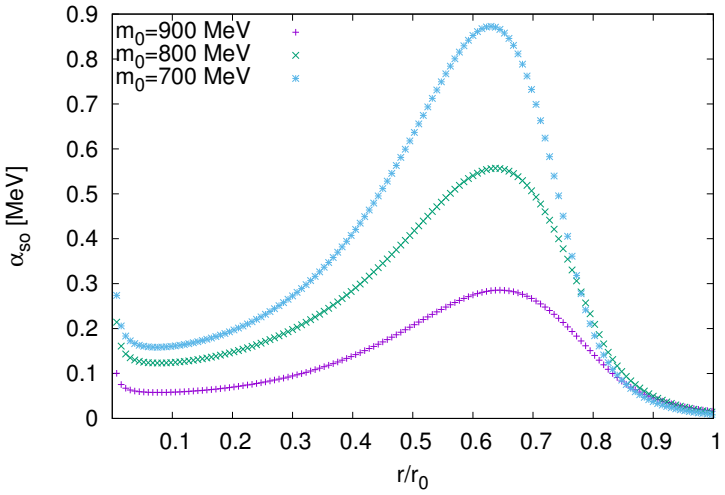

Figure 4.4: α Distributions: here we show the proton distribution. (Because we have assumed ^{4}0Ca, the distribution of protons and neutrons are the same.)

This result also suggests that $m_0 = 500$ MeV is preferred in this model, which is also the case with finite size nuclear matter discussed in a previous chapter. Here, we have showed all $\alpha_{\rm so}^{max}$ even if the density distribution does not conform to the Woods-Saxon distribution. Finally, we show the density distribution of finite-size nuclear matter with m_0 and K as the reference in figure 4.6. As we mentioned earlier, the density distributions that conform to the Woods-Saxon distribution, where the density decreases monotonically, are accepted. If we allow a higher K, the lighter m_0 cases show the Woods-Saxon type distributions.

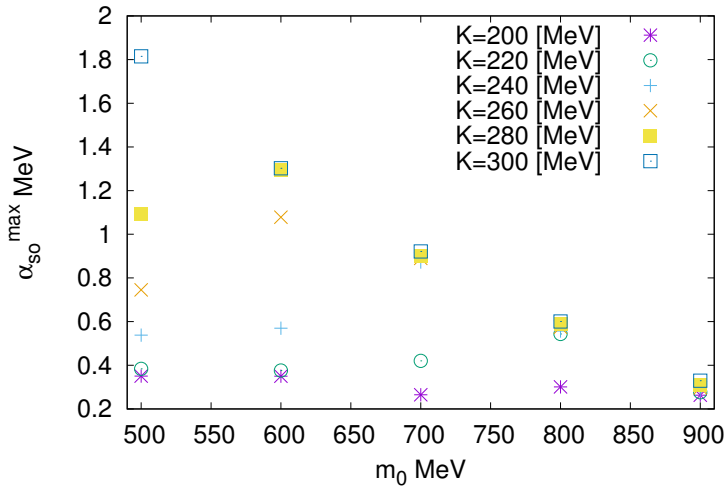

Figure 4.5: $\alpha_{\rm so}^{max}$

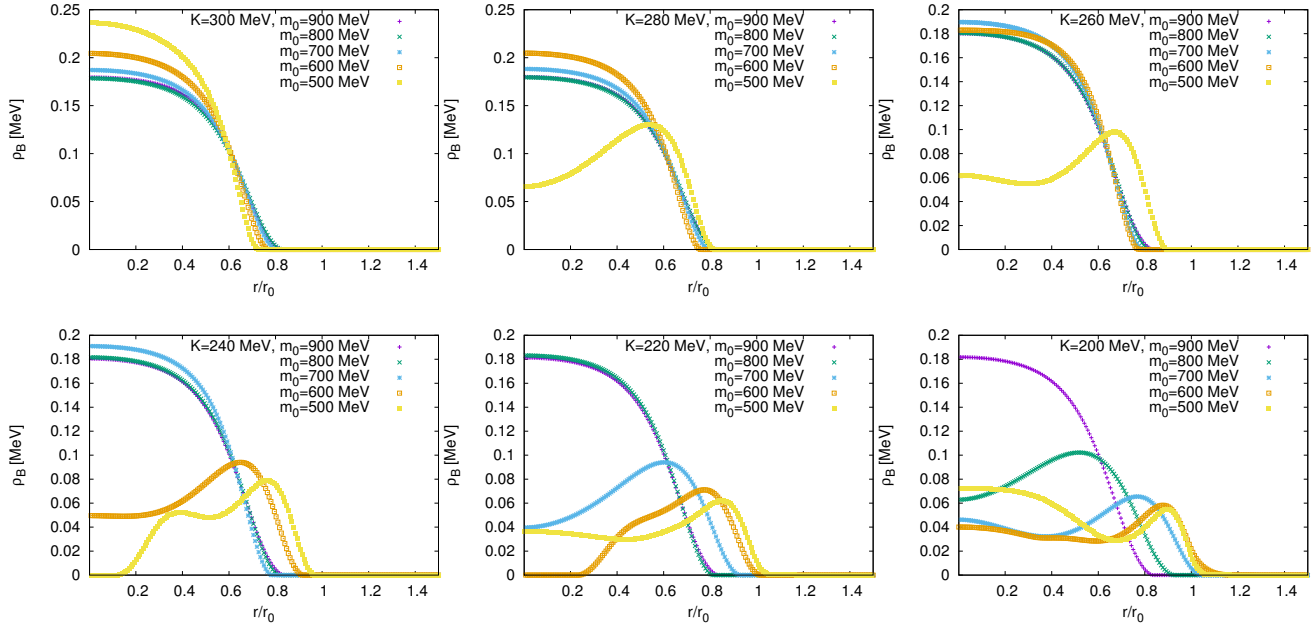

Figure 4.6: Density distributions for values of incompressibility K and chiral invariant mass m_0

Chapter 5

Summary and outlook

We constructed a model for describing nuclear matter based on an SU(2) parity doublet structure. Our model reproduces the saturation density, binding energy, incompressibility, symmetry energy, and slope parameter of nuclear matter for $m_0 = 500$–900 MeV. The six-point scalar interaction that we included in our model plays an important role in reproducing these physical quantities. Our model also reproduces the fist-order liquid-gas phase transition in the symmetric nuclear matter and predicts that this transition is changed to second order in the asymmetric nuclear matter.

We also investigated the pion-decay constant in nuclear matter. When we choose $m_0 = 500$ MeV, the experimental value at normal nuclear matter is reproduced. Effective nucleon masses of positive and negative parity nucleons are approximately equal for different values of m_0 around the saturation density. However, in the higher density regions, the effective masses depend on m_0, which suggests that we may obtain the value of the chiral invariant mass from the observation of effective nucleon masses.

Then, we applied our model to the finite-size nuclear matter and calculated the strength of spin-orbit potential. Although a rough approximation was used, we revealed that the strength of spin-orbit potential is sensitive to m_0 and incompressibility. We showed that, for $m_0 = 500$ MeV and $K = 300$ MeV, the empirical value of the spin-orbit potential is reproduced.

The analysis in this thesis indicates that the chiral invariant mass of the nucleon is $m_0 = 500$ MeV, which is consistent with the value obtained in the analysis in [27] This suggests that we may be able to construct a model that simultaneously describes the vacuum and nuclear matter based on the parity doublet structure.

Next, we discuss the future steps of our study. Our current model does not reproduce the experimental value of the axial charge of nucleons at vacuum. This problem originates because of the choice of the chiral representation of nucleon and may be solved when we use a different representation, for example $(1/2, 1) \oplus (1, 1/2)$. Inclusion of other representations is investigated in [52] with three-flavor parity-doublet model.

We mentioned the "heavy" neutron star in an earlier section. The relation between the mass and radius of a neutron star is an interesting subject to be studied. The existence of the chiral invariant mass may affect the maximum value of the neutron star mass. In addition, neutron stars may contain hyperons. Therefore, extending our model to $\mathrm{SU}(3)_\mathrm{L} \times \mathrm{SU}(3)_\mathrm{R}$ is also interesting and important.

In this study, we have considered only the spin-orbit potential of the finite-size nuclear matter. In addition, our analysis was restricted to symmetric matter. In the future, we can consider other components of the finite-size nuclear matter including asymmetric matter.

It is also interesting to study the temperature dependence of physical quantities of the nuclear matter, pion condensation in the nuclear matter, origin of the chiral invariant mass,

and and the like. We have deferred the interesting topics mentioned above for future studies.

Acknowledgements

I would like to thank Professor Masayasu Harada for his helpful discussions, supervision, and encouragement. Without his patient advice, I may not have continued studying. I would also like to thank Professor Youngman Kim for giving me a chance to visit IBS and for his knowledgeable discussions. He has always given me good advice. I thank Professors Chiho Nonaka and Shinya Matsuzaki for giving me a good environment to study physics. I thank Mr. Hiroki Nishihara for his helpful and interesting discussions that accompanied our study in the laboratory. His deep dedication to physics always inspired me. I also thank Won-Gi Paeng for teaching me a good calculation method during my stay at IBS.

H-lab members and EHQG members, especially my colleagues, helped and interacted with me. They ensured that I had a fruitful time in the laboratory.

My work has been supported in part by the Nagoya University Program for Leading Graduate Schools—“ Leadership Development Program for Space Exploration and Research. ”

Appendix A

Quantum Chromodynamics

In this section, we briefly review QCD. First, we look an overview of the position of QCD and hadron physics. Next, we show the more detail of them.

QCD handles the strong force, one of fundamental forces[1], between quark and gluon, and is a part of standard model of elementary particles. Quarks are fermions which make matter in our world, for example proton and neutron, and gluons are gauge particle of QCD.

Nucleus in our world is of course made by protons and neutrons that are composed from three quarks. These protons and neutrons are bound in nucleus by famous π meson which made by quark and anti-quark pare. Particles bound by strong force are called hadron. Hadron is divided into two groups, one is baryon (figure A.1) which made by three quarks like nucleon and another is meson (figure A.2) that ingredients are quark and anti-quark. Quarks have a

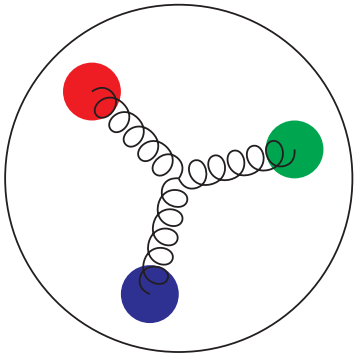

Figure A.1: A rough image of baryon composed by three quarks.

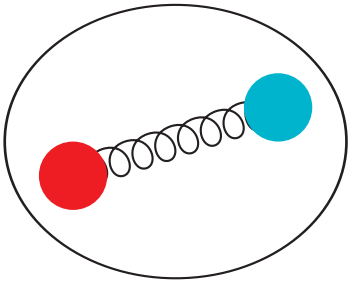

Figure A.2: A rough image of meson composed by quark and anti-quark.

color charge, red, green or blue, and they interact each other via gluons that also have color.

There is one rule that observed hadron state has white color in terms of RGB of quarks. For example, a baryon is made by red, green and blue quarks and a meson is done by red and anti-red (cyan) quarks. On the other words, colored particles like a quark and a gluon are not observed and this fact is called "confinement of color (quark)". We can conclude that the range of strong force is around 1 fm that is hadron size.

We note that we can consider four or more quarks composite which has white color and it is possible theoretically. In addition, gluons composite without quarks can also make white particle called glueball. These composite particles that do not been classified into ordinal baryon and meson are called exotic hadron. Although the glueball state has not been observed, some exotic hadrons are observed and pentaquark state [53] is found recently.

[1]The others are gravity, electromagnetic and weak forces.

QCD is a SU(3) non-abelian gauge theory that describe a physics between color charge. One feature of it is called "asymptotic freedom" that QCD interaction become weak at high energy region and vice versa. Therefore, we can calculate the dynamics of quark and gluon with a perturbative method. This is called perturbative QCD applied to high energy physics like heavy-ion collision experiments and early universe.

On the other hand, the interaction becomes strong and non-perturbative at low energy (long-distance) legion[2]. Then, it is said that quarks move almost freely in a hadron however, interaction becomes strong around boundary of hadron. Therefore, in order to describe 1 fm baryon from quarks and gluons with perturbative calculation is difficult. In addition, the color confinement is a mysterious mechanism that has not been understood and has been discussed. Then we have to use some techniques to handle low energy QCD, effective model of hadron and lattice QCD explained later.

There is other problem of QCD, called origin of hadron mass. Mass of elementary particles is given by Higgs mechanism in standard model of elementary particle. For example, the lightest quark, u, mass is few MeV and the next lightest d-quark has also few MeV. These quark masses obtained by Higgs mechanism is called "current quark mass". The mass of proton composed from two u-quarks and a d-quark seems around 10 MeV naively. However observed proton mass is around 940 MeV and there is large gap between them. It is an idea to

The "spontaneous chiral-symmetry breaking" is considered an idea of solution for it. As we see later, the existence of chiral symmetry of quarks prohibits their mass and the quark obtains mass by breakdown of the chiral symmetry (appendix B). At low energy region, it is considered that a quark and an anti-quark pare is condensed in vacuum by strong interaction and this condensate generates a mass of quarks (their mass is called constituent quark mass). This is a scenario to explain hadron mass. Spontaneous symmetry breaking is discussed in appendix C.

There is a supporting evidence of spontaneous chiral symmetry breaking. Nambu-Goldstone's theorem tells us that the number of generator broken spontaneously corresponds to the generation of massless Nambu-Goldstone (NG) particle (appendix D). In QCD, π meson, the lightest hadron, is considered as NG particle generated by spontaneous chiral-symmetry breaking. In our world, the chiral symmetry is broken slightly by current quark mass and it is the reason why the observed π meson has small mass (approximately 140 MeV).

Describing hadron from quark and gluon degree of freedom is difficult because above reasons. Therefore hadron physics is still interesting field and is investigated by theoretically and experimentally.

Now we move to QCD at finite temperature and density. In early universe, it is considered higher temperature environment than now. Then, there is no longer hadron as bound state of quarks and gluons and they exist as quark-gluon plasma (QGP). In our world, it is low temperature and QGP phase has already turned into hadron phase. Between these two phase, it is considered that confinement and chiral phase transitions occur.

In order to investigate the transition point from hadron phase to QGP phase, heavy-ion collision experiments are running at LHC (CERN) and RHIC (BNL). In those facilities, accelerated heavy-ions (e.g. Au and Pb) are collided and high temperature environment is generated to study QGP. The transition point between hadron and QGP phase is also searched.

High temperature environment is generated in experiment however high density environment is difficult to study experimentally. Only low energy collision experiment using heavy-ion can access the higher density region than saturation density. Recently some experiments have come to be done for investigation[3].

[2]The typical hadron size, 1 fm, gives a scale of QCD. In other words, 200 MeV is a typical scale.

[3]An international collaboration called "the symmetry energy project" explore high density region (https://groups.nscl.msu.edu/hira/sepweb/pages/home.html).

Theoretical point of view, we can assume that the quarks move nearly freely at high density region because of asymptotic freedom. In this region, the quarks can make a Cooper-pare if there is an attractive force and this is called color superconductivity (CSC) phase [54]. The existence of quarks Cooper-pare breaks color SU(3) in this phase. This is an analogy to the BCS type superconductivity of electrons and we do not discuss CSC.

QCD has plenty of phase structure and an image of phase structure is drawn in figure A.3 as an analogy of phase diagram of matter. This figure is just expectation and the transition

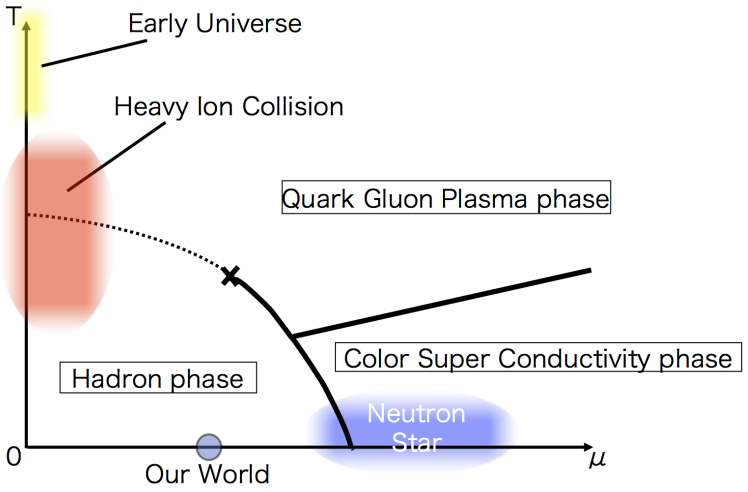

Figure A.3: This is an image of QCD phase structure. Dotted line corresponds to crossover transition and cross mark does to a critical-end-point of second-order.

temperature, density, and order are actually unknown. However, a phase transition from hadron to QGP is predicted as crossover at low density and high temperature by analogy of matter. The second-order critical-end-point is also expected by analogy therefore, it is searched by some heavy-ion collision experiments.

Now we briefly look the lattice QCD (an example of text written in Japanese is [55]). As we looked above, we cannot use perturbative method at low energy QCD and handle the confinement of quarks. The lattice QCD calculates propagator based on first-principle of QCD using computer. In lattice QCD, we divide the space-time into lattice and define discrete QCD on this lattice. Here, quarks are put on the grid points and gluons are defined between each grid points. In this theory, the lattice space plays UV cutoff meanwhile the theory must coincide with continuous QCD when lattice space goes to zero. On the other words, there are some discretization methods to define lattice QCD. Lattice QCD can calculate the non-perturbative region however it depends on the spec of computer. Therefore the full QCD calculation is difficult still now.

From lattice QCD calculation, the phase transition between hadron and QGP phase occurs at $T \sim 200$ MeV and $\mu_B = 0$ MeV, and it is crossover. Lattice QCD is strong method to handle QCD however, it is awkward to handle finite density region because of "sign problem". When we consider the baryon chemical potential in lattice QCD, quark determinant becomes complex and there is uncertainty of phase. This complex value prevent us using Monte Carlo method in calculation. Developing a new method to overcome the sign problem is one of interesting fields.

The other method to study low energy QCD is hadron effective theory. We construct a low energy model with hadrons appeared in low-energy for example, π meson. During construction,

we must respect to the chiral symmetry and its spontaneous breakdown in QCD. We summarize some models to handle low energy hadron physics below.

- Linear sigma model [56]
- Chiral perturbation theory (appendix F)
- Nambu-Jona-Lasinio model [57]
- Based on gauge/gravity correspondence [58, 59]

In this paper, we use a parity doublet model [17] based on chiral linear sigma model.

Finally we briefly review theoretical aspects of QCD and especially focus on the strong interaction of color SU(3). The QCD Lagrangian is written as (A.1):

$$\mathcal{L}_{\rm QCD} = \bar{q}(i\gamma^\mu D_\mu - m_q)q - \frac{1}{2}{\rm tr}(F_{\mu\nu}F^{\mu\nu}) \tag{A.1}$$

$$D_\mu = \partial_\mu - ig_s A_\mu \tag{A.2}$$

$$F_{\mu\nu} = \partial_\mu A_\nu - \partial_\nu A_\mu - ig_s[A_\mu, A_\nu] \tag{A.3}$$

$$A_\mu = A^a_\mu T^a, \quad T^a = \frac{1}{2}\lambda^a. \tag{A.4}$$

Here q is quark field and A_μ is gauge field of SU(3) (gluon). Gell-Mann matrices are λ^a and $a = 1, 2, \cdots 8$. This quark field belongs to the fundamental representation of SU(3) and gauge field does to the adjoint representation. In addition, the parameter of QCD is quark mass, m_q and gauge coupling, g_s.

The transformation properties of them under SU(3) are shown below:

$$q(x) \to U(x)q(x) \tag{A.5}$$

$$A^a_\mu(x) \to U(x)A_\mu U(x)^\dagger - ig_s\partial_\mu U(x)\cdot U^{-1}(x) \tag{A.6}$$

$$U(x) = e^{i\theta^a(x)T^a}. \tag{A.7}$$

Here $\theta^a(x)$ is transformation parameter.

The most different point between non-abelian gauge theory (now we assume QCD) and abelian gauge theory (quantum electrodynamics belongs (QED): U(1)) is self-interaction among gauge fields. In order to investigate the behavior of gauge coupling g_s, we evaluate QCD interaction 1-loop level. When we assume there is N_F flavor symmetry of quarks, the beta function of QCD is

$$\beta(g_s) = -\frac{g_s^3}{(4\pi)^2}\left(11 - \frac{2}{3}N_f\right) \tag{A.8}$$

The coupling constant of QCD at energy-scale Q is given as below by solving the renormalization group equation.

$$\alpha_s(Q^2) = \frac{\alpha_s(M^2)}{1 + \frac{\alpha_s(M^2)}{4\pi}\left(11 - \frac{2}{3}N_f\right)\ln\left(\frac{Q^2}{M^2}\right)} \tag{A.9}$$

Here M is renormalization scale. Equation (A.9) shows that QCD interaction, $\alpha_s(Q^2)$, becomes small at high energy region. This is the asymptotic freedom of QCD and allows us to use the perturbative QCD. Now we introduce a quantity, Λ as

$$-1 = \frac{\alpha_s(M^2)}{4\pi}\left(11 - \frac{2}{3}N_f\right)\ln\left(\frac{\Lambda^2}{M^2}\right). \tag{A.10}$$

This is a condition that the denominator of equation (A.9) equals to zero.

Therefore, $\alpha_s(Q^2)$ is described by one parameter, Λ.

$$\alpha_s(Q) = \frac{4\pi}{\left(11 - \frac{2}{3}N_f\right)\ln\left(\frac{Q^2}{\Lambda^2}\right)} \tag{A.11}$$

Now we write Λ as Λ_{QCD} which is a energy scale that QCD coupling diverges. We note that the perturbation method is not always used when $Q > \Lambda_{\mathrm{QCD}}$ and the value of Λ_{QCD} is known as approximately 200 MeV[4].

The value of strong coupling constant is determined from the scale of Z-bosons mass, m_{Z}, conventionally:

$$\alpha_s(m_Z) = 0.1182. \tag{A.12}$$

This value is quoted from PDG 2016 [60].

[4] $1/\Lambda_{\mathrm{QCD}}$ is same with the order of nucleons radius.

Appendix B

Chiral symmetry

In this section, we review the chiral symmetry of QCD[1]. At first, we summarize the quarks contained in standard model of elementary particle in table B.1. There are six type quarks

Table B.1: Quarks listing and quantities quoted from PDG 2016 [60].

	u	d	s	c	b	t
Mass [MeV]	2.2	4.7	96	1.27×10^3	$4.18 \times 10^3(\overline{\mathrm{MS}})$	1.73×10^5(Direct)
Iso-spin	1/2	-1/2	0	0	0	0
Charge (unit e)	2/3	-1/3	-1/3	2/3	2/3	-1/3

however, u, d, s quarks called "light" are appear in low energy hadron physics. In addition, hadrons including s quark breaks iso-spin symmetry and they are ignored in this work. On the other hand, "heavy" c, b, t quarks are mainly observed as resonances of hadrons in the fireball made at heavy-ion collision experiments.

For light quark flavor, N_F, QCD Lagrangian (A.1) has chiral symmetry, $\mathrm{SU(N}_F)_\mathrm{L} \times \mathrm{SU(N}_F)_\mathrm{R}$, "partially". In other words, QCD Lagrangian (A.1) is invariant "partially" for below transformation:

$$\mathcal{L} = \bar{q}(i\gamma^\mu D_\mu - m_q)q - \frac{1}{2}\mathrm{tr}(F_{\mu_\nu}F^{\mu_\nu}). \tag{B.1}$$

"Partially" means that the current quark mass, m_q breaks the chiral symmetry explicitly as,

$$-m_q(q_l^\dagger q_r + q_r^\dagger q_l) \to -m_0 \bar{q} e^{2i\gamma_5\theta} q, \tag{B.2}$$

under (B.1). However, if we ignore the current quark mass[2] or take a limit of $m_q \to 0$, QCD has chiral symmetry. From here, we omit the quark mass for simplicity. Here r^a, l^a is transformation parameters and T^a is generator of $\mathrm{SU(N}_F)$ group and it satisfies below equation

$$[T^a, T^b] = if^{abc}T^c. \tag{B.3}$$

Here f^{abc} is structure constant of $\mathrm{SU(N}_F)$ and generator is normalized as

$$\mathrm{tr}(T^a T^b) = \frac{1}{2}\delta^{ab}. \tag{B.4}$$

[1]From this section to appendix F, we mainly refer [36] for discussion.

[2]Current quark masses m_u and m_d are smaller than Λ_{QCD} and we usually omit them.

The left- and right-handed quark is written by using projection operators, P_r and P_l defined as

$$q = q_r + q_l \tag{B.5}$$

$$q_r = P_r q \equiv \frac{1+\gamma_5}{2} q, \quad q_l = P_l q \equiv \frac{1-\gamma_5}{2} q. \tag{B.6}$$

The transformation is defined as the commutation relations with a charge in quantum theory. For the chiral transformation, the charge is given from Noether current, $J^a_{R,L\mu}$, of $\mathrm{SU(N}_f)_{R,L}$ transformation:

$$J^a_{R,L\mu} = \bar{q}_{r,l} \gamma_\mu T^a q_{r,l}. \tag{B.7}$$

From this equation, the charges $Q^a_{R,L}$ is given as

$$Q^a_{R,L}(t) = \int d^3x J^a_{R,L0}. \tag{B.8}$$

Now we consider $N_F = 2$ case that means there are only u and d quarks. Then the transformation properties of left- and right-handed quarks are

$$i[Q^a_R, q_r] = -iT^a q_r \tag{B.9}$$

$$i[Q^a_L, q_l] = -iT^a q_l \tag{B.10}$$

$$i[Q^a_R, q_l] = i[Q^a_L, q_r] = 0. \tag{B.11}$$

The commutation relation between charges are

$$[Q^a_R, Q^b_R] = i\epsilon^{abc} Q^c_R \tag{B.12}$$

$$[Q^a_L, Q^b_L] = i\epsilon^{abc} Q^c_L \tag{B.13}$$

$$[Q^a_R, Q^b_L] = 0. \tag{B.14}$$

Then we can say that the chiral transformations are closed each other. We note that subscripts l and r correspond to the representation of Lorentz group and L and R do to the representation of chiral group, $\mathrm{SU(N}_F)_\mathrm{L} \times \mathrm{SU(N}_F)_\mathrm{R}$.

Next, we consider the vector and axial-vector charge that they are linear combinations of $Q^a_{R,L}$:

$$Q^a_V \equiv Q^a_R + Q^a_L, \quad Q^a_A \equiv Q^a_R - Q^a_L. \tag{B.15}$$

Commutation relations of Q^a_V and Q^a_A are

$$[Q^a_V, Q^b_V] = i\epsilon^{abc} Q^c_V \tag{B.16}$$

$$[Q^a_V, Q^b_A] = i\epsilon^{abc} Q^c_A \tag{B.17}$$

$$[Q^a_A, Q^b_A] = i\epsilon^{abc} Q^c_V \tag{B.18}$$

A commutation relation for vector charge is closed however, commutation relations for axial-charge are not closed. It indicates the fact that the chiral symmetry, $\mathrm{SU(N}_F)_\mathrm{L} \times \mathrm{SU(N}_F)_\mathrm{R}$ is broken spontaneously into $\mathrm{SU(N}_F)_V$. The vector and axial-vector charges of quark is obtained by these commutation relations as

$$i[Q^a_V, q] = -iT^a q \tag{B.19}$$

$$i[Q^a_A, q] = -i\gamma_5 T^a q. \tag{B.20}$$

These relations tell us that the vector charge is conserved even if $m_q \neq 0$ however the axial-vector charge is not even if $m_q = 0$.

Spontaneous symmetry breaking generates some Nambu-Goldstone (NG) particles and the number of NG particles correspond to the number of broken generator. These are the consequences of Nambu-Goldstone theorem discussed in appendix D. The NG particle of QCD is considered as π meson that has the lightest hadron.

Appendix C

Spontaneous symmetry breaking

The chiral perturbation theory and hidden local symmetry is based on spontaneous chiral symmetry breaking. In this section, we summarize the general aspect of symmetry and its spontaneous breakdown [36].

We assume a system which action is S is invariant under continues symmetry transformation G with parameter ϵ_A. Noether' theorem tells us that conserved currents j^A_μ and $\partial^\mu j^A_\mu$ corresponding independent generators exist. Then charge operator $Q^A = \int d^3x j^A_0$ plays the small transformation of its symmetry as

$$[i\epsilon_A Q^A, \phi] = \epsilon_A \delta^A \phi, \quad A = 1, 2, \cdots, \dim(G). \tag{C.1}$$

We note that $\delta^A\phi$ is not only a linear transformation of ϕ.

Now we consider a relation between the vacuum and symmetry of this system and we can divide two cases. The vacuum symmetry same with the system or the vacuum symmetry is different from the system. Former case, the vacuum of system is called symmetric phase or Wigner phase. Latter case, it is called spontaneous symmetry broken phase or Nambu-Goldstone phase.

In Wigner phase, the vacuum $|0\rangle$ has no conserving charge as

$$Q^A |0\rangle = 0. \tag{C.2}$$

This is consequence that the charge operator is well-defined like

$$Q^A = \int d^3x j^A_{\mu=0}(x). \tag{C.3}$$

In order to prove equation C.2, we assume Q^A is Lorentz scalar as an example, Q^A must be commutative operator with translation operator P_μ because it is conserved charge and defined on full space-time integral.

$$[P_\mu, Q^A] = 0 \tag{C.4}$$

In addition, the spectral condition gives the eigenvalue of P_μ must be zero at vacuum.

$$P_\mu |0\rangle = 0 \tag{C.5}$$

Because of this vacuum is simultaneous eigenstate of P_μ and Q^A from equation (C.4, $Q^A |0\rangle$ must be proportional to $|0\rangle$.

$$Q^A |0\rangle = c |0\rangle \tag{C.6}$$

Here c is constant of proportion. Then the expectation value of Q^A with vacuum is

$$c = \langle 0 | Q^A | 0 \rangle = \int d^3x \, \langle 0 | j_0^A(x) | 0 \rangle \tag{C.7}$$

On the other hand, the Lorentz symmetry of vacuum give a constraint for expectation value of current as

$$\langle 0 | j_\mu^A(x) | 0 \rangle = \langle 0 | j_\mu^A(0) | 0 \rangle . \tag{C.8}$$

This condition is satisfied only when $c = 0$ and these are the poof of equation (C.2). We can prove the case that Q^A is not Lorentz scalar operator.

Next we move to the Nambu-Goldstone phase. In this case the vacuum is not the eigenstate of charge operator Q^A and we can write this condition like

$$Q^A | 0 \rangle \neq 0. \tag{C.9}$$

We note that this notation is not correct because charge operator is not well-defined if equation (C.2) is not correct[1]. In spontaneous symmetry broken phase, the asymptotic field of ϕ does not correspond with irreducible representation of group G and the symmetry is not explicit. However Nambu-Goldstone's theorem tells us a massless particle called Nambu-Goldstone(NG) particle is generated corresponding with a broken generator. Furthermore the low energy theorem of NG particle gives some constraints to NG particle at low energy limit. We will see the Nambu-Goldstone' theorem and low energy theorem of NG particle.

[1]This statement is contrapositive with the proof of equation (C.2).

Appendix D

Nambu-Goldstone's theorem

In general, some parts of symmetry remain when the global symmetry G is spontaneously broken. The remained generators S^α makes algebra of subgroup H$\subset$ G but broken generators X^a do not. Now we can choose S^α orthogonal to X^a as

$$\mathrm{tr}(S^\alpha X^a) = 0. \tag{D.1}$$

Because the charge operator is not well-defined, equation (C.9) is not suite to the condition of spontaneous symmetry breaking. So we consider the below equation with local operator $\Phi(y)$.

$$[iQ^A, \Phi(y)] = i\int d^3x[j_0^A(x), \Phi(y)] = \delta^A\Phi(y) \tag{D.2}$$

The second equals sign is attained because commutation relation $[j_0^A(x), \Phi(y)]$ exist in vicinity of y and integral is well-defined. Therefore we use $[iQ^A, \Phi(x)]$ which means equation (D.2) and define the spontaneous symmetry breaking as

$$\langle 0|\,[iQ^A, \Phi(x)]\,|0\rangle = \langle 0|\,\delta^A\Phi(x)\,|0\rangle \neq 0. \tag{D.3}$$

This local operator $\Phi(x)$ should not be a Heisenberg field $\phi(x)$ in Lagrangian[1] if and only if it satisfy the translation condition

$$\Phi(x) = e^{iPx}\Phi(0)e^{-iPx}. \tag{D.4}$$

Based on them, we will prove Nambu-Goldstone's theorem below.

Nambu-Goldstone's theorem

When below three condition is satisfied, the theory has massless particle called Nambu-Goldstone particle and it interact with current $j_\mu(x)$.

- The theory has transition and explicit Lorentz invariance.
- There are conserved vector currents $j_\mu, \partial^\mu j_\mu$.
- Symmetry corresponding with charge $Q = \int d^3x j_0(x)$ is broken spontaneously and operator of scalar field $\Phi(x)$ which satisfy equation (D.3) exists[a].

[a] Here we consider the case that there is scalar charge.

[1] A polynomial of $\phi(x)$ in the vicinity of x is enough as an operator $\Phi(x)$.

(PLOOF) The vacuum expectation value of commutation relation between current $j_\mu^A(x)$ and local operator $\Phi(y)$ is written as

$$\langle 0|\left[j_\mu^A(x), \Phi(y)\right]|0\rangle = \int_0^\infty d\sigma^2 \rho(\sigma^2) i\partial_\mu \Delta(x-y;\sigma^2). \tag{D.5}$$

Here we used a spectral function $\rho(\sigma^2)$ defined below.

$$-ik_\mu \rho(\sigma^2 = k^2)\theta(k_0) \equiv (2\pi)^3 \sum_{n,n'} \delta^4(p_n - k) \langle 0|j_\mu(0)|n\rangle \eta^{-1}_{nn'} \langle n'|\Phi(0)|0\rangle \tag{D.6}$$

$$[\phi(x), \phi(y)] = \int \frac{d^4k}{(2\pi)^3 2k_0}(e^{-ik(x-y)} - e^{ik(x-y)}) \equiv i\Delta(x-y;k^2) \tag{D.7}$$

Here we used $\sum_{n,n'} |n\rangle \eta^{-1}_{nn'} \langle n'| = 1$ as a complete set because it is not necessarily eigenstates of transition operator P_μ. If we use a Feynman propagator in this equation, we can write a vacuum expectation value as

$$\langle 0|\,\mathrm{T}\left[j_\mu^A(x)\Phi(0)\right]|0\rangle = \int_0^\infty d\sigma^2 \rho(\sigma^2)\partial_\mu \Delta_F(x;\sigma^2). \tag{D.8}$$

Now we operate $\int d^4x i\partial^\mu$ on the both side of equation (D.8). The left hand side becomes equation (D.9) after some manipulation with current conservation condition $\partial^\mu j_\mu(x) = 0$ and equation (D.3).

$$\int d^4x i\partial^\mu \langle 0|\,\mathrm{T}\left[j_\mu^A(x)\Phi(0)\right]|0\rangle = \langle 0|\delta\Phi(0)|0\rangle \neq 0 \tag{D.9}$$

On the other hand, the right hand side is

$$\int d^4x i\partial^\mu \left[\int_0^\infty d\sigma^2 \rho(\sigma^2)\partial_\mu \Delta_F(x;\sigma^2)\right] = \lim_{p=0} \int d\sigma^2 \frac{\rho(\sigma)(-ip^2)}{i(\sigma^2 - p^2 - i\epsilon)}. \tag{D.10}$$

Here we used ϵ as positive infinitesimal. Therefore below equation is attained from equation (D.9) and (D.10).

$$\langle 0|\delta\Phi(0)|0\rangle = \lim_{p=0} \int d\sigma^2 \frac{\rho(\sigma)(-ip^2)}{i(\sigma^2 - p^2 - i\epsilon)} \neq 0 \tag{D.11}$$

The second not equal demands the existence of massless 1 particle state in the spectral function $\rho(\sigma^2)$ and it is just Nambu-Goldstone particle. Then we divide the spectral function into one-particle pole and continuous part as

$$\rho(\sigma^2) = w\delta(\sigma^2) + \tilde{\rho}(\sigma^2) \tag{D.12}$$

and substitute this for equation (D.11), we obtain

$$w = \langle 0|\delta\Phi(0)|0\rangle \neq 0. \tag{D.13}$$

Equation (D.6) tells us the massless one-particle state $|\mathbf{p}(m=0)\rangle$ exists in the complete set $\{|n\rangle\}$ of this theory. It means that the state $|\mathbf{p}(m=0)\rangle$ interacts with $j_\mu(x)$ and $\Phi(x)$. In other words, these relation are obtained.

$$\langle 0|j_\mu(0)|\mathbf{p}(m=0)\rangle \neq 0, \quad \langle \mathbf{p}(m=0)'|\Phi(0)|0\rangle. \tag{D.14}$$

(QED)

We summarize important consequents and facts of Nambu-Goldstone's theorem below.

- The vacuum expectation value $\langle 0|\,\delta\Phi(0)\,|0\rangle$ is called order parameter. When the order parameter equals to zero, the system has symmetry. However the order parameter become non-zero if the symmetry is broken spontaneously.

- The operator of order parameter $\delta\Phi$ must be scalar quantity from Lorentz symmetry. If the charge operator Q is scalar, the field Φ is also scalar and the NG particle must be scalar from NG theorem. It says that this pole,

$$\text{F.T. } \langle 0|\,\mathrm{T}\left[j_\mu^A(x)\Phi(y)\right]|0\rangle\Big|_{\text{massless pole}} = \langle 0|\,\delta\Phi\,|0\rangle\,\frac{-ip_\mu}{i(-p^2)}, \tag{D.15}$$

  implies the existence of massless asymptotic field ϕ^{as}. This asymptotic field has these characteristics

$$j_\mu(x) \xrightarrow[x_0\to\pm\infty]{} f_\pi\partial_\mu\phi^{as}(x) + \cdots \tag{D.16}$$

$$\Phi(x) \xrightarrow[x_0\to\pm\infty]{} Z^{\frac{1}{2}}\phi^{as}(x) + \cdots \tag{D.17}$$

$$[\phi^{as}(x), \phi^{as}(y)] = iD(x-y) \tag{D.18}$$

$$f_\pi Z^{\frac{1}{2}} = \langle 0|\,\delta\Phi\,|0\rangle\,. \tag{D.19}$$

  Here, Z is renormalization factor. Equation (D.16) is the definition of the decay constant of NG particle.

- Each broken generator X^a has a corresponding asymptotic NG field $\phi^{a,as}$ written as

$$j_\mu^a(x) \to f_\pi^{(a)}\partial_\mu\phi^{a,as}(x) + \cdots\,. \tag{D.20}$$

  Therefore the number of NG particles is given as

$$\dim(G) - \dim(H) = \dim(\mathrm{G/H}). \tag{D.21}$$

These are general aspect of Nambu-Goldstone's theorem and we will use them to construct the non-linear representation of NG boson seen in next appendix.

Appendix E

Non-linear representation of NG boson

In this section, we explain a general formalism that determine the dynamics of NG boson when a symmetry G is broken into H spontaneously. This is called the non-linear representation of NG boson and the lowest order Lagrangian in terms of derivatives is determined uniquely without any parameters. This corresponds to the low-energy theorem of NG boson[1]. Now we assume QCD however, we can apply these discussion to any other symmetries if they break into other symmetry spontaneously.

Now, we move to general discussion. Let $\mathfrak{g}$ be an algebra of G and $\mathfrak{h}$ be an algebra of H. Then we define unbroken and broken generator as S^α and X^a respectively:

$$\{T^A \in \mathfrak{g}\} = \{S^\alpha \in \mathfrak{h}, X^a \in \mathfrak{g} - \mathfrak{h}\} \tag{E.1}$$

$$\mathrm{tr}(S^\alpha X^a) = 0. \tag{E.2}$$

We assume that T^A, S^α and X^A are hermitian and fundamental representation. These generators are normalized as

$$\mathrm{tr}(S^\alpha S^\beta) = \frac{1}{2}\delta^{\alpha\beta}, \quad \mathrm{tr}(X^a X^b) = \frac{1}{2}\delta^{ab}. \tag{E.3}$$

Let us consider the trace of $S^\alpha[S^\beta, X^a]$. By using cyclic-permutation invariance of trace, we can derive

$$\mathrm{tr}(S^\alpha[S^\beta, X^a]) = \mathrm{tr}([S^\alpha, S^\beta]X^a) = 0. \tag{E.4}$$

Then, the commutation relation $[S^\beta, X^a]$ is always contained in broken symmetry H:

$$[\mathfrak{h}, \mathfrak{g} - \mathfrak{h}] \subset \mathfrak{g} - \mathfrak{h}. \tag{E.5}$$

On the other hand, generally, commutation relation of broken generator $[X^a, X^b]$ is expressed with linear combination of broken and unbroken generators. However, if such commutation relation belongs to unbroken algebra,

$$[\mathfrak{g} - \mathfrak{h}, \mathfrak{g} - \mathfrak{h}] = \mathfrak{h}, \tag{E.6}$$

the coset space G/H is called symmetric space.

[1]The scattering amplitude of NG bosom in the low-energy limit is determined from only symmetry structure. It is called the low-energy theorem of NG boson and Goldberger-Treiman relation is an example.

In the symmetric space, the algebra is invariant under a "parity" transformation τ defined as

$$\begin{aligned}\tau(Y) &= +Y, \quad Y \in \mathfrak{h} \\ \tau(Y) &= -Y, \quad Y \in \mathfrak{g} - \mathfrak{h} \\ \tau &: \mathfrak{g} \to \mathfrak{g}, \quad \tau^2 = 1.\end{aligned} \tag{E.7}$$

Here Y is a generator of G.

The number of NG bosons is same with the dimension of G/H from appendix D. In addition, NG bosons transform linearly under unbroken subgroup H (equation (E.6)). These facts indicate that we should identify the NG boson field, π^a as coordinates of the coset space and parametrize representatives of G/H, $\xi(\pi)$ with π^a:

$$\xi(\pi) = e^{i\pi(x)}, \quad \pi(x) \equiv \sum_{a \in \dim(\mathfrak{g}-\mathfrak{h})} \pi^a X^a. \tag{E.8}$$

Let us define the transformation properties of $\pi(x)$ under $g \in G$ as

$$\xi(\pi) \to \xi(\pi') = g\xi(\pi)h^{-1}(\pi, g). \tag{E.9}$$

It means follows. In general, $\xi(x)$ is changed to other representative by transformation g. Then h^{-1} brings $g\xi(x)$ back to the original representative using informations of π and g[2]. This transformation, $\pi(x) \to \pi'(x)$, is non-linear except the case $g = h$. Therefore the representation of G with NG boson is called "non-linear representation". Generally, a set of broken generators $\{X^a\}$ gives us linear and reducible base of H. When $\{X^a\}$ is irreducible for H, G/H is called irreducible coset.

The fundamental building block of non-linear representation is 1-form constructed from $\xi(\pi) \in$G/H as

$$\alpha(\pi) = \frac{1}{i}\xi^{-1}(\pi)d\xi(\pi). \tag{E.10}$$

In terms of coordinate, it is

$$\alpha_\mu(\pi) = \frac{1}{i}\xi^{-1}(\pi)\partial_\mu\xi(\pi). \tag{E.11}$$

This α is called Maurer-Caltan 1-form and it is an element of algebra $\mathfrak{g}$. Hence we can divide α into the parallel or perpendicular parts with unbroken generator S^α as.

$$\alpha_{\parallel\mu}(\pi) \equiv 2\mathrm{tr}(S^\alpha \alpha_\mu(\pi)) \cdot S^\alpha \tag{E.12}$$

$$\alpha_{\perp\mu}(\pi) \equiv 2\mathrm{tr}(X^a \alpha_\mu(\pi)) \cdot X^a. \tag{E.13}$$

Transformation properties of $\alpha_\parallel$ and $\alpha_\perp$ under G transformation are obtained as

$$\alpha_{\parallel\mu}(\pi) \to h(\pi, g)\alpha_{\parallel\mu}(\pi)h^{-1}(\pi, g) - ih(\pi, g)\partial_\mu h^{-1}(\pi, g) \tag{E.14}$$

$$\alpha_{\perp\mu}(\pi) \to h(\pi, g)\alpha_{\perp\mu}(\pi)h^{-1}(\pi, g). \tag{E.15}$$

[2]There is a fact that $g\xi(x)$ is divided into other representative $\xi(\pi')$ and unbroken generator $^\exists h$ uniquely:

$$g\xi(\pi) = \xi(\pi')h(\pi, g), \;\; h(\pi, g) \in \mathrm{H}.$$

Then we conclude that $\alpha_{\perp\mu}(\pi)$ transforms homogeneously however $\alpha_{\parallel\mu}(\pi)$ does not.

From here, we consider the construction of Lagrangian in non-linear representation. For example, we choose the chiral group, $\mathrm{U(N}_f)_L\times\ \mathrm{U(N}_f)_R$, as G which is broken into H=$\mathrm{U(N}_f)_V$ spontaneously. The element of G is pares of $g_L\ \in\mathrm{SU(N}_f)_L$ and $g_R\ \in\mathrm{SU(N}_f)_R$, $(g_L.g_R)$. The unbroken and conserved charge is $Q^a = Q^a_L+Q^a_R$ (vector type) and it is given as (T^a, T^a) in terms of generators. On the other hand, broken charge is axial-vector type written as $Q^a_5 = -Q^a_L+Q^a_R$ and corresponding generators-representation is $(-T^a, T^a)$. Therefore the element of unbroken subgroup, H=$\mathrm{SU(N}_f)_V$ is (g, g). Based on these facts, $\xi(\pi), \alpha_\mu(\pi), \alpha_{\parallel\mu}$ and $\alpha_{\perp\mu}$ are written as

$$\xi(\pi) : (\xi^{-1}(\pi), \xi(\pi)) \equiv (e^{-i\pi^a(x)T^a/f_\pi}, e^{i\pi^a(x)T^a/f_\pi}) \tag{E.16}$$

$$\alpha_\mu(\pi) : (\alpha_{\mu\parallel}(\pi) - \alpha_{\perp\mu}(\pi), \alpha_{\mu\parallel}(\pi) + \alpha_{\perp\mu}(\pi)) \tag{E.17}$$

$$\alpha_{\mu\parallel}(\pi) = \frac{1}{2i}[\xi^{-1}(\pi)\partial_\mu\xi(\pi) + \xi(\pi)\partial_\mu\xi^{-1}(\pi)] \tag{E.18}$$

$$\begin{aligned}\alpha_{\perp\mu}(\pi) &= \frac{1}{2i}[\xi^{-1}(\pi)\partial_\mu\xi(\pi) - \xi(\pi)\partial_\mu\xi^{-1}(\pi)] \\ &= \frac{1}{2i}\xi(\pi)(U^{-1}\partial_\mu U)\xi^{-1}(\pi).\end{aligned} \tag{E.19}$$

Here, we defined $U = e^{2i\pi(x)/f_\pi}$[3] as

$$\xi^2(\pi) \equiv U = e^{2i\pi(x)/f_\pi}. \tag{E.20}$$

Here we normalize π with f_π which is identified as the pion decay constant later. In addition, G/H is irreducible.

The representative $(\xi^{-1}(\pi), \xi(\pi))$ is transformed with $(g_L, g_R)\ \in$G as

$$(\xi^{-1}(\pi), \xi(\pi)) \to (g_L\xi^{-1}(\pi)h^{-1}(\pi, g_L, g_R), g_R\xi(\pi)h^{-1}(\pi, g_L, g_R)). \tag{E.21}$$

From equation (E.21), the transformation property of π is written as equation (E.22):

$$U = \xi^2(\pi) \to g_R\xi^2 g_L^{-1} = g_R U g_L^{-1}. \tag{E.22}$$

Therefore the lowest order Lagrangian in terms of derivatives is written as

$$\begin{aligned}\mathcal{L} =& f_\pi^2 \mathrm{tr}(\alpha_{\perp\mu}(\pi)\alpha_\perp^\mu(\pi)) = -\frac{f_\pi^2}{4}\mathrm{tr}(U^{-1}\partial_\mu U \cdot U^{-1}\partial^\mu U) \\ & \mathrm{tr}(\partial_\mu\pi\partial^\mu\pi) + \cdots.\end{aligned} \tag{E.23}$$

This Lagrangian has the invariance of $\mathrm{SU(N}_f)_L\times\mathrm{SU(N}_f)_R$ transformation which is broken spontaneously. We note that this Lagrangian (E.23) is also called non-linear sigma model.

Finally, we derive the Noether current of $\pi(x)$ respect to X^a:

$$j^a_\mu(x) = f_\pi\partial_\mu\pi^a(x) + (\mathcal{O}(\pi^2)). \tag{E.24}$$

Therefore f_π is exact the decay constant of NG boson. We extend non-linear representation in next appendix F.

[3] U and representative ξ are regarded building blocks of chiral perturbation theory and HLS discussed later.

Appendix F

Chiral perturbation theory

Low-energy effective Lagrangian constructed with respecting to the chiral symmetry is called the chiral perturbation. In this section we briefly review the chiral Lagrangian of QCD [23, 61, 62, 63].

As we have seen, the chiral symmetry of QCD is broken spontaneously at low-energy region. In general, spontaneous global-symmetry breaking generates massless NG bosons and the number of NG bosons corresponds to the number of broken generators. In this situation, a Lagrangian of NG bosons is determined rigorously.

Now we assume $N_f = 3$ ($q = (u, d, s)$) QCD Lagrangian without current quark masses:

$$\mathcal{L}_0 = \bar{q} i\gamma^\mu D_\mu q - \frac{1}{4} G^a_{\mu\nu} G^{a\mu\nu} \tag{F.1}$$

$$D_\mu = \partial_\mu - i g_s G^a_\mu T^a \tag{F.2}$$

$$G^a_{\mu\nu} = \partial_\mu G^a_\nu - \partial_\nu G^a_\mu + f^{abc} G^b_\mu G^d_\nu \tag{F.3}$$

$$q_{L,R} = \frac{1}{2}(1 \pm \gamma_5) q. \tag{F.4}$$

This Lagrangian has $\mathrm{SU(N}_f)_L \times \mathrm{SU(N}_f)_R \times \mathrm{U(1)}_V \times \mathrm{U(1)}_A$ symmetry[1]. $\mathrm{SU(N}_f)_L \times \mathrm{SU(N}_f)_R$ is of course the chiral symmetry and $\mathrm{U(1)}_V$ corresponds to the baryon number conservation.

When there are external fields, the Lagrangian is written as

$$\mathcal{L}_{QCD} = \mathcal{L}_0 + \bar{q}_L \gamma^\mu \mathcal{L}_\mu q_L + \bar{q}_R \gamma^\mu \mathcal{R}_\mu q_R + \bar{q}_L (\mathcal{S} + i\mathcal{P}) q_R + \bar{q}_R (\mathcal{S} - i\mathcal{P}) q_L. \tag{F.5}$$

Here $\mathcal{L}_\mu$ and $\mathcal{R}_\mu$ are external gauge fields of $\mathrm{SU(N}_f)_L$ and $\mathrm{SU(N}_f)_R$ respectively. In addition, $\mathcal{S}$ and $\mathcal{P}$ are scalar and pseudo-scalar external-fields. These external fields are coupled with the theory via gauged chiral symmetry as

$$\mathcal{L}_\mu \to g_L \mathcal{L}_\mu g_L^\dagger - i\partial_\mu g_L \cdot g_L^\dagger \tag{F.6}$$

$$\mathcal{R}_\mu \to g_R \mathcal{R}_\mu g_R^\dagger - i\partial_\mu g_R \cdot g_R^\dagger \tag{F.7}$$

$$(\mathcal{S} + i\mathcal{P}) \to g_L (\mathcal{S} + i\mathcal{P}) g_R^\dagger. \tag{F.8}$$

Now let consider the QCD Lagrangian with quark mass and compare with equation (F.5):

$$\mathcal{L}_{QCD} = \bar{q}(i\gamma^\mu D_\mu - m_q) q - \frac{1}{4} G^a_{\mu\nu} G^{a\mu\nu}. \tag{F.9}$$

[1] $\mathrm{U(1)}_A$ is broken by an anomaly.

We can identify the quark mass, m_q as a scalar source of $\bar{q}q$. Therefore the quark mass is introduced in QCD Lagrangian (F.5) as vacuum expectation value of scalar-external field:

$$< \mathcal{S} >= \begin{pmatrix} m_1 & \cdots & 0 \\ \vdots & \ddots & \vdots \\ 0 & \cdots & m_F \end{pmatrix}. \tag{F.10}$$

As we saw in previous appendixes, the chiral symmetry of QCD, G=SU(N_f)$_L$×SU(N_f)$_R$, is broken into H=SU(N_f)$_V$ at low-energy region. Now we define the representative of coset space, G/H as $U(\pi)$ and parametrize it by $\pi^a(x)$: (appendix E)

$$U(\pi) = e^{2i\frac{\pi(x)^a T^a}{F_\pi}}. \tag{F.11}$$

Here, F_π is the decay constant of NG boson. The chiral transformation properties of U is

$$U \to g_L U g_R^\dagger. \tag{F.12}$$

Based on these facts, we construct low-energy effective model of QCD respecting to QCD symmetries that are chiral, parity and charge conjugation.

At low energy, NG bosons are main degree of freedom and they have small momentum p. Now, we assume that momentum p and/or quark mass m_q are small enough than a certain scale Λ_χ. Then we construct an effective Lagrangian with respecting to the order of $p/\Lambda_\chi, m_q/\Lambda_\chi \ll 1$. This methodology of model construction with the order of small momentum is called the chiral perturbation theory (ChPT). In ChPT, we evaluate the building blocks of model with momentum p and construct the Lagrangian from lowest order of p. During construction, Λ_χ is identified as a breakdown scale of perturbation. Therefore Λ_χ also plays a roll of momentum cutoff in this model.

The energy-scale of this model Λ_χ is given as

$$\Lambda_\chi \sim 4\pi F_\pi \sim 1.1[\text{GeV}]. \tag{F.13}$$

We derive this value later.

In order to construct the Lagrangian respecting to the order of momentum, we evaluate building blocks of it with momentum p. $U(\pi)$ does not include momentum therefore, the order is $\mathcal{O}(1)$. The covariant derivative $D_\mu U$ contains derivative, and external fields $\mathcal{L}_\mu, \mathcal{R}_\mu$ are connected to derivative via transformation (F.6) and (F.7). Hence they have order $\mathcal{O}(p)$. Scalar and pseudo-scalar external fields have $\mathcal{O}(p^2)$. It is because the scalar external field is connected with quark mass (equation F.10) and it is proportional to square of NG boson's mass (equation (F.22)):

$$\mathcal{S} \to m_{u,d} \propto m_\pi^2 = \mathcal{O}(p^2). \tag{F.14}$$

We summarize the order of each building blocks below:

$$U(\pi) \sim \mathcal{O}(1) \tag{F.15}$$

$$D_\mu U, \mathcal{L}_\mu, \mathcal{R}_\mu \sim \mathcal{O}(p) \tag{F.16}$$

$$\mathcal{S}, \mathcal{P} \sim \mathcal{O}(p^2). \tag{F.17}$$

The Lorentz symmetry prohibits the odd-order for p. Therefore the lowest order and renormalizable Lagrangian is order $\mathcal{O}(p^2)$ and it is written as

$$\mathcal{L}_2 = \frac{F_\pi^2}{4}\text{tr}(D_\mu U D^\mu U^\dagger + \chi U^\dagger + \chi^\dagger U) \tag{F.18}$$

$$D_\mu U = \partial_\mu U - i\mathcal{L}_\mu U + iU\mathcal{R}_\mu \tag{F.19}$$

$$\chi \equiv 2B(\mathcal{S} + i\mathcal{P}). \tag{F.20}$$

Here B is a parameter corresponding to the quark condensate and it is defined as

$$\langle 0|\, \bar{q}q \,|0\rangle = -F_\pi^2 B. \tag{F.21}$$

By expanding this Lagrangian, we can reproduce some relations between quark and meson mass, for example Gell-Mann-Oakes-Renner relation [64] (equation (F.22)) and Gell-Mann-Okubo mass formula [65, 66] (equation F.23). After some calculations, we obtain these relations.

$$F_\pi^2 M_\pi^2 = -2\hat{m}\,\langle 0|\, \bar{q}q \,|0\rangle \tag{F.22}$$

$$3M_{\eta_8}^2 = 4M_K^2 - M_\pi^2 \tag{F.23}$$

$$\hat{m} = \frac{m_u + m_d}{2},\ \ M_K = \frac{M_{K^+} + M_{K^0}}{2},\ \ M_\pi = \frac{M_{\pi^0} + M_{\pi^+}}{2}. \tag{F.24}$$

Now we check the uniqueness of order $\mathcal{O}(p^2)$ Lagrangian (F.18). In order to evaluate it, we consider a scattering matrix element,M, of π. If M has N_e of external π lines, the dimension of M written as D_1 is

$$\dim(M) \equiv D_1 = 4 - N_e. \tag{F.25}$$

We assume that the interaction vertex appeared in M contains d derivative operator, k π fields and j quark mass matrix. The interaction term in effective Lagrangian is written with coupling constant, $g_{d,k,j}$, as

$$\mathcal{L}_{int}^{eff} \sim g_{d,k,j}(m_\pi^2)^j(\partial)^d(\pi)^k. \tag{F.26}$$

Then the dimension of $g_{d,k,j}$ is found as $\dim(g_{d,k,j}) = 4-d-2j-k$. If the scattering amplitude M contains $\bar{N}_{d,k,j}$ $g_{d,k,j}$, the total contribution to the dimension M from coupling constants is

$$D_2 = \sum_{j,d,k} \bar{N}_{d,k,j}(4 - 2j - d - k). \tag{F.27}$$

If M contains N_i internal lines of π, each vertices have k π and

$$\sum_k \bar{N}_{d,k,j} k = 2N_i + N_e. \tag{F.28}$$

Now we define $N_{j,d} \equiv \sum_k \bar{N}_{d,k,j}$ and rewrite D_2 as

$$D_2 = \sum_{j,d,k} N_{d,j}(4 - 2j - d) - 2N_i - N_e. \tag{F.29}$$

On the other hand, N_L loops in M is expressed by the number of inner lines and vertices:

$$N_L = N_i - \sum_{j,d} N_{j,d} + 1. \tag{F.30}$$

Finally we get this relation for D_2:

$$D_2 = 2 - 2N_L - N_e + \sum_{j,d,k} N_{d,j}(2 - 2j - d). \tag{F.31}$$

The number of m_π, D_3 also affects to the dimension and order of momentum of M:

$$D_3 = \sum_{j,d} N_{j,d}(2j). \tag{F.32}$$

We note that the order of M is determined from an energy scale E and m_π. Therefore, in general, M is written as

$$M = E^D m_\pi^{D_3} f(\frac{E}{\mu}, \frac{m_\pi}{\mu}). \tag{F.33}$$

Here, $f(\frac{E}{\mu}, \frac{m_\pi}{\mu})$ is a function which represent the energy dependence of M, μ is renormalization scale and D is defined as

$$D = D_1 - D_2 - D_3 = 2 + \sum_{j,d} N_{j,d}(d-2) + 2N_L. \tag{F.34}$$

We expand the Lagrangian with $p/\Lambda_\chi, m_q/\Lambda_\chi \ll 1$ and count the order of expansion with $\bar{D} = D + D_3$:

$$\bar{D} = 2 + \sum_{j,d} N_{j,d}(d + 2j - 2) + 2N_L. \tag{F.35}$$

Since the Lorentz invariance gives us $\bar{D} = 2, 4, \cdots$, we consider $\bar{D} = 2, 4$ cases.

- $\bar{D} = 2$
  This is the lowest order of perturbative expansion and there is no contribution from loop ($N_L = 0$). In other words, the leading term of M does not include any loop. This vertex contains a kinetic term ($j = 0, d = 2$) and mass term ($j = 1, d = 0$) of \$pi. Therefore the Lagrangian (F.18) is unique at $\mathcal{O}(p^2)$.

- $\bar{D} = 4$
  This is next to leading order of M and it can contain a loop. Therefore these two cases are exhaustive:

  ·$N_L = 1$ In this case, $N_{j,d} = 0$, the scattering amplitude M contains one loop and $\mathcal{O}(p^2)$ vertices with (j,d)$\neq$(0,2),(1,0).

  ·$N_L = 0$ In this case M contains one vertex with $\mathcal{O}(p^4)$. In addition we can divide the structure of this vertex into these three cases:

$$\begin{aligned} &N_{0,4} = 1, N_{j,d} = 0, \quad ((j,d) \neq (0,4), (0,2), (1,0)) \\ &N_{1,2} = 1, N_{j,d} = 0, \quad ((j,d) \neq (1,2), (0,2), (1,0)) \\ &N_{2,0} = 1, N_{j,d} = 0, \quad ((j,d) \neq (2,0), (0,2), (1,0)) \end{aligned}$$

Although the loop diagram generate quadratic divergence at $\bar{D} = 4$, it is proved that this divergence is renormalized by tree diagrams of next order. In other words, the quadratic divergence comes from 1-loop diagram derived from $\mathcal{O}(p^2)$ Lagrangian is renormalized by tree diagrams done from $\mathcal{O}(p^4)$ Lagrangian[2]. Therefore, the chiral perturbation theory is renormalizable order by order.

We estimate the energy scale that the perturbative expansion is breakdown at. This is a derivation of equation (F.13). In general, perturbative expansion is valid as long as the next order's contribution is smaller than this order. On the other words, the perturbation does not work when the magnitudes of 1-loop amplitude from $\mathcal{O}(p^2)$ (figure F.2) and tree amplitude from $\mathcal{O}(p^4)$ (figure F.1) are comparable.

[2] $\mathcal{O}(p^4)$ Lagrangian plays a role of counter terms of $\mathcal{O}(p^2)$.

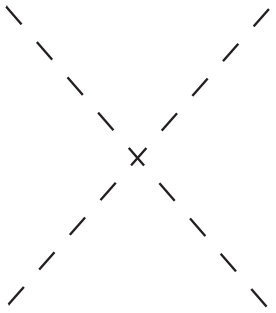

Figure F.1: Tree diagram of 4 π interaction

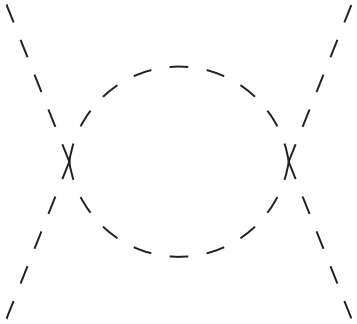

Figure F.2: One loop diagram of 4 π interaction

From Lagrangian (F.18), the factor of 4-point vertex of π is given as p^2/f_π^2. Therefore we can evaluate each scattering amplitudes as

 $\sim \dfrac{p^2}{f_\pi^2}$ (F.36)

 $\sim \dfrac{1}{(4\pi)^2}\dfrac{\Lambda_\chi^2 p^2}{f_\pi^4}.$ (F.37)

Here Λ_χ is a momentum cut-off of loop integral. Since perturbative expansion is broken at

 (F.38)

the energy scale Λ_χ is estimated as

$$\Lambda_\chi \sim 4\pi f_\pi. \tag{F.39}$$

Appendix G

Hidden Local Symmetry

In this section, we review the basics of HLS[21, 22, 23]. Let us consider a system which has $\mathrm{G}_{global}\times$ H_{local} symmetry. Here we assume the global symmetry is the chiral symmetry, G_{global}=$\mathrm{SU(N}_F)_\mathrm{L}\times$ $\mathrm{SU(N}_\mathrm{F})_\mathrm{R}$, and the local symmetry is vector type H_{local}=$\mathrm{SU(N}_F)_\mathrm{V}$[1]. This symmetry is broken into $[\mathrm{SU(N}_F)_\mathrm{V}]_{global}$ spontaneously.

$$[SU(N_F)_\mathrm{L}\times SU(N_F)_\mathrm{R}]_{global}\times[SU(N_F)_\mathrm{V}]_{local}\to[SU(N_F)_\mathrm{V}]_{global},\quad N_\mathrm{F}=2,3$$

Here the remaining symmetry is same with H which is appear in the spontaneous chiral symmetry breaking $\mathrm{G/H}_{global}$:

$$\mathrm{G}=\mathrm{SU(N}_F)_\mathrm{L}\times\mathrm{SU(N}_F)_\mathrm{R},\quad \mathrm{H}=\mathrm{SU(N}_F)_\mathrm{V}.$$

The fundamental quantities $\xi_{\mathrm{L,R}}$ appeared in $\mathrm{G}_{global}\times\mathrm{H}_{local}$ are introduced from U that is a fundamental quantity defined in equation F.10. Now $\xi_{\mathrm{L,R}}$ are written as

$$U=\xi_\mathrm{L}^\dagger\xi_\mathrm{R}. \tag{G.1}$$

The pattern of devision has uncertainty between $\xi_\mathrm{L}^\dagger$ and ξ_R however, we assign a local transformation $h(x)\in H_{Local}$ between them. Therefore $\xi_{\mathrm{L,R}}$ transform under $\mathrm{G}_{global}\times\mathrm{H}_{local}$ as:

$$\xi_{\mathrm{L,R}}(x)\to h(x)\cdot\xi_{\mathrm{L,R}}(x)\cdot g_{\mathrm{L,R}}^\dagger,\quad g_{\mathrm{L,R}}\in G_{Global} \tag{G.2}$$

Explicit forms of $\xi_{\mathrm{L,R}}$ are

$$\xi_{\mathrm{L,R}}(x)=\exp(i\sigma^aT^a/F_\sigma)\exp(\mp i\pi^aT^a/F_\pi),\quad T^a=\frac{\tau^a}{2} \tag{G.3}$$

Here, π^a corresponds to the NG boson generated from spontaneous symmetry breaking. On the other hand, NG-boson σ^a is absorbed into the gauge field that appears in H_{local} and generates the mass of gauge field. $F_{\pi,\sigma}$ are decay constants of NG bosons.

Let us define the V_μ as the gauge field appears in the covariant derivatives of $\xi_{\mathrm{L,R}}$ under H_{Local} transformation. Then the covariant derivative is written as:

$$D^\mu\xi_L\equiv(\partial^\mu\xi_L-iV^\mu\xi_L+i\xi_L\mathcal{L}^\mu) \tag{G.4}$$
$$D^\mu\xi_R\equiv(\partial^\mu\xi_R-iV^\mu\xi_R+i\xi_R\mathcal{R}^\mu) \tag{G.5}$$
$$V_\mu=V_\mu^aT^a. \tag{G.6}$$

[1]As we seen that G is spontaneously broken into global $\mathrm{SU(2)}_V$. Therefore we regard H as the localized version of remaining symmetry. This H is called hidden local symmetry.

Here we added external gauge fields $\mathcal{L}_\mu, \mathcal{R}_\mu$ which transform under gauged chiral symmetry.

Now we define Maurer-Cartan 1-forms as

$$\hat{\alpha}_\perp^\mu = \frac{1}{2i}\left[D^\mu \xi_R \cdot \xi_R^\dagger - D^\mu \xi_L \cdot \xi_L^\dagger\right] \tag{G.7}$$

$$\hat{\alpha}_\parallel^\mu = \frac{1}{2i}\left[D^\mu \xi_R \cdot \xi_R^\dagger + D^\mu \xi_L \cdot \xi_L^\dagger\right]. \tag{G.8}$$

These 1-forms are building block of theory and the meaning of $\perp, \parallel$ is same with appendix E. Transformation properties of $\hat{\alpha}_{\parallel,\perp}^\mu$ are

$$\hat{\alpha}_{\parallel,\perp}^\mu \to h(x)\hat{\alpha}_{\parallel,\perp}^\mu h(x)^\dagger. \tag{G.9}$$

Then the Lagrangian with the lowest derivative is given as

$$\mathcal{L}_\mathrm{A} \equiv F_\pi^2 \mathrm{tr}[\hat{\alpha}_{\perp\mu}\hat{\alpha}_\perp^\mu] \tag{G.10}$$

$$a\mathcal{L}_\mathrm{V} \equiv F_\sigma^2 \mathrm{tr}[\hat{\alpha}_{\parallel\mu}\hat{\alpha}_\parallel^\mu], \quad a \equiv \frac{F_\sigma^2}{F_\pi^2} \tag{G.11}$$

$$\mathcal{L} = \mathcal{L}_\mathrm{A} + a\mathcal{L}_\mathrm{V}. \tag{G.12}$$

Here the order counting method is the same with ChPT (appendix F) and we do not consider the scalar field χ here. The combination $\hat{\alpha}_{\parallel\mu}\hat{\alpha}_\perp^\mu$ breaks the parity invariance and it is prohibited.

Let us check the correspondence between $\mathrm{G}_{global}\times$ H_{local} and G/H. We switch off external fields entire this paragraph for calculation simplicity. The equation of motion of V_μ derived from equation (G.12) is

$$V_\mu = \alpha_{\parallel\mu}. \tag{G.13}$$

Now we substitute equation (G.13) into (G.12) in order to eliminate ${V_\mu}^2$. In addition, $\hat{\alpha}_{\perp\mu}$ is expressed as

$$\hat{\alpha}_{\perp\mu} = \frac{1}{2i}\xi_L \cdot \partial_\mu U \cdot \xi_R^\dagger = \frac{1}{2i}\xi_R \cdot \partial_\mu U^\dagger \cdot \xi_L^\dagger \tag{G.14}$$

with U. Therefore the Lagrangian (G.12) is written as

$$\mathcal{L} = \mathcal{L}_A = \frac{F_\pi^2}{4}\mathrm{tr}(\partial_\mu U \partial^\mu U^\dagger). \tag{G.15}$$

This equation is the same with the equation (F.18)[3]. Therefore the low-energy region of HLS is the same with ChPT theory.

Then we consider the gauge fixing of H_{local}. If we choose $\sigma^a = 0$ gauge called "unitary gauge", the lowest derivative Lagrangian becomes the same thing with equation (F.18) and it is given as

$$\mathcal{L}_A \equiv F_\pi^2 \mathrm{tr}[\hat{\alpha}_{\perp\mu}\hat{\alpha}_\perp^\mu] \tag{G.16}$$

$$a\mathcal{L}_V \equiv F_\sigma^2 \mathrm{tr}[\hat{\alpha}_{\parallel\mu}\hat{\alpha}_\parallel^\mu], \quad a \equiv \frac{F_\sigma}{F_\pi}. \tag{G.17}$$

[2]This is the same manipulation as integrating out the heavy particle from a theory.

[3]Of course the external field is zero.

The appearance is looked the same with (G.12) however, $\xi_{\mathrm{L,R}}$ are different. Let us expand the 1-forms in equation (G.17) and (G.16):

$$\mathcal{L}_A = \mathrm{tr}(\partial_\mu \pi \partial^\mu \pi) + \cdots \tag{G.18}$$

$$a\mathcal{L}_V = \mathrm{tr}[(\partial_\mu \sigma - F_\sigma V_\mu)(\partial^\mu \sigma - F_\sigma V^\mu)] + \cdots. \tag{G.19}$$

Here we absorbed T^a into fields as

$$\sigma = \sigma^a T^a, \ \ \pi = \pi^a T^a. \tag{G.20}$$

Equation (G.18) corresponds to the kinetic term of NG boson and equation (G.19) correspond to vector meson's mass term when we choose the unitary gauge, $\sigma^a = 0$. We briefly discuss the choice of unitary gauge later.

The field strength tensor $V_{\mu\nu}$ and the kinetic term of gauge field is written by ordinal way as

$$V_{\mu\nu} = \partial_\mu V_\nu - \partial_\nu V_\mu - i[V_\mu, V_\nu] \tag{G.21}$$

$$\mathcal{L}_{kin} = -\frac{1}{2g^2}\mathrm{tr}\left[V_{\mu\nu}V^{\mu\nu}\right]. \tag{G.22}$$

Here the transformation property of field strength is

$$V_{\mu\nu} \to h(x) V_{\mu\nu} h^\dagger(x), \tag{G.23}$$

and g is gauge coupling constant of H_{local}. Therefore the lowest derivative Lagrangian ($\mathcal{O}(p^2)$) including kinetic term of vector is written as

$$\begin{aligned}\mathcal{L} &= \mathcal{L}_A + a\mathcal{L}_V + \mathcal{L}_{kin} \\ &= F_\pi^2 \mathrm{tr}(\hat{\alpha}_{\perp\mu}\hat{\alpha}_\perp^\mu) + F_\sigma^2 \mathrm{tr}(\hat{\alpha}_{\parallel\mu}\hat{\alpha}_\parallel^\mu) - \frac{1}{2g^2}\mathrm{tr}(V_{\mu\nu}V^{\mu\nu}).\end{aligned} \tag{G.24}$$

We can consider the next order $\mathcal{O}(p^4)$ Lagrangian as the same way with ChPT.

Next, we consider the assignment of particles in $N_F = 2$ case. If we choose G_{Global}=$\mathrm{U}(2)_L \times \mathrm{U}(2)_R$ and H_{Local}=$\mathrm{U}(2)_V$, the phenomenological NG boson assignment is

$$\begin{aligned}\pi &= \pi^a T^a \\ &= \frac{1}{\sqrt{2}} \begin{pmatrix} \frac{1}{\sqrt{2}}(\pi^0 + \eta) & \pi^+ \\ \pi^- & -\frac{1}{\sqrt{2}}(\pi^0 - \eta) \end{pmatrix} \\ a &= 0, 1, 2, 3, \qquad T^0 = \frac{1}{2}\mathrm{diag}(1, 1)\end{aligned} \tag{G.25}$$

For massive gauge bosons, we assign vector mesons as

$$\begin{aligned}\rho_\mu &= \rho_\mu^a T^a \\ &= \frac{V_\mu}{g} = \frac{1}{\sqrt{2}} \begin{pmatrix} \frac{1}{\sqrt{2}}(\rho_\mu^0 + \omega_\mu) & \rho_\mu^+ \\ \rho_\mu^- & -\frac{1}{\sqrt{2}}(\rho_\mu^0 - \omega_\mu) \end{pmatrix}.\end{aligned} \tag{G.26}$$

Then we finished assignment of vector mesons[4]. If we consider weak bosons, $Z_\mu, W_\mu^\pm$ and photon, A_μ as external fields, we can introduce electroweak interaction into the model. However we does not touch this.

[4]Now we assumed that Okubo-Zweig-Iizuka (OZI) rule [67, 68, 69] works well. OZI rule is phenomenological rule that quark-line disconnected-interaction is prohibited. In other words, double trace term does not appear in the Lagrangian.

After taking unitary gauge $\sigma^a = 0$, the mass term of vector meson is appeared in Lagrangian as

$$\mathcal{L} = \mathrm{tr}(\partial_\mu \pi \partial^\mu \pi) + m_\rho^2 \mathrm{tr}(\rho_\mu \rho^\mu) + \cdots \tag{G.27}$$

$$m_\rho = a g^2 F_\pi^2. \tag{G.28}$$

Then we can determine the interaction among mesons at low-energy region. Here mass of vector is written with gauge coupling and decay constants of NG boson. If we include electromagnetic interaction by introducing photon as an external field, the mass difference between neutral and charged ρ meson is predicted. In addition, HLS can reproduce some phenomenological facts, for example KSRF relations [70, 71] and ρ meson dominance appeared in a $\pi\gamma$ form-factor [72] although we do not consider them.

At the end of this section, we consider unitary gauge $\sigma^a = 0$. When we choose this gauge, $\xi_{\mathrm{L,R}}$ is written as

$$\xi_{\mathrm{L}}^\dagger = \xi_{\mathrm{R}} \equiv \xi = \exp\left(i\frac{\pi}{F_\pi}\right), \tag{G.29}$$

and ξ is not invariant under G_{Global} transformation:

$$\xi_L^\dagger = \xi_R \equiv \xi = \exp\left(i\frac{\pi}{F_\pi}\right). \tag{G.30}$$

Its because the representatives $\xi_{\mathrm{L,R}}$ are moved into other representatives. Now let us choose an element h defined as

$$h \equiv h(\pi, g_{\mathrm{R}}, g_{\mathrm{L}}) \in H_{Local}. \tag{G.31}$$

If we use this local transformation, we can bring the moved representatives back to the original representative. Therefore ξ can be invariant under G_{Global} transformation as

$$h(\pi, g_R, g_L)\xi g_R^\dagger = g_L \xi^\dagger h^\dagger(\pi, g_R, g_L). \tag{G.32}$$

Here the transformation property of gauge field is

$$V_\mu \to h(\pi, g_R, g_L) V_\mu h^\dagger(\pi, g_R, g_L) - i\partial_\mu h(\pi, g_R, g_L) \cdot h^\dagger(\pi, g_R, g_L). \tag{G.33}$$

Therefore, the vector field can obtain a mass without gauge symmetry breaking[5]

[5]This is the same with Higgs mechanism.

Appendix H

Finite-temperature field theory

In this section, we explain how to calculate the fermion determinant including temperature and chemical potential [73].

Free fermion Lagrangian is written as

$$\mathcal{L} = \bar{\psi}(i\gamma^\mu \partial_\mu - m)\psi. \tag{H.1}$$

This Lagrangian has global U(1) symmetry corresponding to fermion (baryon) number conservation and is invariant under $\psi \to e^{-i\theta}\psi$ transformation. Here θ is a transformation parameter. From Noether's theorem, there is conserved current j_μ given as

$$\partial_\mu j^\mu = 0, \quad j^\mu = \bar{\psi}\gamma^\mu\psi. \tag{H.2}$$

The conserved charge of this current is

$$Q = \int d^3x j^0 = \int d^3x \psi^\dagger \psi. \tag{H.3}$$

The momentum conjugate of field ψ is defined as

$$\Pi_\alpha \equiv \frac{\partial \mathcal{L}}{\partial(\partial\psi_\alpha/\partial t)} = i\psi^\dagger_\alpha, \tag{H.4}$$

the Hamiltonian density $\mathcal{H}$ is given as

$$\begin{aligned} \mathcal{H} &= \Pi_\alpha \frac{\partial \psi_\alpha}{\partial t} - \mathcal{L} \\ &= \bar{\psi}(-i\gamma^i\partial_i + m)\psi. \end{aligned} \tag{H.5}$$

Here $\alpha = 1 \sim 4$ is Dirac spinor suffix. Let us consider the chemical potential μ that corresponds to U(1) conserved charge. We introduce it via external field method and use the imaginary time formalism to derive a fermion partition function. As a result, the partition function is written as

$$\int \mathcal{D}\Pi\mathcal{D}\psi \exp\left[\int_0^\beta d\tau \int d^3x \bar{\psi}\left(-\gamma^0\frac{\partial}{\partial\tau} + i\gamma^i\partial_i - m + \mu\gamma^0\right)\psi\right]. \tag{H.6}$$

In order to perform functional integral, we consider the Fourier transformation of fermion field:

$$\psi(\tau, \vec{x}) = \frac{1}{\sqrt{V}}\sum_n \sum_{\vec{p}} e^{i(\vec{p}\cdot\vec{x} + \omega_n\tau)}\tilde{\psi}_{\alpha;n}(\vec{p}). \tag{H.7}$$

Then ω_n is called Matsubara frequency that takes discrete values labeled n since the periodicity of imaginary time formalism. In fermion case, Matsubara frequency is given as

$$\omega_n = (2n+1)\pi T. \tag{H.8}$$

By using above things, the fermionic partition function is given as

$$Z = \prod_n \prod_{\vec{p}} \prod_\alpha \int i d\tilde{\psi}^\dagger_{\alpha;n}(\vec{p}) d\tilde{\psi}_{\alpha;n}(\vec{p}) \exp\left(\sum_n \sum_{\vec{p}} i\tilde{\psi}^\dagger_{\alpha;n}(\vec{p}) D_{\alpha\rho} \tilde{\psi}_{\rho;n}(\vec{p}) \right) \tag{H.9}$$

$$D = -i\beta[(-i\omega_n + \mu) - \gamma^0\gamma^i \cdot p_i - m\gamma^0]. \tag{H.10}$$

After functional integration taking care of anti-commutation relation of fermion field, we obtain

$$Z = \mathrm{Det} D. \tag{H.11}$$

This relation allows us $\ln\det A = \mathrm{tr}\ln A$ (A is matrix.) to obtain the thermodynamic potential of grand canonical ensemble.

$$\ln Z = 2\sum_n \sum_{\vec{p}} \ln\left\{\beta^2[(\omega_n + i\mu)^2 + E^2]\right\} \tag{H.12}$$

$$E = \sqrt{m^2 + \vec{p}^2}. \tag{H.13}$$

By taking Matsubara frequency summation and neglecting terms that do not depend on the temperature $T = 1/\beta$ and chemical potential μ, we get

$$\ln Z = 2V \int \frac{d^3p}{(2\pi)^3} \left[\beta E + \ln\left(1 + e^{-\beta(E-\mu)}\right) + \ln\left(1 + e^{-\beta(E+\mu)}\right)\right]. \tag{H.14}$$

The first term corresponds to the vacuum energy of this system. Second and third terms are contributions from particles and anti-particles respectively. This is coincide with the result from statistical mechanics.

Appendix I

Foldy-Wouthuysen-transformation

Foldy-Wouthuysen-transformation[74, 75] of the Dirac equation is a technique to get the non-relativistic single-particle Hamiltonian for fermion. We consider the Fermion in the some potentials (external fields). Here we consider only vector $V_\mu(x)$ type external fields. We note that the Fermion mass depends on coordinate, $m_+(r)$ in order to consider the parity doublet case.

Then the general form of the Dirac equation for fermion is

$$\left(i\gamma^\mu\partial_\mu + g_v\gamma^\mu V_\mu - m_+\right)\psi = 0 \tag{I.1}$$

$$i\frac{\partial}{\partial x^0}\psi = H\psi = \gamma^0(-i\gamma^i\partial_i - g_v\gamma^\mu V_\mu + m_+)\psi \tag{I.2}$$

Here we note these relations,

$$\gamma^\mu = (\beta, \beta\boldsymbol{\alpha}) \tag{I.3}$$

$$\beta = \begin{pmatrix} 1 & 0 \\ 0 & -1 \end{pmatrix} \tag{I.4}$$

$$\alpha_i = \begin{pmatrix} 0 & \sigma_i \\ \sigma_i & 0 \end{pmatrix} \tag{I.5}$$

Generally, the Hamiltonian mixes the upper and lower components of Dirac spinor. We search the Hamiltonian which has no off-diagonal terms. Here we define the new terms, *even* and *odd* as followings. The operator which mixes the upper component and the lower component of Dirac spinor is called *odd* operator $\mathcal{O}$. The operator which does not mix them is called *even* operator $\mathcal{E}$. Then the Hamiltonian is written with this operators as

$$H = \mathcal{O} + \mathcal{E} \tag{I.6}$$

$$\mathcal{O} = -i\boldsymbol{\alpha}\cdot\boldsymbol{\nabla} - g_v\boldsymbol{\alpha}\cdot\boldsymbol{V} \tag{I.7}$$

$$\mathcal{E} = \beta m_+ - g_v V_0. \tag{I.8}$$

When we consider the non-relativistic limit, the upper and lower components of Dirac spinor become equal each other. Then we consider the unitary transformation U which makes The Dirac spinor into "two component".

$$\psi' = \begin{pmatrix} \varphi \\ \varphi \end{pmatrix} \equiv U\psi \tag{I.9}$$

When we find such unitary transformation, the time evolution does not mix the upper and lower components. The time evolution equation of this new field is written as

$$\begin{aligned} i\frac{\partial}{\partial x^0}\psi' &= (iU(\partial_0\psi) + i(\partial_0 U)\psi) \\ &= UH(U^\dagger U)\psi + i(\partial_0 U)U^\dagger U\psi \\ &= H'\psi' \end{aligned} \tag{I.10}$$

Here we define the diagonalized Hamiltonian as

$$H' = UHU^\dagger - iU(\partial_0 U^\dagger) \tag{I.11}$$

If we use Hermitian operator S, we can write this unitary operator as

$$U = \exp(iS). \tag{I.12}$$

We can expand the H' using the Baker-Campbell-Hausdorff formula as

$$\begin{aligned} H' =& \exp(iS)H\exp(-iS) - i\exp(iS)\frac{\partial \exp(-iS)}{\partial x^0} \\ =& H + [iS, H] + \frac{1}{2!}[iS,[iS,H]] + \frac{1}{3!}[iS,[iS,[iS,H]]] + \cdots \\ & - \left\{ \frac{\partial S}{\partial t} + i\left[S, \frac{1}{2}\frac{\partial S}{\partial t}\right] + \frac{i^2}{2!}\left[S,\left[S,\frac{1}{3}\frac{\partial S}{\partial t}\right]\right] + \frac{i^3}{3!}\left[S,\left[S,\left[S,\frac{1}{4}\frac{\partial S}{\partial t}\right]\right]\right] + \cdots \right\} \\ =& H - \frac{\partial S}{\partial t} + i\left[S, H - \frac{1}{2}\frac{\partial S}{\partial t}\right] + \frac{i^2}{2!}\left[S,\left[S, H - \frac{1}{3}\frac{\partial S}{\partial t}\right]\right] + \frac{i^3}{3!}\left[S,\left[S,\left[S, H - \frac{1}{4}\frac{\partial S}{\partial t}\right]\right]\right] + \cdots \end{aligned} \tag{I.13}$$

We assume S has the order of $O(1/m_+)$ and consider to eliminate the *odd* operator order by order. Here we will consider only static case, we can neglect the derivative terms of S. Then, we get this equation for the first order of m_+.

$$\mathcal{O} + i[S,\beta]m_+ = 0,\ \ O(m_+^0). \tag{I.14}$$

By solving this equation, we get

$$S = \frac{-i}{2m_+}\beta\mathcal{O}, \tag{I.15}$$

here we assume that $\beta S = -S\beta$. Next, we check the H' is *even* or not, order by order.

We separate the *even* operator by mass order and define $\tilde{\mathcal{E}}$ as

$$\mathcal{E} = \beta m_+ + \tilde{\mathcal{E}} \tag{I.16}$$

$$\tilde{\mathcal{E}} = -\, g_v V_0. \tag{I.17}$$

We have to take care the r dependence of m_+ via $\sigma_0(r)$ during calculation.

After some calculations, we get H' as

$$\begin{aligned}
H' =&\beta m_+ + \tilde{\mathcal{E}} + \frac{\beta}{2m_+}[\mathcal{O}, \tilde{\mathcal{E}}] + \frac{i}{2m_+}\left(\boldsymbol{\alpha}\cdot\boldsymbol{\nabla} m_+\right) + \frac{1}{m_+}\beta\mathcal{O}^2 - \frac{1}{2m}\beta\mathcal{O}^2 - \frac{1}{8m}[\mathcal{O}, [\mathcal{O}, \tilde{\mathcal{E}}]] \\
&- \frac{1}{2m^2}\mathcal{O}^3 + \frac{i\beta}{4m_+^2}\left(\boldsymbol{\alpha}\cdot\boldsymbol{\nabla} m_+\right)\mathcal{O} + \frac{\beta}{8m_+^2}(\alpha_i\alpha_j\nabla_i\nabla_j m_+) + \frac{1}{6m^2}\mathcal{O}^3 \\
&- \frac{1}{6m^3}\beta\mathcal{O}^4 + \frac{1}{48m^3}\beta[\mathcal{O}, [\mathcal{O}, [\mathcal{O}, \tilde{\mathcal{E}}]]] - \frac{i}{12m_+^3}\left(\boldsymbol{\alpha}\cdot\boldsymbol{\nabla} m_+\right)\mathcal{O}^2 \\
&- \frac{1}{12m_+^3}(\alpha_i\alpha_j\nabla_i\nabla_j m_+)\mathcal{O} + \frac{i}{48m_+^3}(\alpha_i\alpha_j\alpha_k\nabla_i\nabla_j\nabla_k m_+) + \frac{1}{24m^3}\beta\mathcal{O}^4 + \cdots \\
=&\beta\left(m_+ + \frac{\mathcal{O}^2}{2m_+} - \frac{\mathcal{O}^4}{8m_+^3}\right) + \tilde{\mathcal{E}} - \frac{1}{8m_+^2}[\mathcal{O}, [\mathcal{O}, \tilde{\mathcal{E}}]] + \frac{i\beta}{4m_+^2}\left(\boldsymbol{\alpha}\cdot\boldsymbol{\nabla} m_+\right)\mathcal{O} + \frac{\beta}{8m_+^2}(\alpha_i\alpha_j\nabla_i\nabla_j m_+) \\
&+ \frac{\beta}{2m_+}[\mathcal{O}, \tilde{\mathcal{E}}] + \frac{i}{2m_+}\left(\boldsymbol{\alpha}\cdot\boldsymbol{\nabla} m_+\right) - \frac{\mathcal{O}^3}{3m_+^2} \qquad \text{(I.18)} \\
\equiv&\beta m_+ + \tilde{\mathcal{E}}' + \mathcal{O}' \qquad \text{(I.19)}
\end{aligned}$$

$$\mathcal{E}' \equiv \beta\left(m_+ + \frac{\mathcal{O}^2}{2m_+} - \frac{\mathcal{O}^4}{8m_+^3}\right) + \tilde{\mathcal{E}} - \frac{1}{8m_+^2}[\mathcal{O}, [\mathcal{O}, \tilde{\mathcal{E}}]] + \frac{i\beta}{4m_+^2}\left(\boldsymbol{\alpha}\cdot\boldsymbol{\nabla} m_+\right)\mathcal{O} + \frac{\beta}{8m_+^2}(\alpha_i\alpha_j\nabla_i\nabla_j m_+) \qquad \text{(I.20)}$$

$$\mathcal{O}' \equiv \frac{\beta}{2m_+}[\mathcal{O}, \tilde{\mathcal{E}}] + \frac{i}{2m_+}\left(\boldsymbol{\alpha}\cdot\boldsymbol{\nabla} m_+\right) - \frac{\mathcal{O}^3}{3m_+^2} \qquad \text{(I.21)}$$

Here we have eliminated the *odd* term with $O(m_+^0)$. Next, we use another Foldy-Wouthuysen transformation to delete $O(m_+^{-1})$. Same as above, we get hermitian matrix S' as

$$S' = \frac{-i}{2m_+}\beta\mathcal{O}' \qquad \text{(I.22)}$$

Then we eliminate the *odd* $O(m_+^{-1})$ terms and get

$$\begin{aligned}
H'' =&\exp(iS')H'\exp(-iS') \\
=&\beta m + \tilde{\mathcal{E}}' + \frac{1}{2m}\beta[\mathcal{O}', \tilde{\mathcal{E}}'] + \frac{i\beta}{4m_+^2}\left[\alpha_i\nabla_i m_+, \tilde{\mathcal{E}}\right] + \mathcal{O}\left(\frac{1}{m^3}\right) \qquad \text{(I.23)} \\
\equiv&\beta m + \tilde{\mathcal{E}}' + \mathcal{O}'' \qquad \text{(I.24)} \\
\mathcal{O}'' =&\frac{1}{2m_+}\beta[\mathcal{O}', \tilde{\mathcal{E}}'] + \frac{i\beta}{4m_+^2}\left[\alpha_i\nabla_i m_+, \tilde{\mathcal{E}}\right] \qquad \text{(I.25)}
\end{aligned}$$

We continue the same procedure.

$$S'' = \frac{-i}{2m_+}\beta\mathcal{O}'' \qquad \text{(I.26)}$$

Then

$$H''' = \beta m_+ + \tilde{\mathcal{E}}' + \mathcal{O}'' + \frac{1}{2m_+}[\beta\mathcal{O}'', \beta m_+ + \tilde{\mathcal{E}}' + \mathcal{O}''] \qquad \text{(I.27)}$$

Then we get the *even* Hamiltonian up to $\mathcal{O}(m_+^{-2})$ as

$$\begin{aligned}
H''' =& \beta\left(m_+ + \frac{\mathcal{O}^2}{2m_+} - \frac{\mathcal{O}^4}{8m_+^3}\right) + \tilde{\mathcal{E}} - \frac{1}{8m_+^2}[\mathcal{O}, [\mathcal{O}, \tilde{\mathcal{E}}]] \\
&+ \frac{i\beta}{4m_+^2}\left(\boldsymbol{\alpha}\cdot\boldsymbol{\nabla} m_+\right)\mathcal{O} + \frac{\beta}{8m_+^2}(\alpha_i\alpha_j\nabla_i\nabla_j m_+) + \mathcal{O}\left(\frac{1}{m_+^3}\right) \qquad \text{(I.28)}
\end{aligned}$$

We have to calculate the products of operators and we get them below.

$$\begin{aligned}\frac{\mathcal{O}^2}{2m_+} =&\frac{1}{2m_+}\alpha_i\alpha_j(i\nabla+g_vV)_i(i\nabla+g_vV)_j\\ =&\frac{1}{2m_+}(\delta_{ij}+i\epsilon_{ijk}\Sigma_k)(i\nabla+g_vV)_i(i\nabla+g_vV)_j\\ =&\frac{1}{2m_+}\left[(i\boldsymbol{\nabla}+g_v\boldsymbol{V})^2-g_v\epsilon_{ijk}(\nabla_iV_j)\Sigma_j\right]\end{aligned} \tag{I.29}$$

here,

$$\Sigma_i=\begin{pmatrix}\sigma^i & 0\\ 0 & \sigma^i\end{pmatrix}. \tag{I.30}$$

The other terms are

$$\begin{aligned}\left[\mathcal{O},\tilde{\mathcal{E}}\right] =&[-\alpha_i(i\nabla_i+g_vV_i),-g_vV_0]\\ =&ig_v\alpha_i\nabla_iV_0 \qquad\text{(I.31)}\\ \left[\mathcal{O},\left[\mathcal{O},\tilde{\mathcal{E}}\right]\right] =&[-\alpha_i(i\nabla_i+g_vV_i),ig_v\alpha_j\nabla_jV_0]\\ =&\alpha_i\alpha_j(g_v\nabla_i\nabla_jV_0)+2\ \alpha_i\alpha_j(g_v\nabla_jV_0)(\nabla_i-iV_i)|_{i\neq j}\\ =&g_v\nabla^2V_0+i\epsilon_{ijk}\nabla_i(g_v\nabla_jV_0)\Sigma_k+2i\epsilon_{ijk}\Sigma_k(g_v\nabla_iV_0)\nabla_j \qquad\text{(I.32)}\\ (\boldsymbol{\alpha}\cdot\boldsymbol{\nabla}m_+)\,\mathcal{O} =&(\nabla_im_+)(-i\nabla_i-g_vV_i)-i\epsilon_{ijk}\Sigma_k(\nabla_im_+)(i\nabla_j+g_vV_j) \qquad\text{(I.33)}\\ (\alpha_i\alpha_j\nabla_i\nabla_jm_+) =&\nabla^2m_++i\epsilon_{ijk}\Sigma_k\nabla_i(\nabla_jm_+) \qquad\text{(I.34)}\end{aligned}$$

Then we get the *even* Hamiltonian as

$$\begin{aligned}H''' =&\beta\left(m_++\frac{1}{2m_+}\left[(i\boldsymbol{\nabla}+g_v\boldsymbol{V})^2-g_v\epsilon_{ijk}(\nabla_iV_j)\Sigma_j\right]+\cdots\right)-g_vV_0\\ &-\frac{1}{8m_+^2}\left(g_v\nabla^2V_0\right)-\frac{i}{8m_+^2}\epsilon_{ijk}\nabla_i(g_v\nabla_jV_0)\Sigma_k\\ &-\frac{i}{4m_+^2}\epsilon_{ijk}\Sigma_k(g_v\nabla_iV_0)\nabla_j-\frac{i\beta}{4m_+^2}(\nabla_im_+)(i\nabla_i+g_vV_i)\\ &+\frac{i\beta}{4m_+^2}\epsilon_{ijk}\Sigma_k(\nabla_im_+)\nabla_j+\frac{g_v\beta}{4m_+^2}\epsilon_{ijk}\Sigma_k(\nabla_j)V_j+\frac{1}{8m_+^2}\nabla^2m_+^2+\frac{i}{8m_+^2}\epsilon_{ijk}\Sigma_k\nabla_i(\nabla_jm_+)\end{aligned} \tag{I.35}$$

The spin-orbit interaction comes from

$$H'''_{so}=-\frac{i}{4m_+^2}\epsilon_{ijk}\Sigma_k(g_v\nabla_iV_0)\nabla_j+\frac{i\beta}{4m_+^2}\epsilon_{ijk}\Sigma_k(\nabla_im_+)\nabla_j. \tag{I.36}$$

To check this, we assume the inhomogeneous matter. Then angular depending terms become dropped and the gradient of fields are simple form. Finally, the operator act on the upper component of Dirac field are

$$\frac{1}{2m_+^2r}(g_v\frac{dV_0}{dr}-\frac{dm_+}{dr})\frac{\boldsymbol{\sigma}}{2}\cdot(\mathbf{r}\times(-i\nabla)). \tag{I.37}$$

When we take spin-average, the spin-orbit term is written as

$$V_{so}=\frac{1}{2m_+^2r}(g_v\frac{dV_0}{dr}-\frac{dm_+}{dr})\boldsymbol{s}\cdot\boldsymbol{L}. \tag{I.38}$$

Bibliography

[1] K. Yagi, *Gensikaku Butsurigaku* (Nuclear Physics), Tokyo, Asakura Shoten (1971), p. 81

[2] P. Danielewicz, R. Lacey and W. G. Lynch, Science **298**, 1592 (2002) doi:10.1126/science.1078070 [nucl-th/0208016].

[3] P. Demorest, T. Pennucci, S. Ransom, M. Roberts and J. Hessels, Nature **467**, 1081 (2010) [arXiv:1010.5788 [astro-ph.HE]].

[4] J. Antoniadis, P. C. C. Freire, N. Wex, T. M. Tauris, R. S. Lynch, M. H. van Kerkwijk, M. Kramer and C. Bassa *et al.*, Science **340**, 6131 (2013) [arXiv:1304.6875 [astro-ph.HE]].

[5] M. Alford, M. Braby, M. W. Paris and S. Reddy, Astrophys. J. **629**, 969 (2005) [nucl-th/0411016].

[6] I. Bombaci and U. Lombardo, Phys. Rev. C **44**, 1892 (1991).

[7] H. Muller and B. D. Serot, Phys. Rev. C **52**, 2072 (1995) doi:10.1103/PhysRevC.52.2072 [nucl-th/9505013].

[8] B. A. Li, C. M. Ko and Z. Ren, Phys. Rev. Lett. **78**, 1644 (1997) [nucl-th/9701048].

[9] F. Hofmann, C. M. Keil and H. Lenske, Phys. Rev. C **64**, 034314 (2001) [nucl-th/0007050].

[10] B. Liu, V. Greco, V. Baran, M. Colonna and M. Di Toro, Phys. Rev. C **65**, 045201 (2002) [nucl-th/0112034].

[11] W. Zuo, I. Bombaci and U. Lombardo, Phys. Rev. C **60**, 024605 (1999) [nucl-th/0102035].

[12] E. N. E. van Dalen, C. Fuchs and A. Faessler, Phys. Rev. Lett. **95**, 022302 (2005) [nucl-th/0502064].

[13] L. W. Chen, C. M. Ko and B. A. Li, Phys. Rev. C **76**, 054316 (2007) [arXiv:0709.0900 [nucl-th]].

[14] P. Gogelein, E. N. E. van Dalen, K. Gad, K. S. A. Hassaneen and H. Muther, Phys. Rev. C **79**, 024308 (2009) [arXiv:0809.3325 [nucl-th]].

[15] M. Drews and W. Weise, arXiv:1412.7655 [nucl-th].

[16] B. W. Lee, *Chiral Dynamics*, New York, Gordon and Breach Science Publishers (1972), p. 21

[17] C. E. DeTar and T. Kunihiro, Phys. Rev. D **39**, 2805 (1989).

[18] D. Jido, M. Oka and A. Hosaka, Prog. Theor. Phys. **106**, 873 (2001) doi:10.1143/PTP.106.873 [hep-ph/0110005].

[19] C. E. Detar and J. B. Kogut, Phys. Rev. D **36**, 2828 (1987). doi:10.1103/PhysRevD.36.2828

[20] G. Aarts, C. Allton, S. Hands, B. Jäger, C. Praki and J. I. Skullerud, Phys. Rev. D **92**, no. 1, 014503 (2015) doi:10.1103/PhysRevD.92.014503 [arXiv:1502.03603 [hep-lat]].

[21] M. Bando, T. Kugo, S. Uehara, K. Yamawaki and T. Yanagida, Phys. Rev. Lett. **54**, 1215 (1985).

[22] M. Bando, T. Kugo and K. Yamawaki, Phys. Rept. **164**, 217 (1988).

[23] M. Harada and K. Yamawaki, Phys. Rept. **381**, 1 (2003)

[24] T. Hatsuda and M. Prakash, Phys. Lett. B **224**, 11 (1989).

[25] D. Zschiesche, L. Tolos, J. Schaffner-Bielich and R. D. Pisarski, Phys. Rev. C **75**, 055202 (2007) [nucl-th/0608044].

[26] V. Dexheimer, S. Schramm and D. Zschiesche, Phys. Rev. C **77**, 025803 (2008) [arXiv:0710.4192 [nucl-th]].

[27] S. Gallas, F. Giacosa and D. H. Rischke, Phys. Rev. D **82**, 014004 (2010)

[28] C. Sasaki and I. Mishustin, Phys. Rev. C **82**, 035204 (2010) [arXiv:1005.4811 [hep-ph]].

[29] S. Gallas, F. Giacosa and G. Pagliara, Nucl. Phys. A **872**, 13 (2011) [arXiv:1105.5003 [hep-ph]].

[30] J. Steinheimer, S. Schramm and H. Stocker, Phys. Rev. C **84**, 045208 (2011) [arXiv:1108.2596 [hep-ph]].

[31] S. Benic, I. Mishustin and C. Sasaki, arXiv:1502.05969 [hep-ph].

[32] J. Weyrich, N. Strodthoff and L. von Smekal, arXiv:1504.02697 [nucl-th].

[33] A. Bohr and B. R. MotteIson (A. Arima, M. Ichimura and K. Kubodera Trans.) , *Nuclear Structure* (Gensikakukouzou), Tokyo, Koudansha (1979), p. 177

[34] F. E. Serr and J. D. Walecka, Phys. Lett. B **79**, 10 (1978) Erratum: [Phys. Lett. B **84**, 529 (1979)]. doi:10.1016/0370-2693(79)91255-3, 10.1016/0370-2693(78)90423-9

[35] Y. Motohiro, Y. Kim and M. Harada, Phys. Rev. C **92**, no. 2, 025201 (2015) [arXiv:1505.00988 [nucl-th]].

[36] T. Kugo, *Gauge-ba no ryoushiron II* (Quantum theory of gauge field, II), Tokyo, Baifukan (1989)

[37] D. H. Youngblood, H. L. Clark and Y.-W. Lui, Phys. Rev. Lett. **82**, 691 (1999). doi:10.1103/PhysRevLett.82.691

[38] S. Shlomo, V. M. Kolomietz, and G. Colo, Eur. Phys. J. A 30, 23 (2006).

[39] J. M. Lattimer and Y. Lim, Astrophys. J. **771**, 51 (2013) doi:10.1088/0004-637X/771/1/51 [arXiv:1203.4286 [nucl-th]].

[40] I. Vidana, C. Providencia, A. Polls and A. Rios, Phys. Rev. C **80**, 045806 (2009) doi:10.1103/PhysRevC.80.045806 [arXiv:0907.1165 [nucl-th]].

[41] J. A. López, E. Ramírez-Homs, R. González and R. Ravelo, Phys. Rev. C **89**, no. 2, 024611 (2014) doi:10.1103/PhysRevC.89.024611 [arXiv:1311.6134 [nucl-th]].

[42] C. Wellenhofer, J. W. Holt and N. Kaiser, Phys. Rev. C **92**, no. 1, 015801 (2015) doi:10.1103/PhysRevC.92.015801 [arXiv:1504.00177 [nucl-th]].

[43] C. J. Horowitz *et al.*, J. Phys. G **41**, 093001 (2014) doi:10.1088/0954-3899/41/9/093001 [arXiv:1401.5839 [nucl-th]].

[44] J. Pochodzalla *et al.*, Phys. Rev. Lett. **75**, 1040 (1995). doi:10.1103/PhysRevLett.75.1040

[45] P. Kienle and T. Yamazaki, Prog. Part. Nucl. Phys. **52**, 85 (2004). doi:10.1016/j.ppnp.2003.09.001

[46] J. Gasser, H. Leutwyler and M. E. Sainio, Phys. Lett. B **253**, 252 (1991). doi:10.1016/0370-2693(91)91393-A

[47] D. T. Son and M. A. Stephanov, Phys. Rev. Lett. **86**, 592 (2001) doi:10.1103/PhysRevLett.86.592 [hep-ph/0005225].

[48] H. Nishihara and M. Harada, Phys. Rev. D **89**, no. 7, 076001 (2014) doi:10.1103/PhysRevD.89.076001 [arXiv:1401.2928 [hep-ph]].

[49] J. B. Kogut and D. K. Sinclair, Phys. Rev. D **70**, 094501 (2004) doi:10.1103/PhysRevD.70.094501 [hep-lat/0407027].

[50] R. D. Woods and D. S. Saxon, Phys. Rev. **95**, 577 (1954). doi:10.1103/PhysRev.95.577

[51] C. A. Bertulani, *Nuclear Physics in a Nutshell*, Princeton, Princeton University Press (2007).

[52] H. Nishihara and M. Harada, Phys. Rev. D **92**, no. 5, 054022 (2015) doi:10.1103/PhysRevD.92.054022 [arXiv:1506.07956 [hep-ph]].

[53] R. Aaij *et al.* [LHCb Collaboration], Phys. Rev. Lett. **115**, 072001 (2015) doi:10.1103/PhysRevLett.115.072001 [arXiv:1507.03414 [hep-ex]].

[54] M. G. Alford, K. Rajagopal and F. Wilczek, Phys. Lett. B **422**, 247 (1998) doi:10.1016/S0370-2693(98)00051-3 [hep-ph/9711395].

[55] S. Aoki, *Koushijou no Banoriron* (Field theory on lattice), Tokyo, Maruzen shuppan (2005)

[56] M. Gell-Mann and M. Levy, Nuovo Cim. **16**, 705 (1960). doi:10.1007/BF02859738

[57] Y. Nambu and G. Jona-Lasinio, Phys. Rev. **124**, 246 (1961). doi:10.1103/PhysRev.124.246

[58] J. Erlich, E. Katz, D. T. Son and M. A. Stephanov, Phys. Rev. Lett. **95**, 261602 (2005) doi:10.1103/PhysRevLett.95.261602 [hep-ph/0501128].

[59] T. Sakai and S. Sugimoto, Prog. Theor. Phys. **113**, 843 (2005) doi:10.1143/PTP.113.843 [hep-th/0412141].

[60] C. Patrignani *et al.* [Particle Data Group Collaboration], Chin. Phys. C **40**, no. 10, 100001 (2016). doi:10.1088/1674-1137/40/10/100001

[61] J. Gasser and H. Leutwyler, Annals Phys. **158**, 142 (1984). doi:10.1016/0003-4916(84)90242-2

[62] J. Gasser and H. Leutwyler, Nucl. Phys. B **250**, 465 (1985). doi:10.1016/0550-3213(85)90492-4

[63] G. Ecker, Prog. Part. Nucl. Phys. **35**, 1 (1995) doi:10.1016/0146-6410(95)00041-G [hep-ph/9501357].

[64] M. Gell-Mann, R. J. Oakes and B. Renner, Phys. Rev. **175**, 2195 (1968). doi:10.1103/PhysRev.175.2195

[65] M. Gell-Mann, Phys. Rev. **125**, 1067 (1962). doi:10.1103/PhysRev.125.1067

[66] S. Okubo, Prog. Theor. Phys. **27**, 949 (1962). doi:10.1143/PTP.27.949

[67] S. Okubo, Phys. Lett. **5**, 165 (1963). doi:10.1016/S0375-9601(63)92548-9

[68] G. Zweig, CERN-TH-401.

[69] J. Iizuka, Prog. Theor. Phys. Suppl. **37**, 21 (1966). doi:10.1143/PTPS.37.21

[70] K. Kawarabayashi and M. Suzuki, Phys. Rev. Lett. **16**, 255 (1966). doi:10.1103/PhysRevLett.16.255

[71] Riazuddin and Fayyazuddin, Phys. Rev. **147**, 1071 (1966). doi:10.1103/PhysRev.147.1071

[72] J.J.Sakurai, *Currents and Mesons*, Chicago, Chicago University Press, (1969)

[73] J. I. Kapusta and C. Gale, *Finite-Temperature Field Theory Principles and Applications Second Edition*, Cambridge, Cambridge University Press, (2006)

[74] L. L. Foldy and S. A. Wouthuysen, Phys. Rev. **78**, 29 (1950).

[75] W. A. Barker and Z. V. Chraplyvy, Phys. Rev. **89**, 446 (1953).